FUNCTIONAL CHARACTERIZATION OF AZINOMYCIN BIOSYNTHETIC ENZYMES

A Dissertation

by

HILLARY CHIDI AGBO

Submitted to the Office of Graduate Studies of
Texas A&M University
in partial fulfillment of the requirements for the degree of

DOCTOR OF PHILOSOPHY

August 2012

Major Subject: Chemistry

Functional Characterization of Azinomycin Biosynthetic Enzymes

FUNCTIONAL CHARACTERIZATION OF AZINOMYCIN BIOSYNTHETIC ENZYMES

A Dissertation

by

HILLARY CHIDI AGBO

Submitted to the Office of Graduate Studies of
Texas A&M University
in partial fulfillment of the requirements for the degree of

DOCTOR OF PHILOSOPHY

Approved by:

Chair of Committee,	Coran M. H. Watanabe
Committee Members,	Tadhg P. Begley
	Wenshe Liu
	Michael Manson
Head of Department,	David H. Russell

August 2012

Major Subject: Chemistry

ABSTRACT

Functional Characterization of Azinomycin

Biosynthetic Enzymes. (August 2012)

Hillary Chidi Agbo, B.Sc., University of Nigeria, Nsukka

Chair of Advisory Committee: Dr. Coran M.H. Watanabe

Azinomycins A and B are antitumor compounds isolated from soil bacteria, *Streptomyces sahachiroi*. The azinomycin structure contains an unusual aziridine [1,2a] pyrrolidine ring and an epoxyvaline moiety which are used in forming DNA cross-links. The biosynthetic gene cluster of azinomycin B has been characterized but the biosynthetic routes to these intermediates and overall architecture of this compound is not well understood.

This work investigates the role of *aziW*, a *lysW* homologue in azinomycin biosynthesis. Gene replacement of *aziW* by homologous exchange abolished the production of azinomycin thereby implicating the gene in azinomycin biosynthesis. Complementation of *aziW* in the mutant strain, however, did not restore production of this natural product as observed by HPLC analysis, which suggests that *aziW* as well as genes downstream could be responsible for lack of azinomycin production. Sequence analysis of *aziW* suggests co-transcription with the downstream genes which are homologous to lysine biosynthetic genes in *T. thermophilus*. The mRNA expression profile of the genes downstream of *aziW* exhibited a down-regulation or transcription

termination for these genes which appear to be in the same operon. The impact is stronger the further away the gene is from *aziW*. Negative lysine auxotrophy test showed that this gene is not involved in lysine biosynthhesis but is crucial to azinomycin biosynthesis. This dissertation also discusses the investigation of the role of *ORF10*, a dehydrogenase which is located at the terminal end of the gene cluster. Gene disruption of *ORF10* had no effect in azinomycin production but established the boundary of the azinomycin gene cluster. *AziC9* was charaterized as an authentic cytochrome P450 through gene expression in *E.coli*, purification, carbon monoxide binding and activity assay with a putative substrate.

DEDICATION

To

My Wife & Kids, Friends & Family; and to my relatives and friends who could not live to see this day.

ACKNOWLEDGEMENTS

I want to thank my labmates Dr. D. Simkhada (postdoc), Shogo Mori, Rachel Lee, Vishruth Gowda, and Michelle Lebo for being such a family. My deep sense of gratitude goes to my former labmates, Dr. Huitu Zhang, a postdoctoral fellow that taught me gene disruption in Streptomyces, Dr. Eun Jin Kim, Dr. T. Kelly, Dr. B. J. Bench and Dr. J. Foulke-Abel for teaching me how to get things done at my early stages in the group. I thank Dr. B. Philmus (BJ) for all the scientific advice and suggestions in my research and Felix Yu for making agarose gels for me.

I would like to thank my committee chair, Dr. Watanabe for her guidance and support throughout the course of this research. I want to specifically thank her for showing a lot of understanding when I became a father of two in quick succession as well as a graduate student.

Finally, thanks to my wife, Helen and my daughters Muna and Akachi for being such a source of strength even when I can't get enough sleep.

TABLE OF CONTENTS

Page

ABSTRACT iii

DEDICATION v

ACKNOWLEDGEMENTS vi

TABLE OF CONTENTS vii

LIST OF FIGURES x

LIST OF TABLES xiii

CHAPTER

I INTRODUCTION 1

Natural Products 1
Natural Product Biosynthesis 3
Fatty Acids and Polyketides 5
Ribosomal Peptides 11
Non-Ribosomal Peptides (NRP) 14
Terpenes and Alkaloids 19
Terpenes 19
Carotenoids 22
Combinatorial Chemistry & Engineering of Secondary Metabolic Pathways 26
Azinomycin B 30
Biosynthesis of Azinomycin B 32
Statement of Purpose 33

II GENETIC DISRUPTION OF *ORF10*, A DEHYDROGENASE AND THE IMPACT ON AZINOMYCIN PRODUCTION 34

Introduction 34
Materials and Methods 38
Media Conditions 39
Cloning of *ORF10* Disruption Cassette 39
Conjugal Transformation of Disruption Plasmid 41

CHAPTER Page

Fermentation and Isolation of Metabolites 42
Results and Discussion 43
Generation of *OFR10* Deletion Mutant 43
Fermentation and Analysis of Metabolites 45

III PROBING THE ROLE OF *aziW*, A LYSINE BIOSYNTHETIC GENE (*lysW*) HOMOLOGUE IN AZINOMYCIN PRODUCTION .. 50

Introduction 50
Materials and Methods 55
Media Conditions 57
Cloning of aziW Disruption Construct 58
E.coli-S. sahachiroi Interspecies Conjugation 59
Generation of ^{32}P-ATP-labeled Gene Probes and Southern Hybridization 61
Construction of Recombinant Integrative Plasmid, pSET152-lysW 62
E.coli-S. sahachiroi Interspecies Conjugation 63
Fermentation and Isolation of Metabolites 63
RNA Isolation and Northern Hybridization 64
Reverse Transcription (RT)-PCR Analysis of Genes Downstream of *aziW* 66
Testing of Lysine Auxotrophy of *aziW* Mutant 66
Results and Discussion 67
Generation of *aziW* Disruptant 67
Recombinant Integrative Plasmid, pSET152-lysW 69
Fermentation and Characterization of Metabolites 70
Organization of lysW Operon and Northern Blot Analysis 73
The mRNA Expression Profile of Genes Downstream of *aziW* 74
Lysine Auxotrophy in *aziW* Deletion Mutant 76

IV BIOCHEMICAL EVALUATION OF THE ROLE OF CYTOCHROME P450 (*aziC9*) IN AZINOMYCIN BIOSYNTHESIS 78

Introduction 78
Applications of Cytochrome P450 82
Cytochrome P450 as Epoxidases 84
aziC9, a Cytochrome P450 in the Azinomycin Gene Cluster .. 85
Materials and Methods 87
Cloning, Overexpression and Purification of *aziC9* 87
Carbon Monoxide (CO) Binding Assay 90
aziC9, Cytochrome P450 Assay 90

CHAPTER Page

Results and Discussion 90
Expression and Purification of *aziC9*..... 90
Spectral Properties of aziC9 91
Sequence Alignmentof aziC9 92
Conversion of 3-methyl-2-oxobut-3-enoate to the Epoxide..... 94

V CONCLUSION 95

REFERENCES 98

APPENDIX 114

LIST OF FIGURES

Page

Figure 1.Distribution of approved small molecule drug sources from 1981 to 2010 2

Figure 2.Structures of some natural products used as drugs 3

Figure 3.Proposed routes to natural product biosynthesis 5

Figure 4.Reaction scheme for the FAS system 7

Figure 5.Comparison of the domain arrangement in type I and II PKS systems 8

Figure 6.Biosynthesis of 6-deoxyerythronolide B..... 9

Figure 7 (a).Biosynthetic pathway of fungal polyketide 6-methylsalicylic acid..... 10

Figure 7 (b).Illustration of type III PKS system..... 11

Figure 8.Structures of some ribosomal natural products 13

Figure 9.Generic steps in bacterial ribosomal peptide biosynthesis..... 14

Figure 10.Illustration of surfactin A biosynthesis 17

Figure 11.Some natural products of NRPS origin..... 18

Figure 12.Mevalonate biosynthesis pathway of isopentenyl pyrophosphate (IPP)... 21

Figure 13.The deoxy-xylulose phosphate pathway for IPP 22

Figure 14.Condensation of IPP and DMAPP..... 23

Figure 15. Tail-to-tail condensation of FPP in squalene biosynthesis 23

Figure 16.Structures of carotenoids, lycopene, vitamin E and β-carotene 24

Figure 17.Enzymatic cleavage of β-carotene to retinal and conversion to retinol.... 24

Figure 18.Human vision cycle..... 25

Figure 19.Structures of natural products whose gene clusters have been identified. 29

Figure 20.Structures of azinomycin A, azinomycin B and epoxyamide 31

Figure 21.Azinomycin interaction with duplex DNA 31

Figure 22.Structures of some aziridine-containing natural products..... 33

Figure 23.Structures of azinomycin A and B 34

Figure 24.Revised azinomycin gene cluster..... 35

Figure 25.Biosynthetic route to the epoxide moiety in the azinomycins..... 37

Figure 26.Valine degradation pathway 37

Figure 27.Gene disruption strategy for *ORF10*..... 46

Figure 28.Confirmation of *ORF10* gene disruption 47

Figire 29.^{1}H-NMR analysis of extracts from *ORF10* disruptant (A) and wild-type (B) strains 48

Figure 30.RP-HPLC analysis of *S.sahachiroi* wild-type and *ORF10* disruptant..... 49

Figure 31.Revised azinomycin gene cluster showing boundary of the cluster 49

Figure 32.Some of the precursors that are incorporated into the azinomycin..... 52

Figure 33.Proposed biosynthetic pathway to the azibicyclic ring 52

Figure 34.Lysine biosynthesis and location of *aziW* in azinomycin gene cluster 53

Figure 35.Enzymatic activities of *lysW* & *lysX* and structures of some truncation products of arginine and lysine biosyntheses..... 54

Figure 36.Comaparison of gene orientation of lysine biosynthetic gene clusters..... 54

Figure 37.*aziW* disruption strategy 69

Figure 38.Confirmation of *aziW* disruption 70

Figure 39.Vector diagram of pSET152 and the complementation plasmid 71

Figure 40.RP-HPLC analysis of metabolites from *S. sahachiroi* wild-type (top) and *aziW* deletion mutant (bottom)..... 72

Figure 41.RP-HPLC analysis of metabolites from *S. sahachiroi aziW* compement (top) and *aziW* deletion mutant (bottom)..... 72

Figure 42.Promoter analysis of *aziW* sequence and Northern hybridzation 73

Figure 43.The mRNA expression profile of *aziW* downstream genes 76

Figure 44.Lysine auxotrophy experiment on minimal agar plates 77

Figure 45.Protoporphyrin IX with a bound iron..... 80

Figure 46.Proposed catalytic cycle of cytochrome P450..... 82

Figure 47.Cytochrome P450 catalyzed epoxidation reactions 85

Figure 48.Aznomycin gene cluster showing cytochrome P450 in blue color..... 86

Figure 49.*aziB1*, cytochrome P450 catalyzed hydroxylation of 5-methyl-NPA..... 86

Figure 50.Oxidation steps in azinomycin shown in red color..... 87

Figure 51.pET24b-AziC9 plasmid and SDS PAGE analysis of *aziC9*..... 91

Figure 52.Carbon Monoxide (CO) binding study of *aziC9* 92

Figure 53.Multiple sequence alignment of *aziC9* with its homologues..... 93

Figure 54.Multiple sequence alignment of *aziC9* with other P450 epoxidases 93

Figure 55.*azic9* reaction with 3-methyl-2-oxobut-3-enoate..... 94

Figure 56.Multiple protein sequence alignment of *ORF10* with its homologues 114

Figure 57.Mass spectrum of azinomycin B (peak B) collected from RP-HPLC 114

Figure 58.Mass spectrum of azinomycin A (peak A) collected from RP-HPLC..... 115

LIST OF TABLES

Page

Table 1.Bacterial strains, plasmids and primers used in *ORF10* study 44

Table 2.Bacterial strains, plasmids and primers used in *aziW* study 56

Table 3.Classes of P450 systems classified based on components involved in the electron transfer to the P450 enzyme 81

Table 4.Bacterial strains, plasmids and primers used in *aziC9* study 88

CHAPTER I

INTRODUCTION

NATURAL PRODUCTS

Humans are inventive and adaptive; they have found ways of treating various illnesses since life began on earth. In the pre-historic era, plants and their extracts were the dominant sources of active medicinal compounds. Plant-derived metabolites were used as flavors for food, colorants, fragrances, sweeteners. Natural products, as the term is applied in this write-up, refer mostly to biologically active natural products and their precursors. The discovery of natural products of microbial origin started with the use of molds and warm soil in the treatment of wounds and infections. The birth of modern medicine was heralded by Sir Alexander Fleming's serendipitous discovery in 1928 of the β-lactam antibiotic, penicillin, produced by the fungus *Penicillium notatum* and the follow-up clinical studies in the 1940s.[1] The advance in science and technology has overcome the barriers met by earlier efforts in the discovery of natural products. Natural products, their derivatives, and natural product- inspired compounds remain invaluable to the pharmaceutical industry and medicine in general. In the period between 1981 and 2010, the FDA approved the use of 1073 small molecules as drugs; ~60% of these were natural products, their derivatives, or natural product-inspired compounds (Figure 1).[2]

This dissertation follows the style of *Biochemistry*.

Romidepsin (Figure 2) is one of the six antitumor agents approved in 2010. It is a histone deacetylase inhibitor (HDAC) and a microbial natural product. Although the total synthetic route exists for this compound, it is still being produced by fermentation of *Chromobacterium violaceum*.[3-7] This approval came after a roughly 20-year shift by big pharmaceutical companies from natural product-based discovery programs.[2]

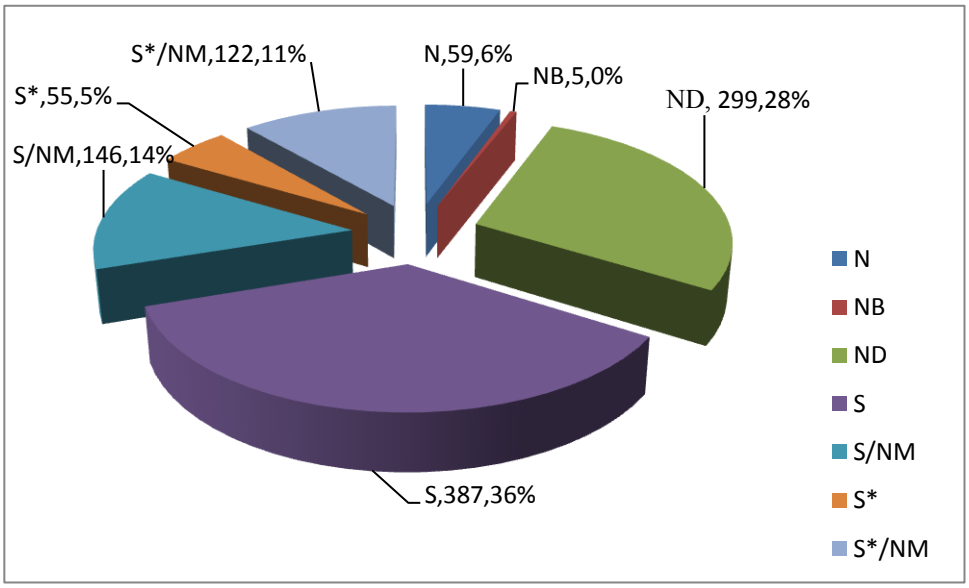

Figure 1.Distribution of approved small molecule drug sources from 1981 to 2010.[2]
N, natural product; NB, Natural product botanical (in general these have been recently approved); ND, derived from a natural product and usually a semisynthetic modification; S, totally synthetic drug often found by random screening/modification of an existing agent; S*, made by total synthesis, but the pharmacophore is/was from a natural product; NM subcategory, natural product mimic.

The discussion of natural products in this era cannot be complete without the mention of two very important drugs, taxol and vancomycin (Figure 2). The story of these two drugs has been a motivation to both researchers and investors, who are in constant search of another blockbuster drug. Taxol was discovered in 1967, isolated

from the Pacific yew tree and is used in treating soft-tissue cancer.[8-9] Between 1967 and 1993, taxol was almost completely produced from the bark of the Pacific yew. A semisynthetic route was later established, and taxol generated $1.6 billion in annual sales to Bristol-Myers Squibb in 2000.[10-12] Vancomycin, on the other hand, is a glycopeptide antibiotic produced by the soil organism, *Amycolatopsis orientalis*. It is used as the last line of defense in treating methicillin-resistant *Staphylococcus aureus* (MRSA) and penicillin-resistant *Streptococcus pneumonia* infections.[13]

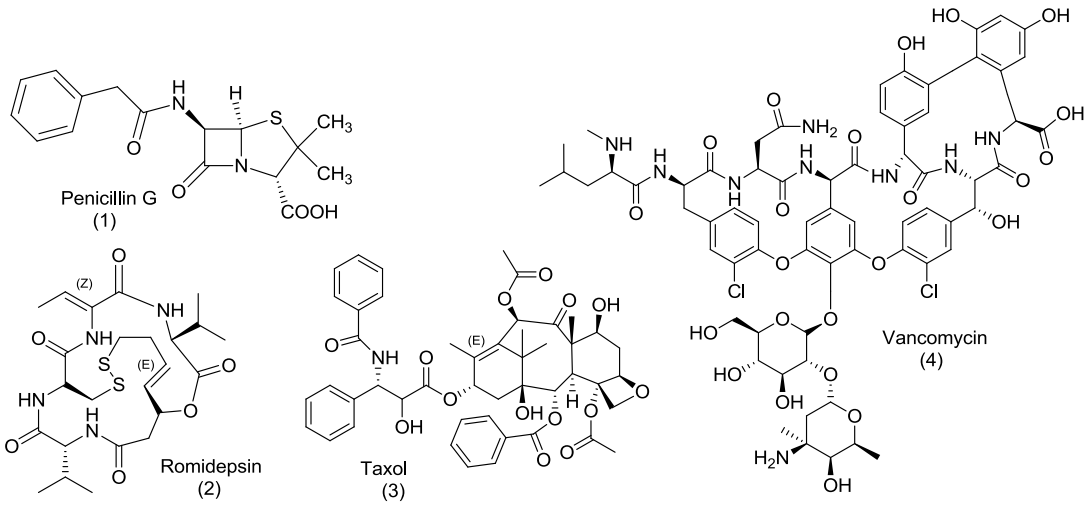

Figure 2.Structures of some natural products used as drugs.

NATURAL PRODUCT BIOSYNTHESIS

Nature is the best chemist ever known and carries out a plethora of chemical reactions required for sustaining living organisms. While this primary metabolism is indispensible to the daily existence of the organism, the need arises for these organisms to carry out chemical reactions through clearly defined pathways during adverse conditions like starvation, disease and the presence of chemical agents. Secondary

metabolites represent a pool of chemical structures ranging from very simple to complex architectures. The products and intermediates of primary metabolism form the building blocks; they are fed into the biosynthetic pathways of these secondary metabolites and form the basis of secondary metabolic products classification. In 1907, James Collie, a chemist at London University proposed his ideas on the biosynthesis of polyphenols.[14] At the time, there were no biological chemists, and organic chemists do not have much idea of reaction pathways in the living system. His ideas were dismissed as premature and overly ambitious. In 1917, Robert Robinson proposed a scheme (Figure 3A) for the biosynthesis of tropinone, a synthetic precursor to atropine, which is an extract from plant and serves as drug with a variety of effects.[15–16] The chemists of Robinson's time were more receptive to his ideas and his proposal was accepted. Arthur Birch, the chemist who coined the term "poly ketides," had his early training in Robinson's laboratory at Oxford. In 1950, he proposed the biosynthetic route for the aromatic polypeptide, 6-methylsalyicylic acid (Figure 3B), produced by the fungus, *Penicillium patulum*.[17,18] The study of natural product biosynthesis has been enhanced by the development of radioactive-labeling studies, NMR and MS spectroscopies, and more recently, advancement in the genomic and proteomic technologies. Natural products are biosynthesized through limited but complex pathways including the fatty acid synthases (FAS), the polyketides synthases (PKS), the non-ribosomal peptide synthetases (NRPS), terpenes and alkaloids pathways.

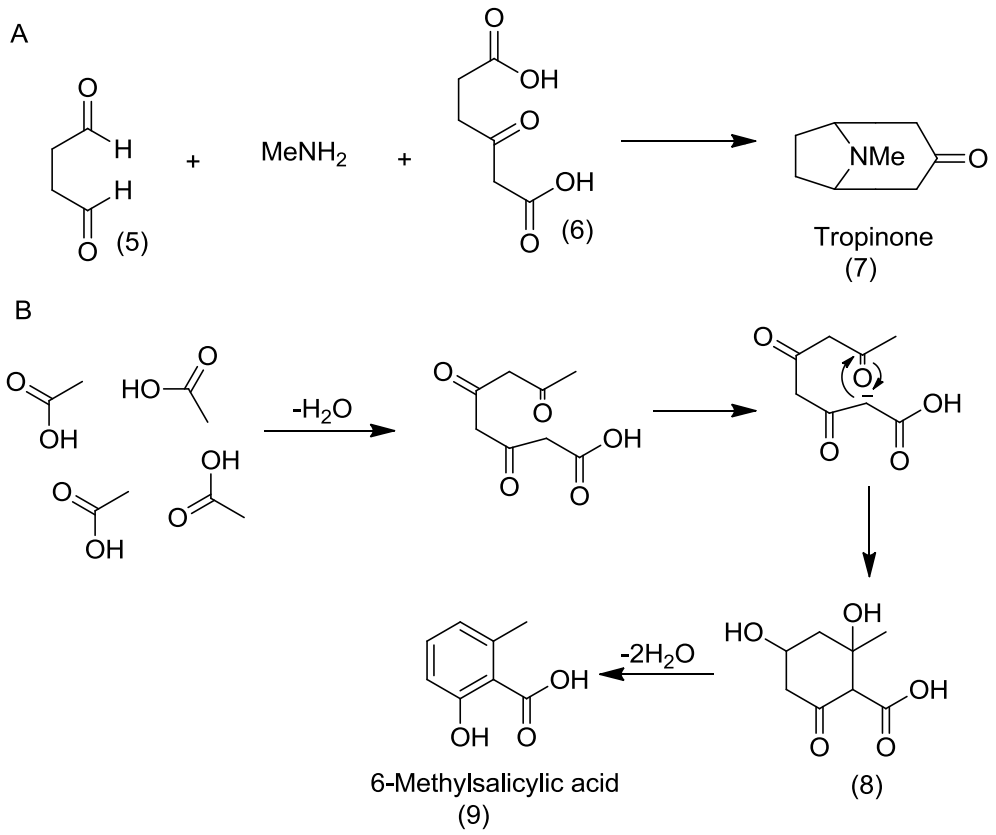

Figure 3.Proposed routes to natural product biosynthesis. (A) Robinson's biomimetic synthesis of tropinone. (B) Birch's route to biosynthesis of 6-methylsalicylic acid.

FATTY ACIDS AND POLYKETIDES

Fatty acid synthases (FAS) are multi-functional enzyme complexes that catalyze the synthesis of fatty acids through a decaboxylative Clasien condensation of the starter unit, acetate, and a decarboxylated malonyl-unit by the action of the keto synthase (KS) domain.[19-21] The extended unit is released from the enzyme and further converted to β–hydroxy thioester by the keto reductase (KR) domain. A β-unsaturated thioester is formed from the β–hydroxy thioester by the loss of a water molecule by the action of the dehydratase (DH) domain. The enoyl reductase (ER) domain then reduces the above intermediate to produce a saturated fatty acid (Figure 4). This sequence of reactions is

repeated, and the growing fatty acid chain is transferred between active sites while covalently attached to the phosphopantetheinyl arm of the acyl carrier protein (ACP) until the desired chain length is reached. The mature fatty acid is then released by the action of the thioesterase (TE) domain.

The fatty acid synthases (FAS) resemble the polyketide systems in that they share some catalytic domains. However, the PKSs are deficient in some of the reductive catalytic domains necessary for the saturated alkyl chains produced in FAS systems. The core domains of PKS system are the keto synthase (KS), acyltransferase (AT), and thiolation (T) domain. The structural diversity of polyketides is controlled by the variation in the choice of starter (acetyl-CoA, malonyl-CoA, methylmalonyl-CoA) and the extender units, as well as by the number of condensations and reduction cycles. The two main types of PKS systems found in bacteria are the type I & II PKSs. Type I PKSs are multi-domain proteins encoded by single gene, whereas type II PKSs are trans-acting iterative protein complexes in which each domain is encoded by one gene.[22] The cis/trans wiring of the domains of type I and type II PKS systems are illustrated in Figure 5. Catalytic domains in type II PKSs are used multiple times during chain elongation, whereas those in type I PKSs are only used once per catalytic cycle.

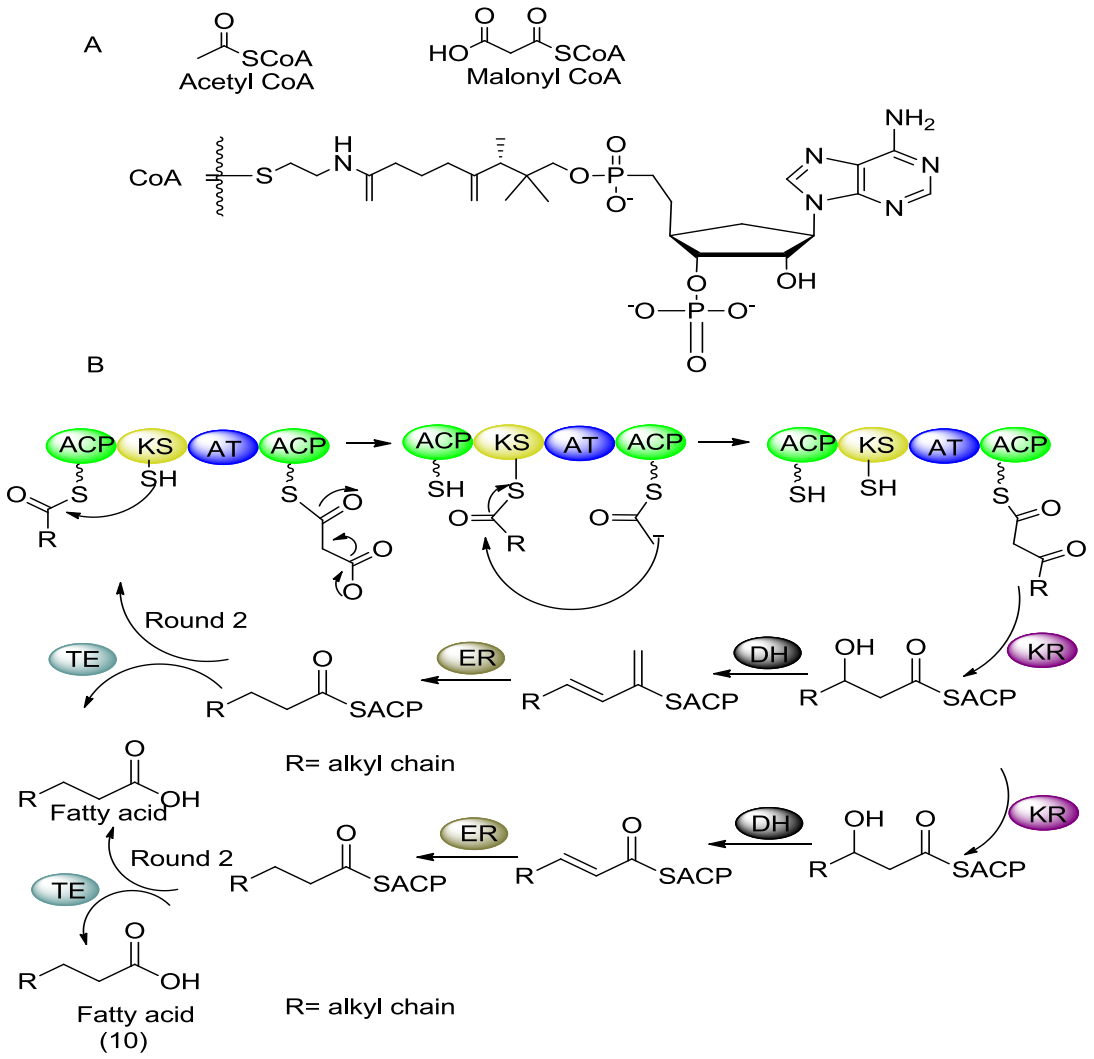

Figure 4.Reaction scheme for the FAS system. (A) Acetyl-CoA and Malonyl-CoA units (B) KS, AT domains that catalyze the decaboxylative Claisen condensation of the starter units; KR, DH, ER modify unit, TE release product.

A classical example of type I or modular PKS is the erythromycin PKS. The structural genes responsible for synthesizing the first macrolide intermediate, 6-deoxyerythronolide B (6-DEB), are three giant open reading frames coding for multienzyme polypeptides, 6-deoxyerythronolide B synthase (DEBS) 1, 2 and 3.[23-25] Each of the DEBS proteins contains two functional modules, which in turn contain the

core domains, KS, AT and ACP (Figure 6). These modules contain variable sets of domains, KR, DH and ER, which are required for the modification of the keto group. The intermediate, 6-DEB, is released by the TE domain in DEBS 3 and further modified by other tailoring enzymes to produce erythromycin B. There are unusual cases of aromatic compounds derived from type I PKSs in which either the domains or modules are used in iterative manner.[26-29] The 6-methylsalicylic acid synthase (6-MSAS) is an

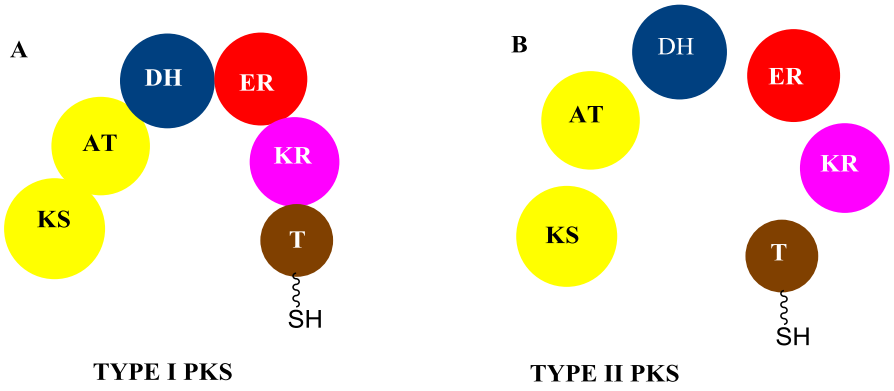

Figure 5.Comparison of the domain arrangement in type I and II PKS systems. (A) Type I PKS system, domains are connected in cis; (B) Type II PKS system, domains are trans-acting.[17]

example of an iterative type I PKS. 6-MSAS contains KS, MAT, DH, KR, and ACP domains in that order, and forms 6-MSA from one molecule of acetate starter unit and three molecules of malonate extender units.[18] What is remarkable about the 6-MSAS (Figure 7a) is that it lacks the thioesterase (TE) domain, so that release of the chain from the PKS occurs not by TE domain-mediated hydrolysis but by some other mechanism. It was initially proposed that the release of the product proceeded through a ketene intermediate.[18] The actual domain involved in the release of the product was identified

two decades later.[30] The 6-MSA is released hydrolytically from 6-MSAS by the action of the domain initially called DH but later renamed thioester hydrolase (TH) domain. Type III PKSs do not share domains with FAS and are seen as a unique type of PKS.

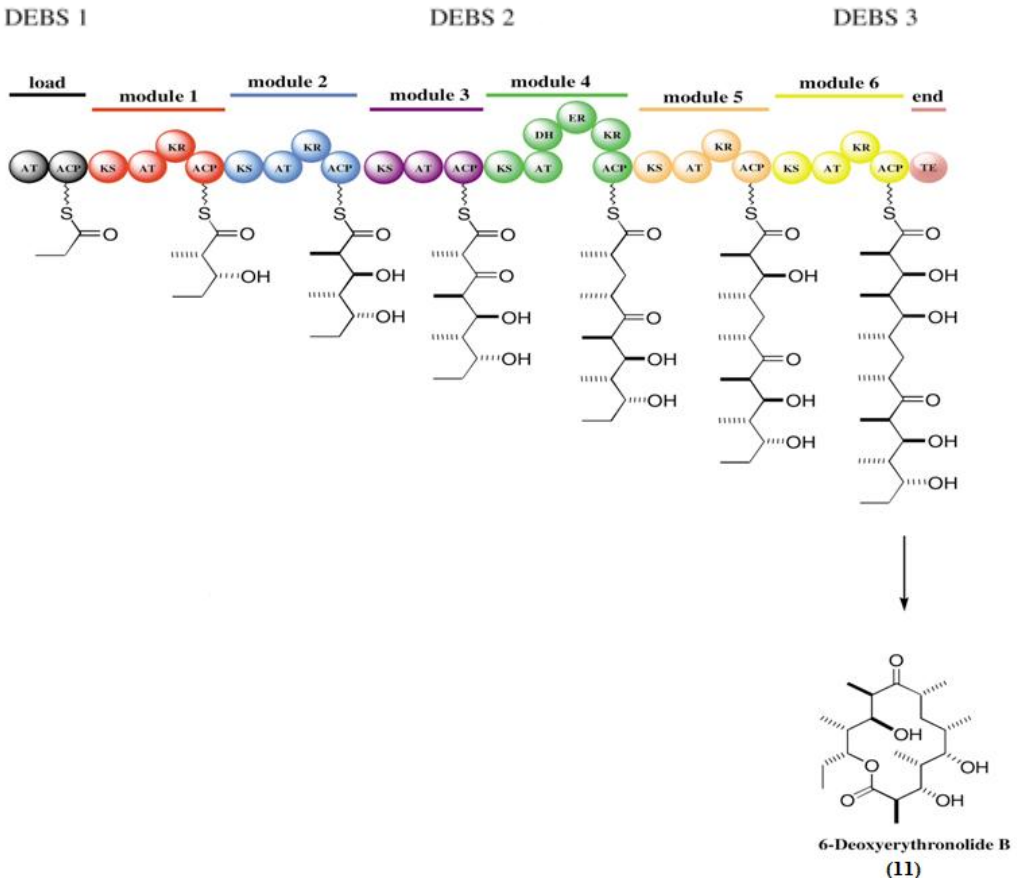

Figure 6.Biosynthesis of 6-deoxyerythronolide B.

Examples of type III PKSs are the chalcone synthase (CHS), a plant polyketide synthase that uses p-coumarin-CoA as the starter unit, and acridone synthase (ACS) (Figure 7b), which uses *N*-methylanthraniloyl-CoA as the starter unit.[31-34] Chalcones are

natural phenols and form the central core of a variety of biologically active compounds.[35,36] Acridone forms the scaffold for a variety of synthetic compounds with interesting pharmacological properties.[37,38] Although the initial steps of Claisen condensation and cyclisation in CHS resembles that of type I and II PKS systems, there are differences in the mode of transfer of the intermediates among active sites. The PKSs use the phosphopantetheine arm of ACP to shuttle substrates and intermediates through the active sites, whereas CHS uses CoA thioesters directly.[39]

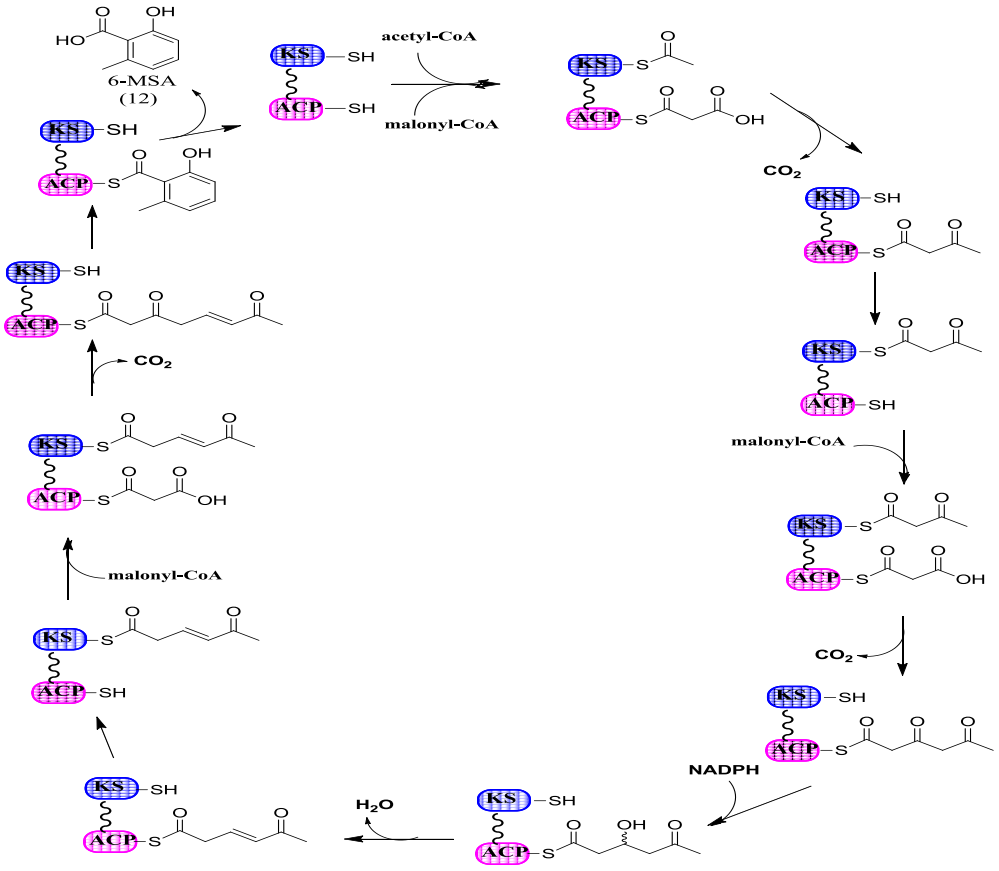

Figure 7(a).Biosynthetic pathway of fungal polyketide 6-methylsalicylic acid.

The decarboxylation, condensation, cyclization and aromatization events in CHS are all carried out in a single active site, in contrast to type I or II PKSs.[39]

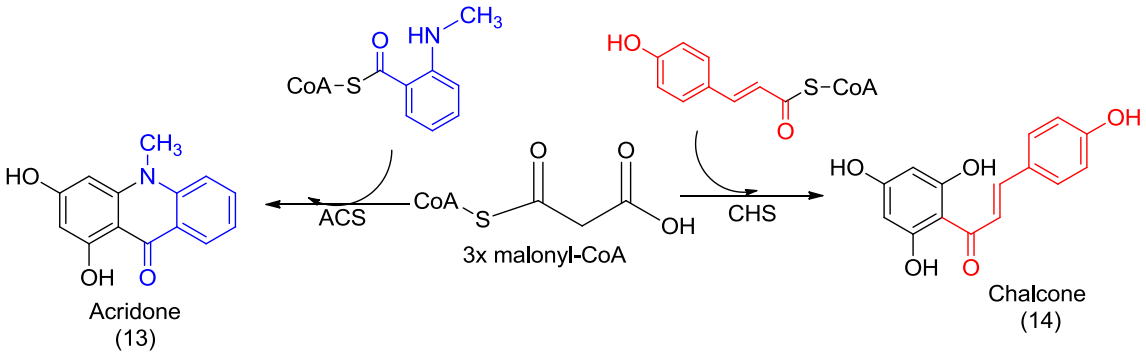

Figure 7(b).Illustration of type III PKS system.

RIBOSOMAL PEPTIDES

Ribosomal peptides are natural products that are produced by the ribosomal machinery. They exhibit broad structural and functional diversity. Unlike non-ribosomal peptides, their structural diversity is limited by the pool of amino acid residues accessible to ribosomal peptide enzymes. There is no evidence yet of the ability of the ribosomal peptide machinery to explore amino acids beyond the standard twenty proteinogenic ones. In spite of this limitation, ribosomal peptides display as much structural diversity as non-ribosomal peptides because of the extensive post-translational modification found in the ribosomal peptide system. Some modifications that were initially thought to be unique to the non-ribosomal peptides are also found in the ribosomal system. Compared to the non-ribosomal system, the ribosomal peptide system offers a simple platform for the modification of the natural product. The manipulation of

a few codons for ribosomal peptide sequence results in an increase in structural and functional diversity; this is in contrast to the non-ribosomal peptides, which require extensive genetic engineering to effect changes in structure. [40, 41] In the ribosomal peptide synthesis pathway, short peptide precursors are translated in the ribosome followed by modification by enzymes to produce very complex natural products.[42] The modifications can be so extensive, for example in pyrroloquinoline quinone (Figure 8), that the natural product is no longer readily recognizable as derived from amino acids. Another example of a ribosomal peptide natural product is the lantibiotics (Figure 8), which are produced by a number of streptococcus and streptomyces species and are used in food preservation and treatment of infection in human.[43]

A generic form of the ribosomal peptide biosynthesis is shown in Figure 9 below. The gene for a precursor peptide is usually clustered with the modifying enzyme. Following translation, the precursor peptide is post-translationally modified, and an active natural product is formed.[42] One common post-translational modification of amino acid residues is the dehydration of serine and threonine. This modification results in intermediates that can react by both intramolecular and intermolecular mechanisms to form well-known ribosomal peptides like lanthionine, nisin and subtilin.[44,45] Another known side-chain modification is prenylation which enhances their lipophilicity and helps in membrane targeting.[46] Disulfide bond formation is common to proteins and small peptides. In ribosomal peptides, it plays a role in constraining small peptide sequences into active conformations.[47] Conopeptides are biologically potent ribosomal peptides that contain multiple disulfide bridges; incorrect disulfide bridging during

synthesis or disruption of disulfide bridges by mutagenesis has been shown to inactivate this class of compounds.[48]

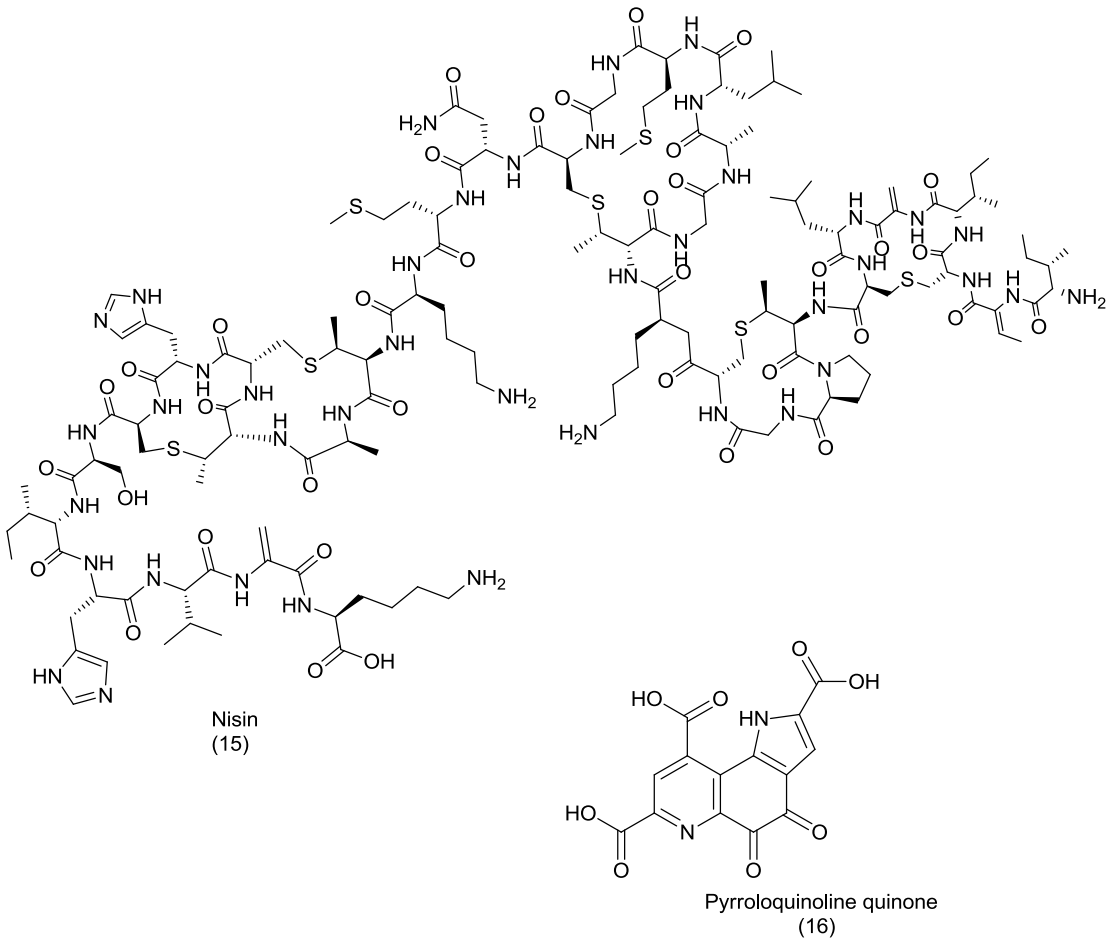

Figure 8.Structures of some ribosomal natural products.

One common feature of ribosomally synthesized peptides is proteolytic cleavage from precursor peptides. The primary site for proteolysis is the N-terminus of the peptide (Figure 9); however, pyrroloquinoline quinone (Figure 8) and cyanobactins are cases in which both N-terminal and C-terminal proteolytic cleavage occur.[49] Proteolysis has

been shown, in some cases to activate the peptide, and is in some cases tightly coupled to the ABC transport proteins for export from the cytoplasm.[50-55] Other documented types of main-chain modification of ribosomal peptides are macrocyclization, formylation, lactone formation, addition of a nucleotide base and glycosylation.[56-60]

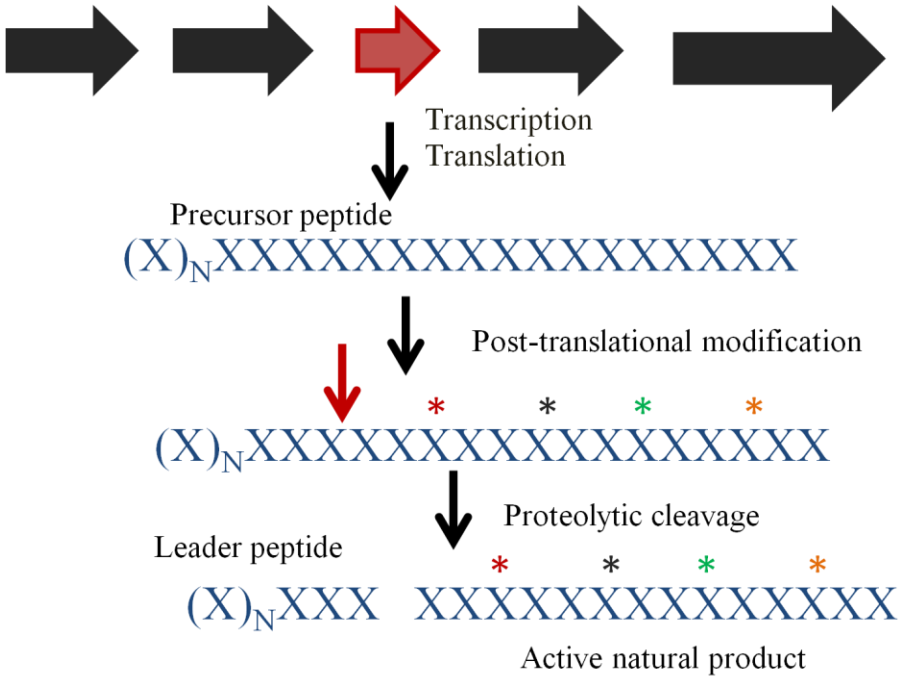

Figure 9.Generic steps in bacterial ribosomal peptide biosynthesis.

NON-RIBOSOMAL PEPTIDES (NRP)

Bacteria and fungi use large multifunctional enzymes to produce peptide natural products of diverse structure and broad biological activity. The large multifunctional enzymes involved in the biosynthesis of non-ribosomal peptides are called Non-Ribosomal Peptide Synthetases (NRPS). Unlike the ribosomal peptides, the non-ribosomal peptides are produced independent of messenger RNA (mRNA) and the

ribosomal machinery. Although similarities exist between the ribosomally and non-ribosomally derived peptide natural products, there are differences in the architecture and the pool of over 500-building blocks available to NRPSs.[61] A number of NRPs contain non-proteinogenic amino acid residues and other molecules like fatty and α-hydroxyl acids that are not usually found in ribosomally synthesized natural products.[62-64] The structural diversity provided by the large pool of precursors contributes to the broad clinical application of NRP natural products.

In terms of the arrangement of the catalytic domains, NRPSs differ remarkably from ribosomal peptide systems but resemble the type I fatty acid system. Individual catalytic domains are stitched together into modules that are responsible for incorporation of the building blocks into the growing polypeptide chain.[65] The core components of a module are the adenylation (A), peptidyl carrier protein (PCP or T), and condensation (C), domains except for the initiation module, which lacks a C-domain. In addition to the core domains, there exists a number of tailoring enzymes that aid in the maturation of the NRP product.

The selection of the building blocks to be added to the NRPS system is similar to the ribosomal synthesis of protein. In the same way that the amino acid t-RNA (aa-tRNA) synthetase charges the amino acid residue to be incorporated into the growing peptide chain, the adenylation of an amino acid or other substrate activates it for incorporation into the growing chain. These enzymes are structurally unrelated despite the similarity in the enzymatic activities of the A-domain of NRPS and aa-tRNA synthetase.[66] Activated amino acid is transported to the PCP domain, where it gets

covalently tethered to the phophopantetheinyl cofactor as a thioester.[67] The thioester acts like a flexible arm that allows the movement of the bound amino acyl and peptidyl substrates between different catalytic centers. The condensation domains are responsible for the formation of the peptide bonds between the PCP-bound amino acyl substrates of adjacent modules.[68] Occasionally, the modules contain tailoring domains: for example formylation (F), oxidation (O), reduction (Red), N-methylation (NMT), epimerization (E) and cyclization (Cy). The synthesis of NRP is a highly controlled process that starts with substrate-specific activation and incorporation that is dictated by the NRPS template. The termination of the synthesis occurs in an ordered sequence and is signaled by the presence of a thioesterase domain (TE) in the termination module. Figure 10 Illustrates the arrangement of NRPS modules in the biosynthesis of surfactin A. Surfactin A synthetase is made up of seven modules, each of which contains the core domains C, A and T. Modules 3 and 6 contain an epimerization domain each, and the terminal module 7 contains a TE domain that carries out the cyclization and release of the natural product. Because fungi often use a single NRPS for natural product biosynthesis, these multifunctional enzymes can reach a staggering size. *Tolypocladium niveum* uses a single NRPS of about 1.6 MDa, which contains 11 modules for the synthesis of cyclosporine A (Figure 11), an immunosuppressant used in the prevention and treatment of graft-versus-host reactions in bone-marrow transplantation and in prevention of rejection of kidney, heart and liver after transplants.[69]

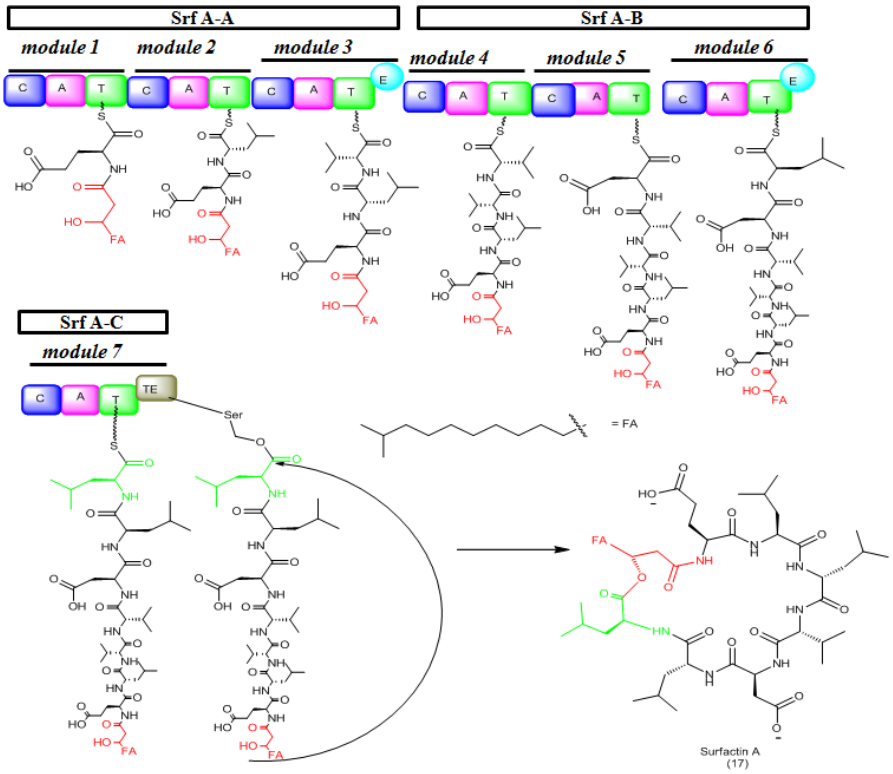

Figure 10.Illustration of surfactin A biosynthesis.

In bacteria, the modules are usually organized into operons, which may contain as much as eight modules. An example is the syringomycin synthetase E, produced by *Pseudomonas syringae*. It is one of the largest know bacterial NRPS and produces syringomycin E (Figure 11), an antifungal cyclic lipodepsinonapeptide that inhibits growth of *Sacchromyces cerevisiae*.[70] During the early days of NRPS research, the dogma of the colinearity rule (the notion that the sequence of an NRP directly reflects the linear arrangement of the modules and domains in the enzyme) was believed to be

the strategy for controlling natural product biosynthesis in this system.[71-73] NRPSs that follow this rule are classified as type A or linear systems.

Recent characterizations of NRPS systems have shown that the colinearity rule does not apply to all NRPSs. For instance, the cyclic lipoheptapeptide surfactin (Figure 10) is synthesized following this rule;[74] however, the colinearity rule falls apart when applied to the gramicidin S (Figure 11) synthetases GrsA and GrsB.[75-76] GrsA contains one module and incorporates one amino acid, whereas GrsB contains four modules that

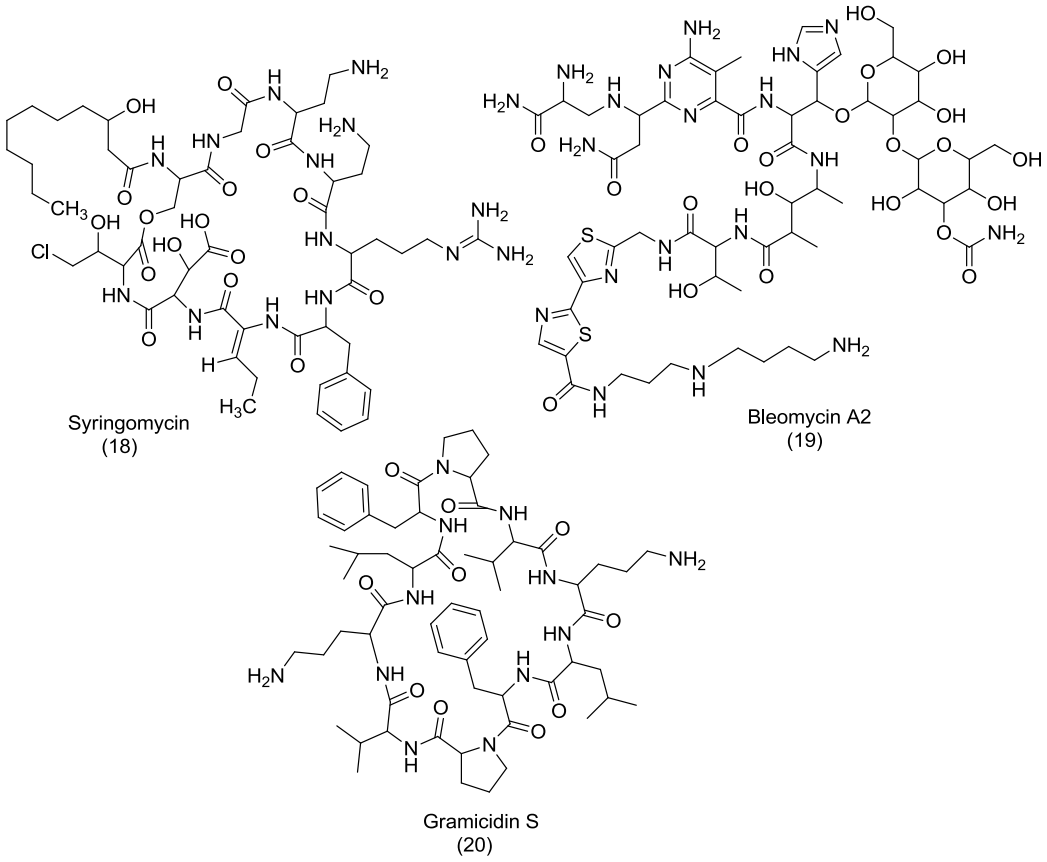

Figure 11.Some natural products of NRPS origin.

activate and load five amino acids into the natural product. This type of NRPS is used repeatedly or iteratively and classified as type B or iterative NRPS.[73] The third class, type C (non-linear) of the NRPS system is more complicated and deviates from the classical (C-A-T) arrangement of modules.[73] Bleomycin A2 (Figure 11) synthetase, BlmIII, has a modular arrangement containing A-PCP-Ox in place of the classical C-A-PCP arrangement.[77]

The knowledge of the preceding types of NRPS systems has been useful in predicting the arrangement of modules and domain in the NRPS templates. However, nonfunctional domains cannot easily be predicted based on the primary sequence of the natural product.[78] The biosynthetic logic of NRPSs with unusual domain architecture cannot easily be explained by the sequence of the natural product. This makes biochemical characterization imperative for better understanding of the logic of these unusual enzymes.

TERPENES AND ALKALOIDS

Terpenes

Terpenes are natural products that are built up from isoprene subunits. They are widespread in nature and are the main constituents of plant essential oils. The name originated from turpentine, the so called “resin of pine trees” that flows upon cutting or carving the bark of pine trees. Many terpenes are hydrocarbons but may also exist as terpenoids containing alcohols, aldehydes, ketones, carboxylic acids, ethers, esters or glycosides as functional groups. Plants produce different volatile terpenes to attract

specific insects for pollination or to repel certain animals that could eat these plants.[79] There are other terpenes that play roles in growth regulation in plants.[79]

Terpenes are classified based on the number of isoprene units $(C)_n$, called the isoprene rule. Hemiterpenes contain single isoprene unit (isovaleric acid, prenol), monoterpenes contain 10-carbon (citral, geraniol, camphor, limonene, menthol), diterpenes contain 20-carbons (taxols, retinal, retinol, phytol), sestererpenes contain 25-carbons (geranylfarnesol), triterpenes contain 30-carbons (squalene, lanosterol), tetraterpenes contain 40-carbons (carotenes). Polyterpenes are made up of many units of isoprene, an example of which is rubber.[80] Isoprene units may be joined head-to-tail or tail-to-tail to form linear chains or re-arranged to form ring compounds.[81] The reactive isoprene units are isopentenyl pyrophosphate/diphosphate (IPP) and dimethylallyl pyrophosphate (DMAPP). There are two possible routes to the formation of IPP, namely the mevalonate and the non mevalonate pathways. Three molecules of acetyl-coenzyme A (CoA) are used in mevalonate pathway to form IPP, and this pathway occurs in mammals and yeasts.[81] Two acetyl-CoA molecules are initially combined in a Claisen condensation to give acetoacetyl-CoA, and the last molecule is incorporated by stereospecific aldol addition to produce 3-hydroxy-3-methylglutaryl-CoA (HMG-CoA). HMG-CoA undergoes dehydration, reduction, decarboxylation and phosphorylation to form IPP.[81] Figure 12 illustrates the biosynthesis of IPP via the mevalonate pathway.

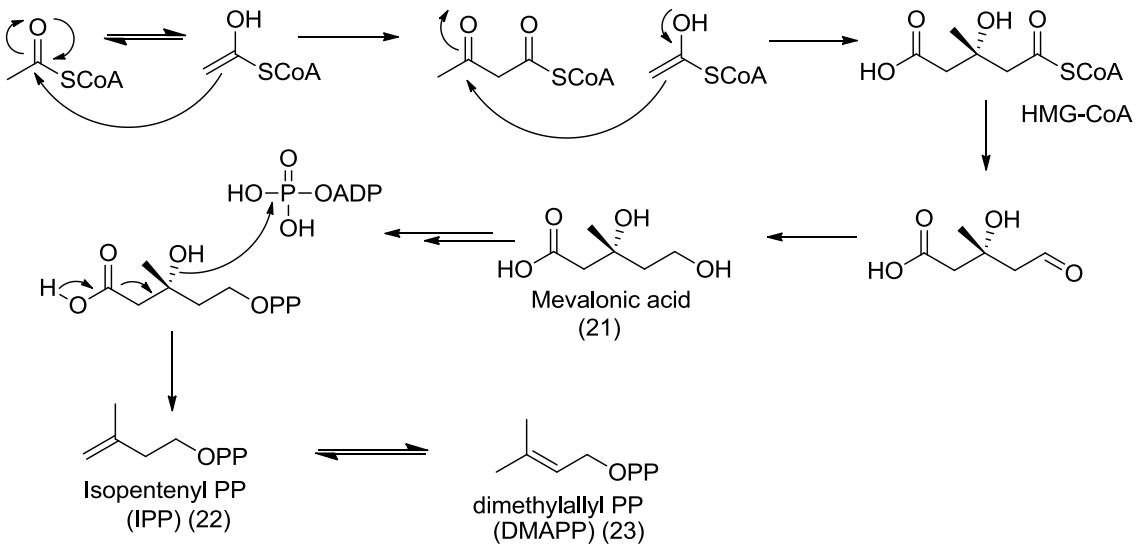

Figure 12.Mevalonate biosynthesis pathway of isopentenyl pyrophosphate (IPP).

The non-mavelonate or mavelonate-independent pathway to the biosynthesis of IPP starts with a thymine pyrophosphate (TPP)–mediated condensation of one unit of pyruvic acid and one unit of glyceraldehyde-3-phosphate to give 1-deoxy-D-xylulose 5-phosphate. This intermediate undergoes several rearrangement and reduction steps to produce IPP.[82] The deoxy-xylulose phosphate pathway to IPP is illustrated in Figure 13. Head-to-tail condensation of IPP and DMAPP (Figure 14) leads to the formation of geranyl pyrophosphate (GPP). Condensation of IPP and DMAPP is catalyzed by farnesyl diphosphate synthase which can also catalyze the addition of isoprene units unto GPP to produce up to sesterterpenes, C_{25}.[83] Triterpenes (C_{30}), however, are not produced by the addition of IPP to the growing chain. Two molecules of farnesyl pyrophosphate are instead joined tail-to-tail to yield a squalene, an example of a triterpene (Figure 15).

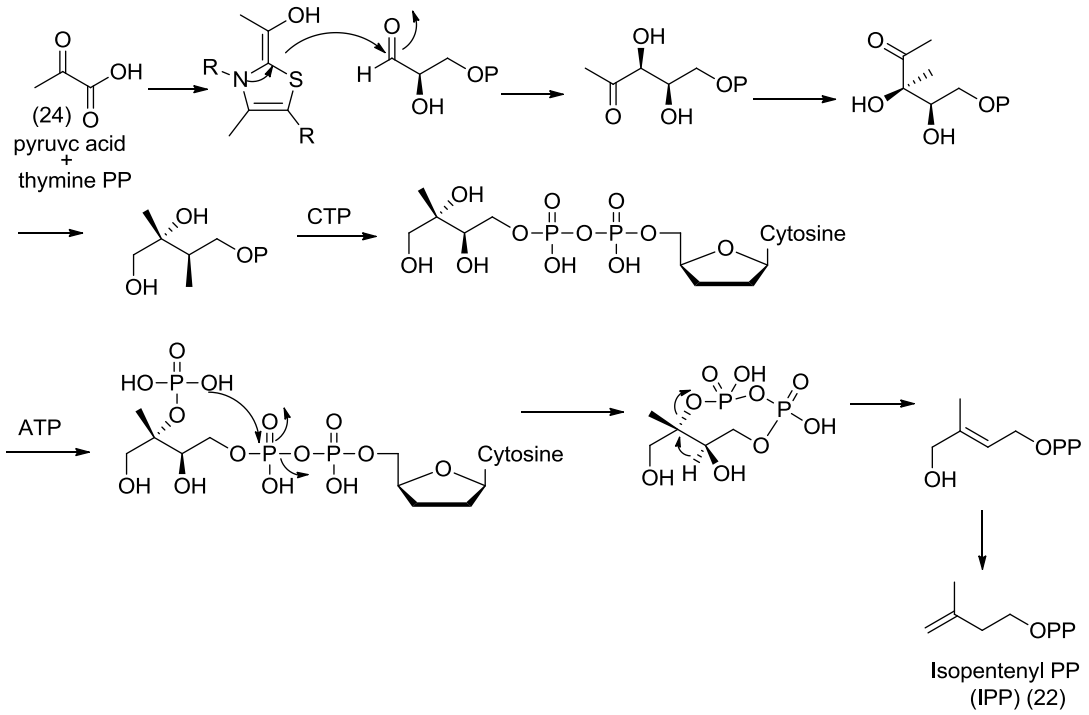

Figure 13.The deoxy-xylulose phosphate pathway for IPP.

Carotenoids

Carotenoids are an important class of terpenoids because they play a significant role in energy-transfer process such as photosynthesis. They are formed by the tail-to-tail coupling of two molecules of geranylgeranyl diphosphate (GGPP). Lycopene (Figure 16), one example of carotenoid, is a class of anti-oxidant that acts by scavenging free radical species within the human body.[84] Lycopene is 100 times more effective in quenching singlet-oxygen species than vitamin E (Figure 16).[85] It is an intermediate in the biosynthesis of β-carotene (Figure 16), a precursor to vitamin A.

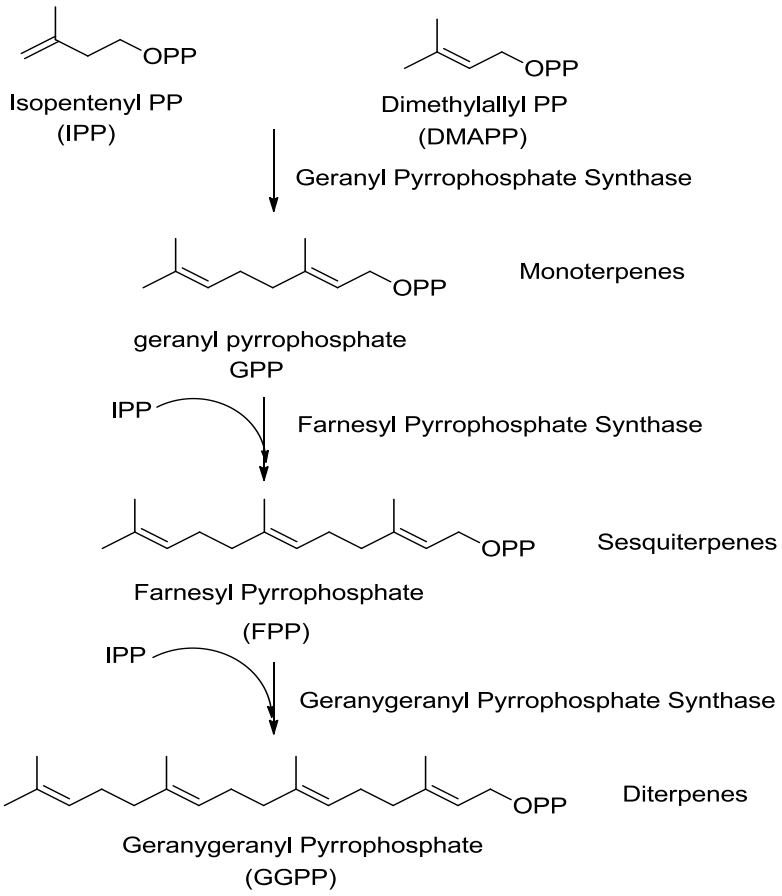

Figure 14.Condensation of IPP and DMAPP.

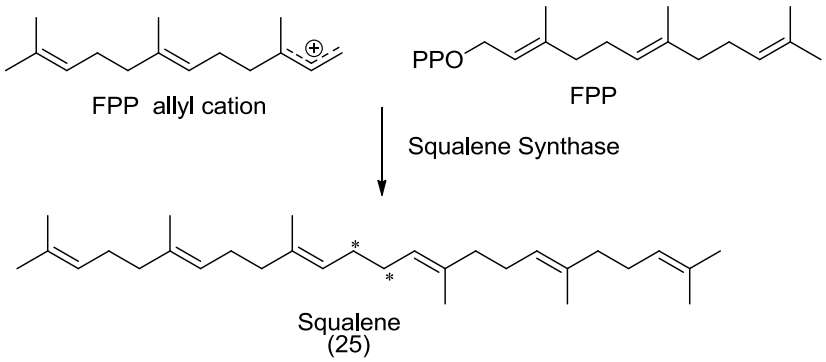

Figure 15. Tail-to-tail condensation of FPP in squalene biosynthesis.

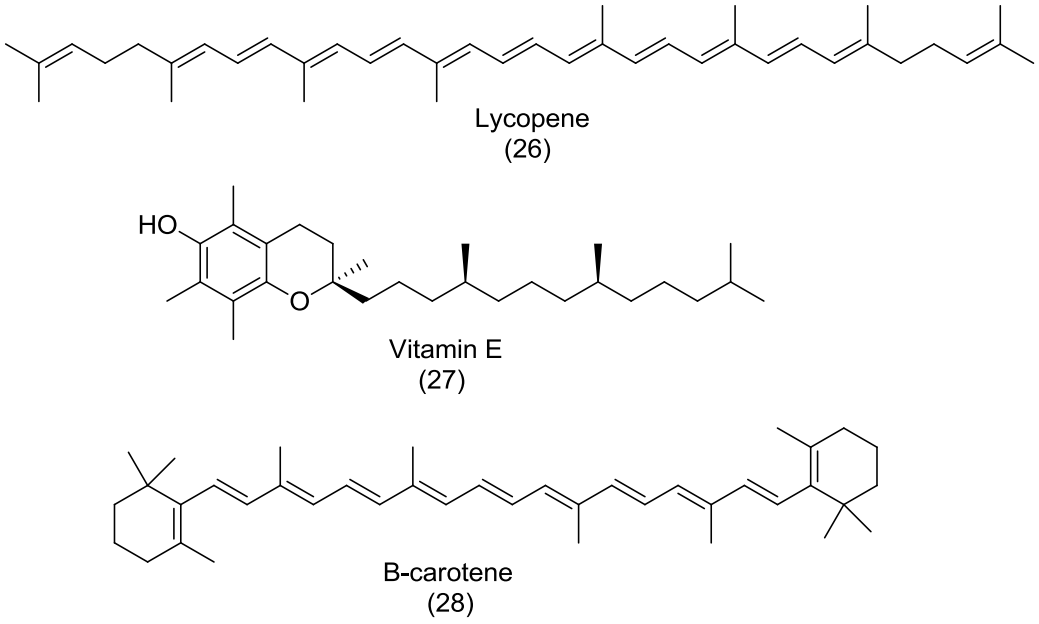

Figure 16.Structures of carotenoids, lycopene, vitamin E and β-carotene.

β-carotene can be enzymatically cleaved by the β-carotene 15,15'-monoxygenase to form two molecules of retinal (Figure 17).[86-88] The reduction of

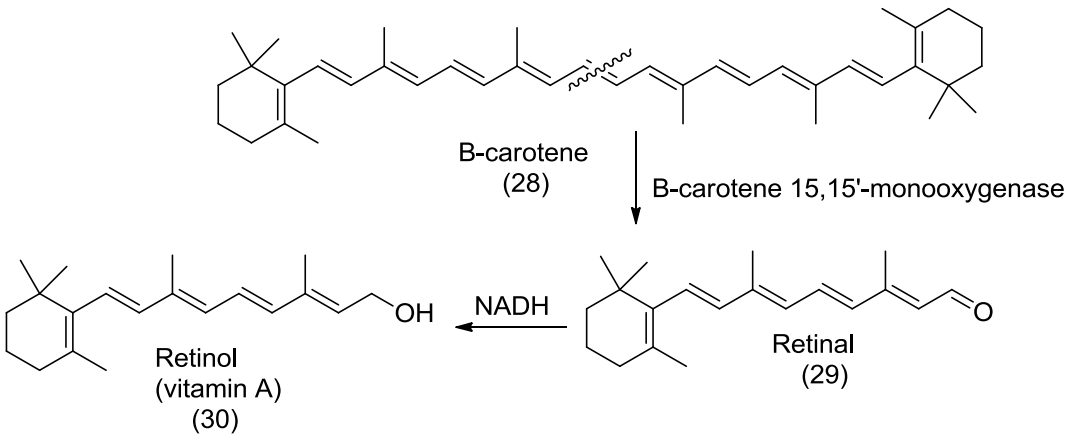

Figure 17.Enzymatic cleavage of β-carotene to retinal and conversion to retinol.

retinal, produces retinol commonly known as vitamin A, which plays a key role in signal transduction in the vision cycle (Figure 18).[89] Some of the vision cycle intermediates, such as all-trans-retinal (ATR) has been shown to accumulate in the rod outer segment (ROS) of the human eye. The incomplete digestion of the ROS by the retinal pigment epithelium (RPE) results in autoflourescent by-products known as lipofuscins. These lipofuscin have been implicated in a disease state known as age-related macular degeneration, a leading cause of blindness in people over 60-years of age.[90]

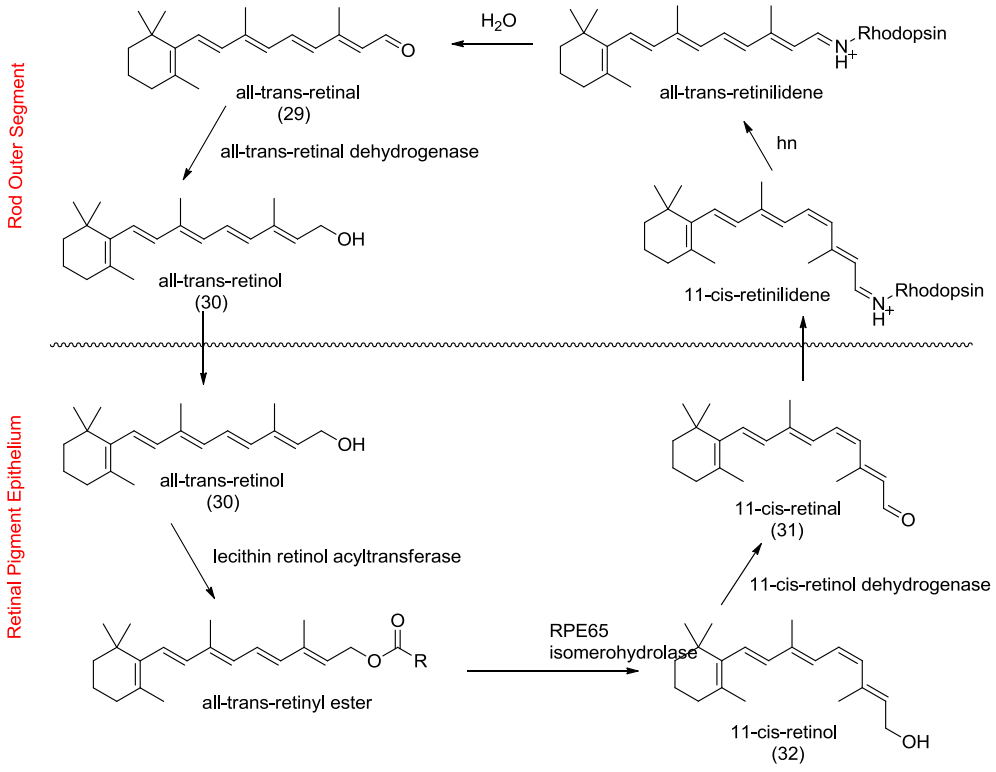

Figure 18.Human vision cycle.

COMBINATORIAL CHEMISTRY & ENGINEERING OF SECONDARY METABOLIC PATHWAYS

Nature has a vast collection of chemists in the form of microorganisms harboring millions of specific pathways to produce a wide variety of chemicals. The synthetic chemists have contributed significantly in crafting pathways for making some of these important compounds in the laboratory. In spite of the advances in synthesis of bioactive compounds, disease conditions continue to exert a substantial pressure on mankind to bolster the lean resources to combat all these diseases. Combinatorial chemistry was introduced to increase the number of different but structurally related molecules that could be synthesized in the same reaction steps. The field of combinatorial chemistry reached an advanced stage early in 1980s.[91] This was marked by a shift from extraction of compounds from natural sources to synthesis of large libraries of compounds. The advances in the use of nuclear magnetic resonance (NMR) spectroscopy for characterization of natural products was an impetus to combinatorial chemistry w,hich in turn became the mainstream tool of drug discovery.[92] This new method of synthesis of pools of chemical compounds necessitated the improvement in purification and screening methods. The labor and time requirements that could have been a major set-back for combinatorial chemistry were overcome by the use of powerful computer simulation for combinatorial synthesis and subsequent high-throughput screens based on molecular targets.

Although combinatorial chemistry has succeeded as a method for optimizing structures that were recently approved as therapeutic agents by the FDA, only one de

novo combinatorial compound has been approved in the last 30-years.[2] Sorafenib (Nexavar), a multikinase inhibitor, was developed by Bayer and approved by the FDA for the treatment of renal cell and hepatocellular carcinoma.[2] One major limitation of combinatorial chemistry is that it is not particularly effective as a de novo drug discovery tool; however, the capability for structural optimization is tremendous once an active natural product skeleton is discovered.[93]

Total synthesis of complex natural products, although often successful for use as a model, has limited practical and economic value.[178] The dependence of the large-scale production of synthetic drugs on petroleum-derived precursors has also raised the issue of sustainability and environmental impact of hazardous chemical wastes generated by these methods. Human beings as adherents of Le Chatelier's principle have resorted to emerging methodologies and technologies in the production of important natural products.

The endogenous biosynthetic pathways in microbes are precise and efficient; less harmful waste is generated and the processes are in tune with the global order of "green environment". Combinatorial biosynthesis or metabolic engineering involves the rational manipulation of genes governing the secondary metabolic pathways in microorganisms to increase the structural diversity and activity of the new products.[94-96]

Gene clusters encoding many natural products (Figure 19) have been characterized and whole-genome sequencing, which has become increasingly fast and cheap has uncovered hundreds of cryptic or "orphan" secondary metabolic pathways.[97] This suggests that the potential for discovery of natural products is underestimated by

the number of natural products described to date. Rational manipulations by insertion, deletion or swaping of elements of biosynthetic gene clusters are possible, and they greatly increase the possibilities of new natural products.

The analysis of modular type I PKS has shown that the total number of modules determines the polyketide chain length before cyclization, whereas the catalytic domains contained in each modules control the level of oxidation of the polyketide.[98,99] Some of the achievements so far recorded in combinatorial biosynthesis include structural diversity in a polyketide system made by introducing a loading domain in the first module that could accept a wide range of starter units, such as 3-amino-5-hydroxybenzoic acid, isobutyryl CoA and 3, 4-dihydroxycyclohexanecarboxylic acid.[100] Ring-contraction of polyketides has been effected by movement of the terminal thioesterase to different modules of the PKS.[101,102] The analogues of parent polyketides have also been produced by deletion, insertion and switching of catalytic domains and modules.[103-105]

Successful combinatorial biosynthesis will not be possible if multi-modular enzymes cannot transfer the intermediate from the last module to the downstream module that will further tailor the intermediate. Docking-domain studies, which involves a computer-simulated replacement of specific residues and analysis of the activity of the engineered enzymes have helped in understanding the requirement for transfer of intermediates between unrelated modules.[106,107] Combinatorial biosynthesis in the polyketide system has had quite some difficulties to overcome, and developing high-

throughput combinatorial strategies with multi-modular enzymes still remains a challenge.

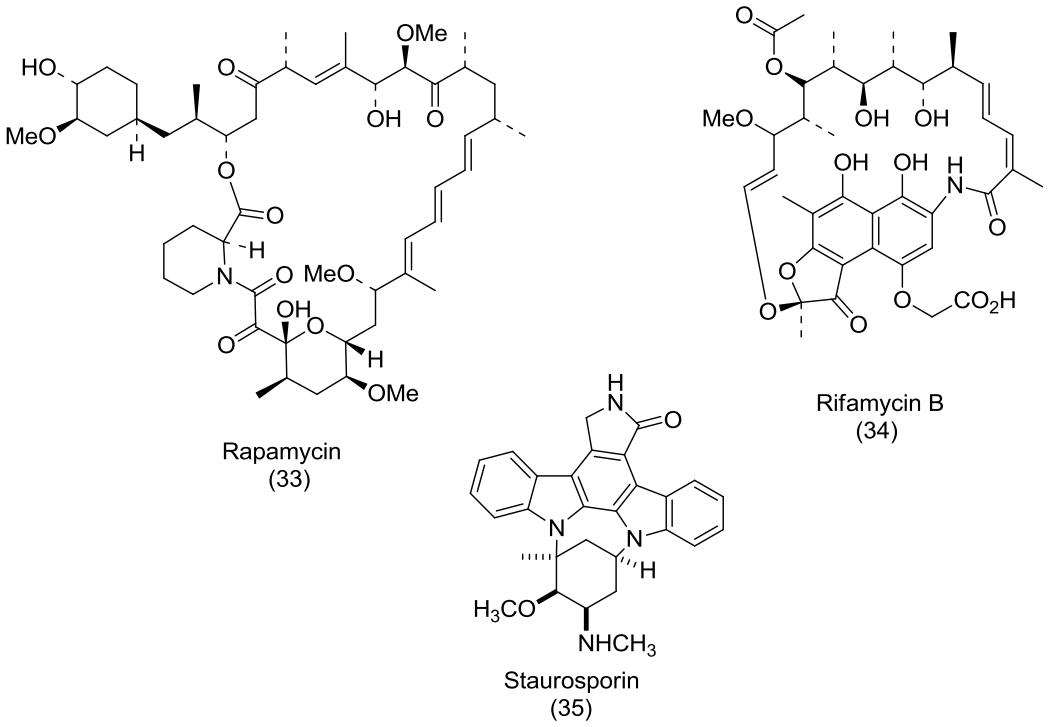

Figure 19. Structures of natural products whose gene clusters have been identified.

Many organisms producing natural products are understudied and introducing DNA into them is difficult. Some of these organisms are slow-growing, unculturable, or do not contain systems for regulated gene expression.[108-111] The multi-modular enzyme systems present even greater difficulties because of their extraordinarily large sizes (35 to > 200kb) and lack of conserved restriction sites to facilitate domain or module switches.[111]

A breakthrough in high–throughput combinatorial biosynthesis was achieved in the PKS gene set of the 6-deoxyerythronolide B synthase, DEBS (Figure 6). Fourteen modules from eight PKS clusters were synthesized with optimized codons for expression in *E.coli*, and they were shuffled into 154 bimodular combinations. Almost 50% of the combinations successfully mediated polyketide biosynthesis in *E.coli*.[112] What these findings suggest is that the inter-domain/module architecture should be understood for successful combinatorial biosynthesis involving domain or module switching. The design and inclusion of appropriate inter-module or domain linker sequences is crucial for transfer of modules between these units[109].

AZINOMYCIN B

Azinomycins B is a secondary metabolite first isolated from *S. sahachiroi* as carzinophlin A.[113] Three decades later azinomycin B, its analogue azinomycins A, and expoxamide (Figure 20) were isolated from S. *griseofuscus*.[114] With improvement in the purification methods and spectroscopic analysis, carzinophilin A was found to be the same compound as azinomycin B. Azinomycin B is of specific interest to the research community since it exhibits anticancer and antibacterial properties.[113-115] The anticancer activity is ascribed to the DNA cross linking effect arising from the aziridine and epoxide moieties of azinomycin B. It was initially concluded that since epoxamide lacked the 1-azabicyclo-[3.1.0] ring, the antibacterial and antitumor activities should be negligible. It was later found that epoxamide exhibited a strong cytotoxic effect [IC_{50} =

0.0036μg/mL] against P388 murine leukemia.[116] The antitumor activity was weak in an *in vivo* antitumor assay against P388 murine leukemia.

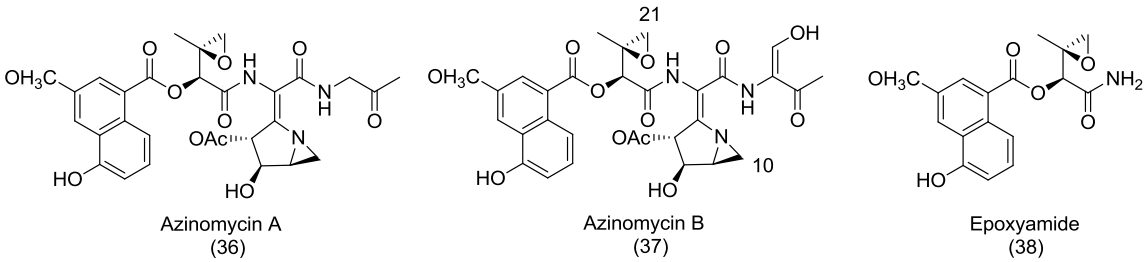

Figure 20.Structures of azinomycin A, azinomycin B and epoxamide.

In vitro studies have shown that aziomycin B forms inter-strand cross-links with DNA via the electrophilic C10 and C21 carbons of azinomycin and the N7 positions of suitably disposed purine bases (Figure 21).[117]

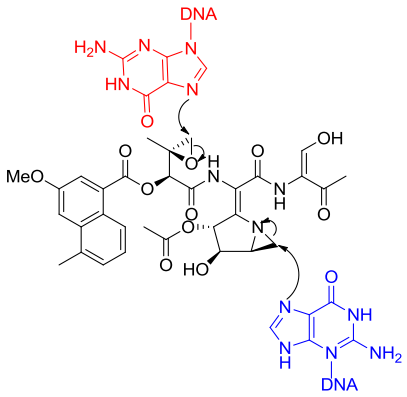

Figure 21.Azinomycin interaction with duplex DNA.

BIOSYNTHESIS OF AZINOMYCIN B

The biosynthesis of azinomycins is of utmost importance to the science community because of its unique architecture. It contains the azabicyclo [3.1.0] hexane ring and is one of the few compounds (Figure 22) containing the three member nitrogen heterocycle (aziridine ring). The biosynthetic gene clusters of azinomycin B, mitomycin C, azicemicin A and maduropeptin have been discovered but the biosynthetic route to the azabicyclic ring has not been successfully established.[29,118-120] The biosynthetic reactions leading to the epoxide moiety of azinomycin B are also not well understood. The structures of azinomycins A and B are suggestive of hybrid PKS and NRPS biosynthetic origins. The naphthoate moiety of azinomycin B is analogous to that in neocarzinostatin, an anti-cancer compound with a gene cluster encoding an iterative type I PKS.[121]

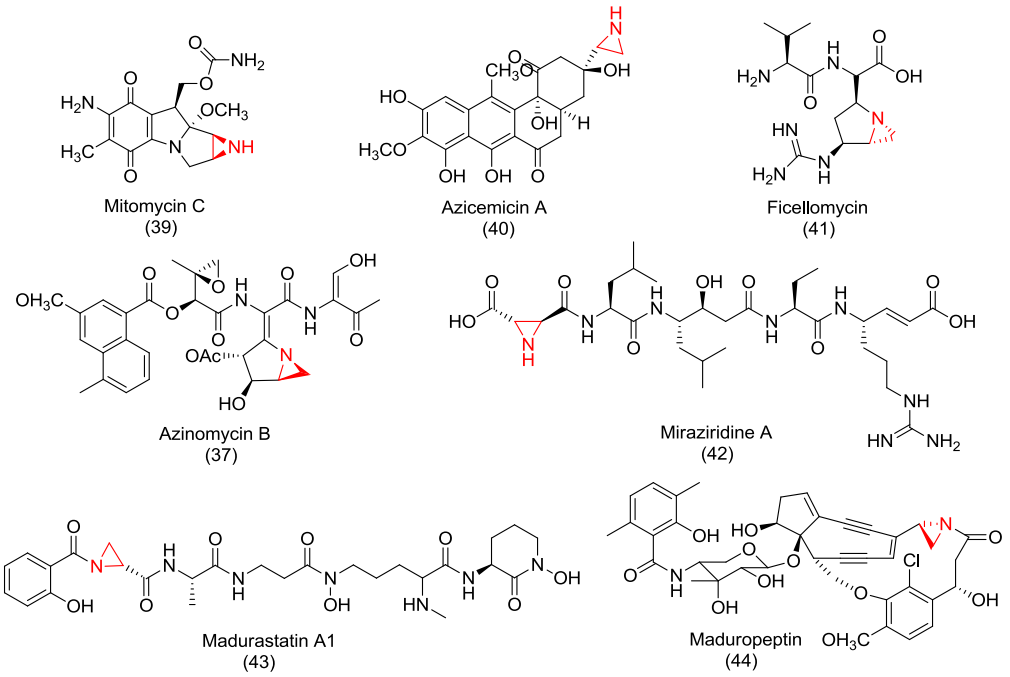

Figure 22.Structures of some aziridine-containing natural products.

A milestone in understanding of the precursor origin in azinomycin B biosynthesis has been reached through the use of isotopically-labeled precursors in fermentation cultures. Details of some of these studies and their results will be pointed out in later chapters.

STATEMENT OF PURPOSE

An overview of natural product biosynthesis has been presented in the introduction. Against this backdrop, the goals of this study are to identify the roles and to characterize the genes involved in the azinomycin biosynthesis so as to enhance future bioengineering effort and the design of a custom drug delivery system against cancer.

CHAPTER II

GENETIC DISRUPTION OF *ORF10*, A DEHYDROGENASE AND THE IMPACT ON AZINOMYCIN PRODUCTION

INTRODUCTION

Azinomycins (Figure 23) are antitumor agents that contain an epoxide moiety and an aziridino pyrrolidine (1-azabicyclo [3.1.0] hexane) ring system.[113,114] Although mitomycin C is already in use in cancer therapies, azinomycin B shows similar antitumor activities at much lower doses but has been limited by natural product availability.[115] *In vitro* studies have shown that these agents form interstand cross-links with DNA via the electrophilic C10 and C21 carbons of azinomycin and the N7 positions of suitably disposed purine bases.[121] Biosynthetic studies on the azinomycins were initially limited by difficulties with the fermentation system resulting in unreliable production of the natural products. Because this limitation persisted, a cell-free system was developed to study the *in vitro* biosynthesis of the azinomycins.[123]

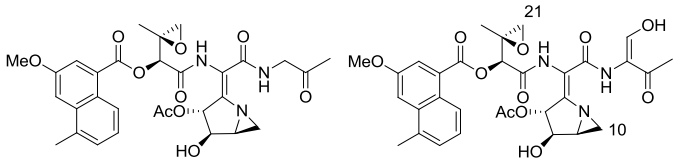

Figure 23.Structures of azinomycin A and B.

These investigations led to precursor assignments, [124] sequencing of the genome and the identification of the biosynthetic gene cluster in *S. sahachiroi* (Figure 24).[125, 126]

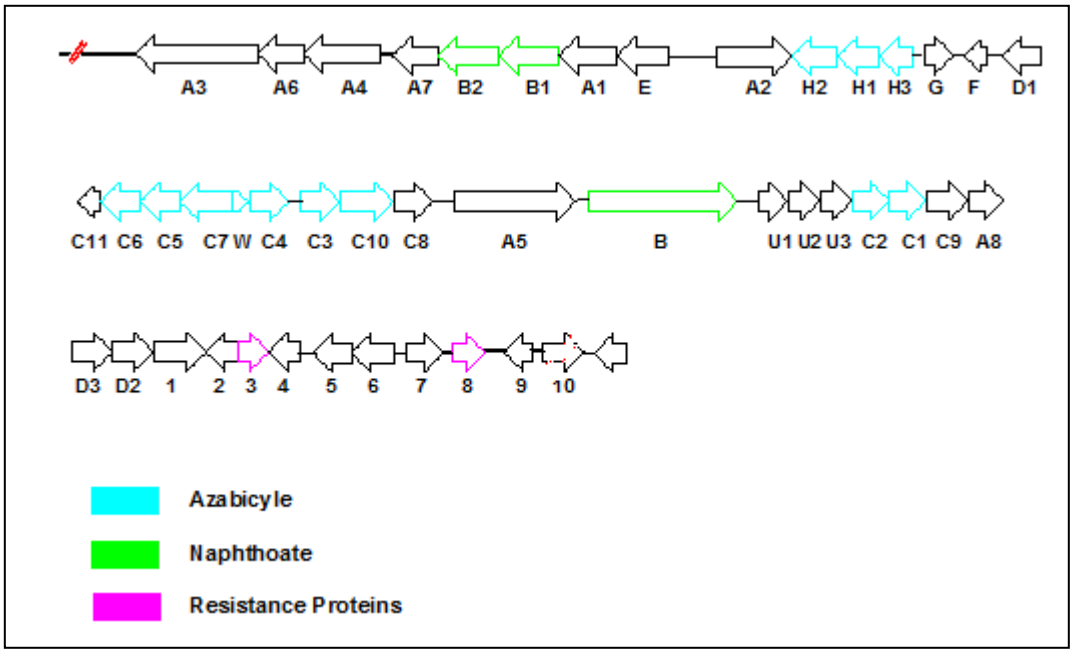

Figure 24. Revised azinomycin gene cluster.

The cell-free studies established L-Valine as the precursor in the formation of the epoxide moiety.[123]

Once we optimized our fermentation procedure, a feeding experiment with ^{13}C-labeled valine and several advanced precursors was conducted, and a biosynthetic route (Figure 25**)** to the formation of the epoxide moiety in the azinomycins was postulated based on these results.[125] The compound 3-methyl-2-oxobutenoate (Figure 25) is the most advanced precursor of valine that is found to be incorporated into the epoxide by feeding experiment.[125] However, the valine degradation pathway (Figure 26) suggests

that methylacryl-CoA (**51)**, an analogue of **48** could be further modified to 3-hydroxyisobutyrate (**52b)**, an analogue of **47** by the intervening enzymes. Apart from valine, most of these precursors appear to have be been derived from the valine degradation pathway. Based on the proximity of ORF10 to the gene cluster (Figure 24), we postulated that ORF10 might play a role in azinomycin biosynthesis. A BLAST search of ORF10 showed that it has ~ 60 % sequence identity to 3-hydroxyisobutyric acid dehydrogenase from *E.coli* (Appendix). The conversion of compound **52b** to **53** is thought to represent a shunt system that reduces the valine intermediate flux towards azinomycin production.

The blockage of shunt pathways to natural products or other metabolite production is routinely used to increase the titer of the natural products or metabolites.[127] This chapter explores the use gene disruption of ORF10 to evaluate its role in azinomycin biosynthesis. Disruption of 3-hydroxyisobutyric acid dehydrogenase is expected to lead to the accumulation of compound **52b**, thereby increasing the flux towards azinomycin formation. The disruption could also clearly define the end of the azinomycin biosynthetic gene cluster.

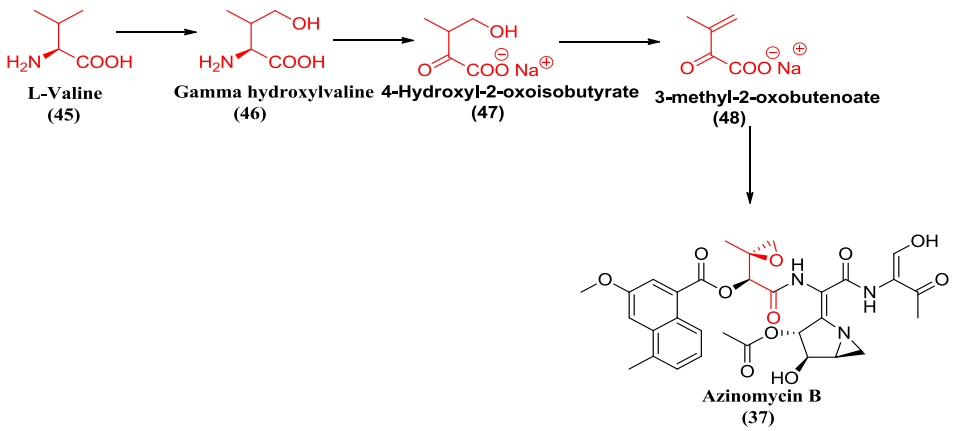

Figure 25.Biosynthetic route to the epoxide moiety in the azinomycins.

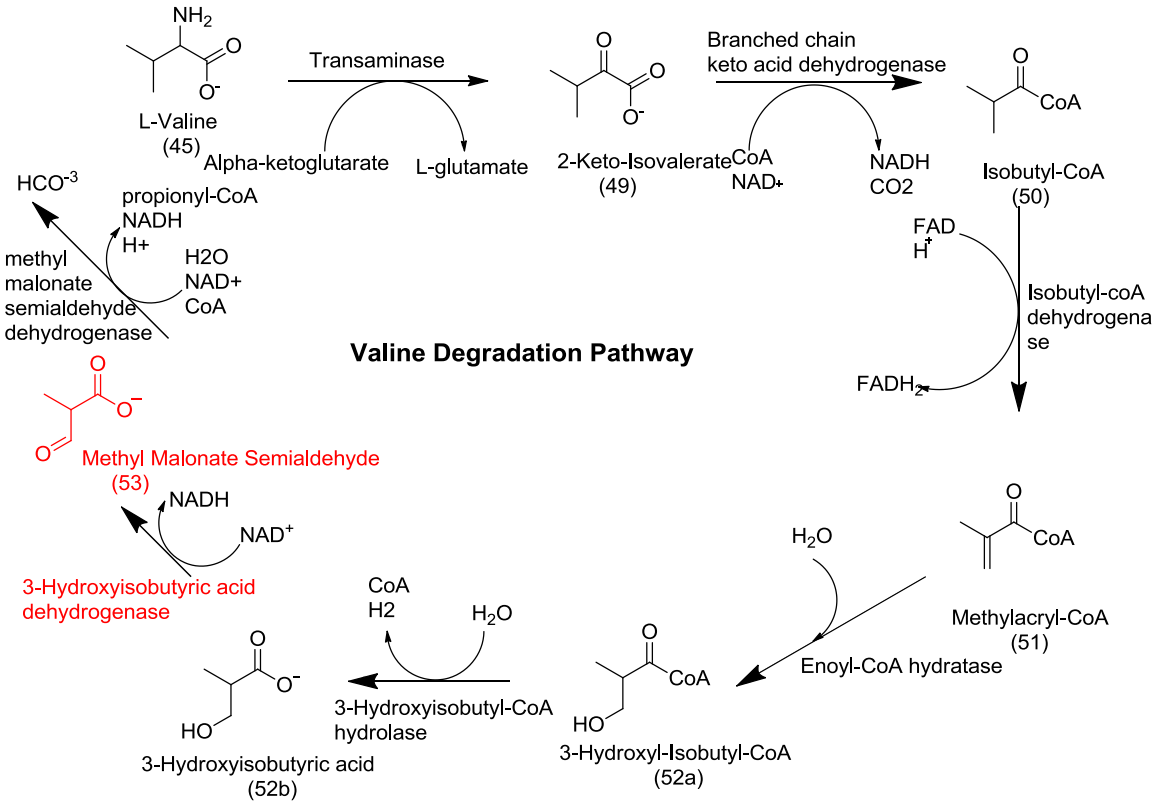

Figure 26.Valine degradation pathway.

MATERIALS AND METHODS

Unless otherwise specified, biochemical reagents were purchased from Sigma (St. Louis, MO). Oligonucleotide primers were ordered from Integrated DNA Technologies (Idtdna), USA, and PCR kit (Phusion DNA polymerase, buffer, dNTPs, DMSO), all enzymes and regular DNA ladders were obtained from NEB (Ipswich, MA). All PCR was carried out with PTC-200 Peltier Thermal cycler by MJ Research (Waltham, MA). All other media, reagents, glassware, petri dishes, dichloromethane and dimethyl sulfoxide (DMSO) were purchased from VWR International (West Chester, PA). DNA miniprep (QIAprep) and Gel extraction (QIAquick) kits were purchased from Qiagen (Valencia, CA). Oligonucleotide primers, plasmids, and bacterial strains used in this study are summarized in Table 1. Reverse-phase high performance liquid chromatography (RP-HPLC) separations were conducted on a Waters 600 Controller equipped with Waters 2487 dual λ absorbance detector (Milford, MA) by using a Phenomenex Prodigy 5μ C8 (250 x 4.6 mm) column (Torrance, CA). ^{1}H NMR spectra were recorded on a Varian Inova 300 (Chemistry Dept., Texas A&M University). ^{1}H NMR chemical shifts are reported as δ values in ppm relative to $CDCl_3$ (7.26 ppm) and coupling constants (*J*) are reported in Hertz (Hz).

Radioactive labeled adenosine triphosphate (^{32}P ATP) was purchased from Perkin Elmer (Walthan, MA), and the 1Kb Plus DNA ladder used in Southern hybridization was obtained from Life Technologies (Carlsbad, CA).

Media Conditions

All components are per liter of deionized water and autoclaved before use. R2YE (Required Growth Factor added/Yeast Extract): Yeast extracts, 4 g; Bacto-peptone, 4 g; Bacto-tryptone, 2 g; Glucose, 10 g; Sucrose, 103 g; K_2SO_4, 0.25 g; $MgCl_2.6H_2O$, 10.12 g; Casaminoacids, 1g; 10 mL KH_2PO_4 (0.5%); 80 mL $CaCl_2.2H_2O$ (3.68 %); 15 mL L-proline (20 %); 2 mL *Trace element solution; 5 mL NaOH (1N); 25 mL Tris-HCl (1M, pH 7.5); adjust to pH 6.8 with HCl or NaOH. *Trace element solution contained the following components per liter: $ZnCl_2$, 40 mg; $FeCl_3$ •$6H_2O$, 200 mg; $CuCl_2$ •$2H_2O$, 10 mg; $MnCl_2$•$4H_2O$, 10 mg; $Na_2B_4O_7$• $10H_2O$, 10 mg; $(NH_4)_6Mo_7O_2$ • $4H_2O$, 10 mg; and deionized water.MS (Manntol/Soy): Mannitol, 20 g; Soy Flour, 20 g PS5 (Pharmamedia/Starch): Pharmamedia (yellow cotton seed flour), 5 g; Soluble Starch, 5 g, adjust pH to 7 prior to sterilization. LB (Luria-Bertani): Bacto-Peptone, 10 g; Yeast Extract, 5 g; Sodium Chloride, 5 g.

Cloning of the *ORF10* Disruption Cassette

Genomic DNA was isolated from *Streptomyces sahachiroi* cultured on R2YE for 2-days at 30 ^oC with shaking. The salting out method was used for DNA extraction, and the DNA used as template to amplify the 950 base pair regions flanking the target gene, Orf10. Primer pair Orf10-UP-F which has a *Hind*III restriction site and Orf10-UP-R containing an *Xba*I restriction site (Table1) was used in the amplification of the upstream region whereas Orf10-DS-F which contained an XbaI restriction site and Orf10-DS-R which contained an *EcoR*I restriction site were used in the amplification of the

downstream region. The selective marker gene, thiostrepton (TSR), was amplified from a plasmid, pRF, a gift from Rongfeng (Table 1) using the TSR primer pair containing XbaI restriction sites in both the forward and reverse direction. Amplification was achieved in each case using a cycling condition: 98^{o}C for 30 s followed by 29 iterative steps of 98 ^{o}C for 10 s, 63 ^{o}C for 20 s, 72 ^{o}C for 30 s and a final 72 ^{o}C for 10 mins. The PCR reaction mixtures were separated on a 1% agarose gel, and the desired bands were extracted from the agarose using a QIAquick Gel Extraction Kit. Purified PCR products were digested with appropriate enzymes and purified on a mini-column packed with Sephadex G50 (GE Healthcare, Uppsala, Sweden). An *E.coli–Streptomyces* shuttle vector, pKC1139, a gift from Rongfeng (Table 1) was digested with HindIII and XbaI, separated on a 1 % agarose gel, and purified using a QIAqick Kit. Digested upstream and pKC1139 fragments were ligated to produce the intermediate plasmid pKC1139-Orf10-1. pKC1139-Orf10-1 was digested with XbaI and EcoRI, and this fragment was ligated to the rear-arm fragment to generate the intermediate plasmid, pKC1139-Orf10-2. Finally, pKC1139-Orf10-2 was digested with XbaI and ligated to the TSR fragment to generate pKC-ORF10-KO. All the ligation steps above were followed by transformation of *E.coli* DH10B (Table 1) and transformants were spread on LB-agar plates containing 25 ug/mL apramycin and incubated at 37 ^{o}C for at least 13 hr to allow for selection of positive clones. Positive clones were identified by both restriction digestion and plasmid sequencing performed using ABI Big Dye Chemistry at the Gene Technology Laboratory, Texas A&M University.

Conjugal Transformation of Disruption Plasmid

One positive plasmid, pKC-ORF10-KO was transformed in *E.coli* S17-1 (Table 1), spread on LB-agar plates containing 25ug/mL apramycin and incubated at 37 ^{o}C for at least 13 hr. A solid state culture of *S. sahachiroi* MS-agar plate medium (mannitol 2 %; soy flour 2 %; bacto-agar 1.5 % in distilled water) was incubated at 28 ^{o}C for 5-days. The spores were scraped off the plate with a sterile scraper and suspended in 15 mL Falcon tubes containing 2xYT medium (1.6 % tryptone and 1 % yeast extract in distilled water) and sterile glass beads. The spores were vortexed for 1 min and filtered through sterile cotton followed by heat shock at 50 ^{o}C for 10 min. Spores were incubated with shaking at 37 ^{o}C for 3 hr, centrifuged to pellet the spores, and re-suspended in fresh 2xYT medium. The spores were centrifuged one more time and re-suspended in 4 mL of 2xYTmedium. The donor, *E. coli* S17-1, carrying the disruption construct (pKC-OR10-KO), was prepared according to standard *E. coli* competent cell preparation. Cells were grown overnight at 37 ^{o}C with shaking and used to subculture 5 mL LB medium in a 15 mL Falcon tube to an OD_{600}, of 0.4. The cells were centrifuged at 5000 rpm for 8 min and washed twice with 2xYT medium while maintaining the temperature at 4 ^{o}C. Finally, the cell pellet was resuspended in 2 mL of 2xYT medium, and 1 mL each of donor and recipient cells were mixed and plated on ISP4-agar medium supplemented with 10 mg/ml sterile magnesium chloride solution. After 18 hr of incubation at 28 ^{o}C, the plates were overlaid with 1 mL water containing 0.5 mg nalidixic acid and 1 mg apramycin. The *S. sahachiroi* exconjugants resulting from single crossover of the plasmid into the chromosome were first isolated after 5-days. Thiostrepton-resistant; but

apramycin-sensitive colonies derived from a second crossover were identified after 10 rounds of selection on MS-agar plates containing 50 μg/mL thiostrepton. ^{32}P-labeling of 1kb Plus DNA ladder was carried out according to the Life Technologies protocol using T4 DNA polymerase and the 500 bp DNA probe was generated by PCR. Unincorporated nucleotides were removed by purification using a Sephadex G-50 spin column. Correct replacement of ORF10 was checked by both PCR and Southern hybridization. For Southern hybridization, genomic DNA of both the wild-type and ORF10 disrupted *S.sahachiroi* were digested with *Pvu*II restriction enzyme. The digested DNA was concentrated by ethanol precipitation and separated on a 1% agarose gel. Hybridization, washing and detection were performed according to the protocol in Molecular Cloning, a Laboratory Handbook, Volume 1.[128]

Fermentation and Isolation of Metabolites

Fermentation of ΔORF10/*S.sah* and wild-type *S. sahachiroi* followed a three stage fermentation and extraction protocol.[125] The fermentation broth was extracted with ethyl acetate and the crude extract subjected to HPLC analysis. Each extract was dissolved in 50 % acetonitrile to a concentration of 1 mg/mL and passed through a 0.2 μm syringe filter. To each filtered solution, 10 μL was withdrawn and diluted ten times; 20 μL was finally drawn from each sample for RP-HPLC analysis. A linear gradient of acetonitrile and water (solvent A = acetonitrile; solvent B = water; 0-1 min 10 % A; 1-14 min 10 % A to 95 % A; 14-15 min 95 % A; 15-20 min 95 % A to 10 % A; 20-25 min 10 % A) was used to separate metabolites in a Phenomenex Prodigy 5μ C8 (250 x 4.6 mm)

column and a detector set at 254 nm and 320 nm. ^{1}H NMR was carried out using 20 mg/mL solution of each sample in $CDCl_3$.

RESULTS AND DISCUSSION

Generation of *ORF10* Deletion Mutant

A thiostrepton antibiotic marker was installed in place of ORF10, a dehydrogenase located downstream of azinomycin gene cluster. This was done by creating a gene disruption cassette and ligating into the *E.coli-Streptomyces* shuttle vector pKC1139. The resulting plasmid, pKC-ORF10-KO (Figure 27) contained sequences homologous to those flanking the ORF10 gene in addition to the selection marker gene, TSR. The pKC-ORF10-KO plasmid was first introduced into an *E.coli* donor strain, S17-1, and introduced into wild-type *S. sahachiroi* by conjugation. 10 rounds of selection (see methods) for the antibiotic TSR resistance resulted in isolation of clones that had lost the shuttle vector, pKC1139 (Figure 27). Figure 27 shows the strategy used to achieve ORF10 gene disruption by homologous recombination and MS agar plates showing positive colonies generated. Verification of the replacement of ORF10 was done by PCR method using two pairs of oligonucleotide primers that targeted two different genes. The first target is the TSR gene which is inserted into the chromosome in the disruptant and the second target is the ORF10 gene. When an ORF10 gene primer pair (ORF10-F+ORF10-R) was used for PCR, only the wild-type genomic DNA produced the expected 900bp PCR product. This showed that the ORF10 gene has been eliminated in the disruptants. However, when the TSR primer pair (TSR-F

and TSR-R) was used for PCR, the disruptants gave the expected 1105 bp PCR product, whereas the wild-type strain did not give any PCR product.

Table 1 Bacterial strains, plasmids and primers used in ORF10 study

Strains, plasmids or primers	Relevant characteristics or primer sequence	Reference or source
Strains		
S. sahachiroi	Wild type azinomycin A and B-producing strain	ATCC
E.coli DH10B	General cloning host	Epicentre
E.coli S17-1	Conjugative donor	Rongfeng*
ΔORF10/*S.sah*	*S.sahachiroi* lacking ORF10	This study
Plasmids		
pKC1139	*Streptomyces-E.coli* shuttle vector	Rongfeng
pKC-ORF10-KO	Gene disruption construct	This study
Primers		
TSR –F	GCGTCTAGATGATCAAGGCGAATACTTCATATG	This study
TSR -R	CGCTCTAGAATCACTGACGAATCGAGGTCGAG	This study
ORF10-UP-F	GTCAAGCTTGGACCCCGAGGGCAACGAGTTCG	This study
ORF10-UP-R	GCTTCTAGACCCTCCATGCTCGGAGAGTG	This study
ORF10-DS-F	CTGTCTAGACCGTGCGCGGCCACCCGACGTTC	This study
ORF10-DS-R	GACGAATTCAGGCCACAGGACACCGTCGCC	This study
ORF10-probe-F	CGGCCGGGCATAGGTAGCGTG	This study
ORF10-probe-R	ACTACTCTCAGAAGTACCCACACT	This study
ORF10-F	GCATGAACGAACAACAGAAC	This study
ORF10-R	GCGCGGTCCTCGGATGCTG	This study

* Johns Hopkins University

This confirmed the integration of TSR gene into the chromosome of *S. sahachiroi*. However; the site-specific integration of the TSR gene has to be established by Southern blotting. A 500 bp PCR fragment located upstream of the target gene was amplified using the primer pairs ORF10-probe-F and ORF10-probe-R (Table 1).This PCR probe as well as the 1 Kb Plus ladder DNA ladder was labeled with ^{32}P-ATP according to the Life Technologies protocol. The Southern hybridization strategy and

analysis (Figure 27) showed a strong contrast between the wild type and the ORF10-disrupted strains of *S. sahachiroi*. Site-specific replacement of ORF10 by the TSR gene was confirmed by the presence of 3.1 kb and 1.7 kb fragments in the wild-type and mutant DNA respectively.

Fermentation and Analysis of Metabolites

The spores of mutant and wild-type strains were spread on MS agar plates and incubated at 30^{o} C until brownish spores developed (usually 5 -7 days). Fermentation of the first and second starter cultures and third-stage fermentation under nutrient-starved condition were performed.[125] Extraction of the supernatant recovered an amorphous yellowish extract. The extract was divided into two equal parts, and one portion was used for further purification and the remainder was used as crude sample for HPLC analysis. *S. sahachiroi* produces azinomycin A and B, and purification of the extract selectively eliminates the amount of azinomycin A while increasing the percentage recovery of azinomycin B. Azinomycin B ^{1}H-NMR spectrum displays a signature doublet at about 13 ppm owing to the presence of the enol hydroxyl group derived from threonine.[125] ^{1}H-NMR analysis of purified product from both the wild-type and mutant strains showed the presence of the azinomycin B signature doublet at 13 ppm (Figure 29). This result indicates that the disruption of ORF10 has little or no effect on the production of Azinomycin B. Sample preparation and HPLC conditions were as described in the methods and materials section. Reverse phase HPLC profiles (Figure

30) of the extract from the mutant and wild-type strains are consistent with the ^{1}H-NMR results.

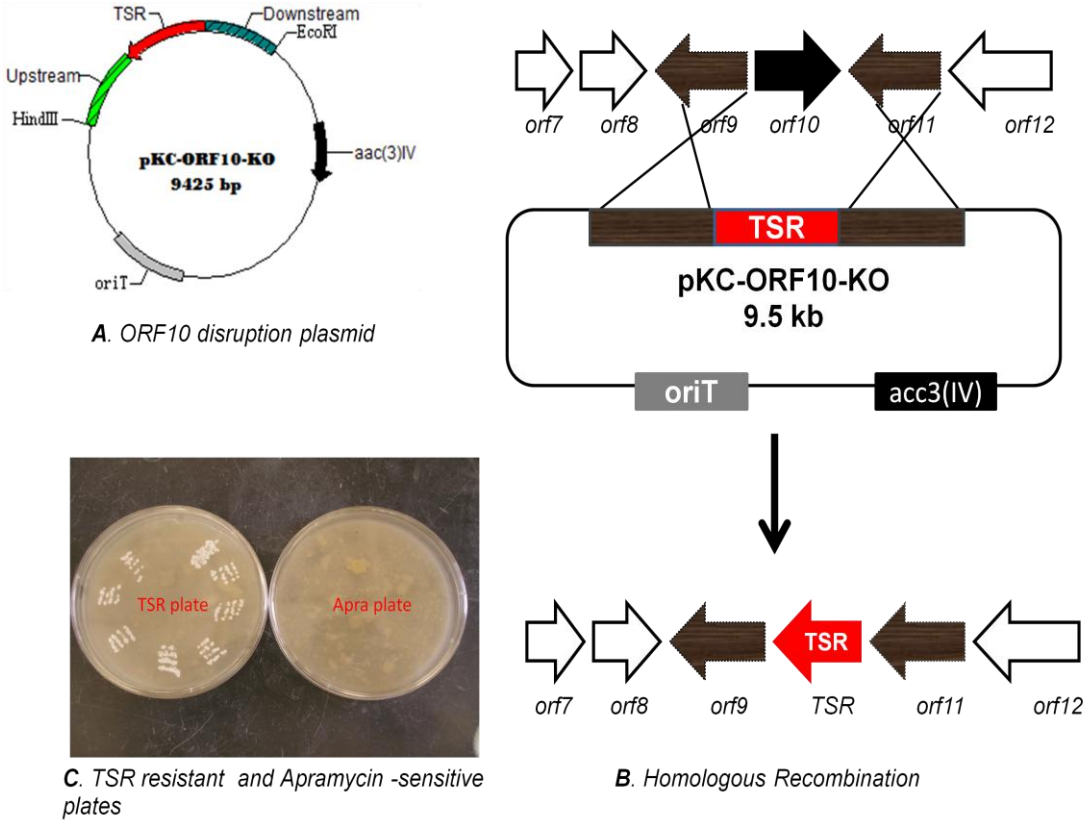

Figure 27. Gene disruption strategy for *ORF10*. (A) Gene disruption plasmid, pKC-ORF10-KO containing TSR gene and the flanking regions of target gene, ORF10. (B) Homologous recombination strategy. (C) MS-agar plates containing TSR and apramycin antibiotics establishing a double crossover event; mutant strains are resistant to TSR while sensitive to apramycin.

Differences in the metabolite profiles exist when extraction is performed with different solvents; however, the profiles are quite similar when wild-type and knockout strains are compared for the same solvent system. These results indicate that ORF10, a 4-hydroxyisobutric acid dehydrogenase homologue, is not directly involved in the

azinomycin biosynthetic pathway. It also shows that disruption of ORF10 does not lead to any substantial increase in azinomycin production. However, an apparent increase in azinomycin production could not be detected if the step involving the valine degradation

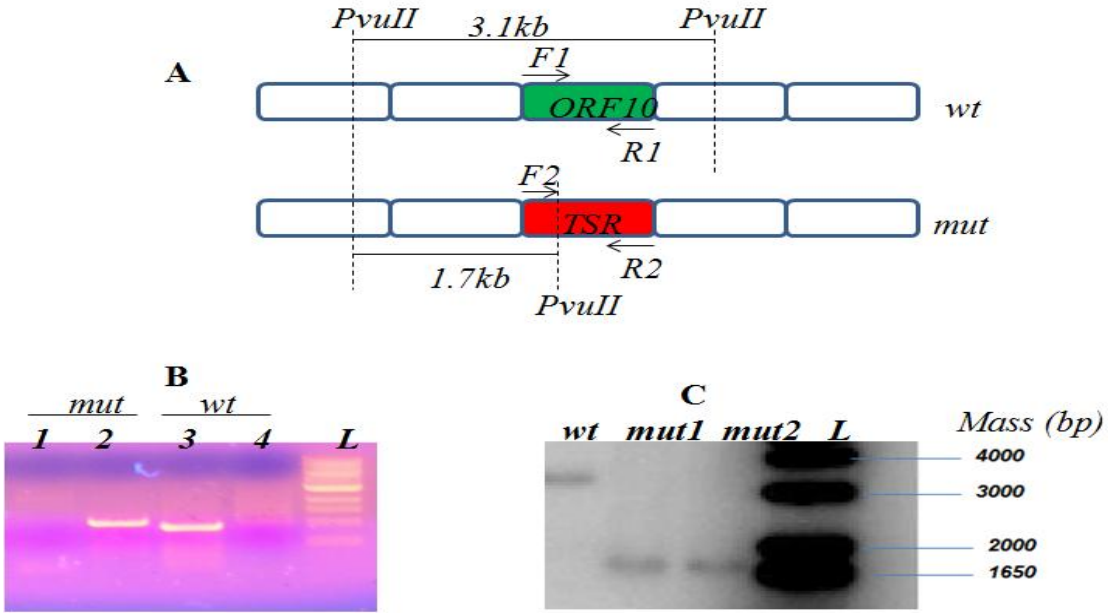

Figure 28.Confirmation of ORF10 gene disruption. (A) PCR and enzyme digestion strategies. (B) PCR using primer pairs F1&R1 (lane 1&3) and F2&R2 (lane 2&4). (C) Southern hybridization.

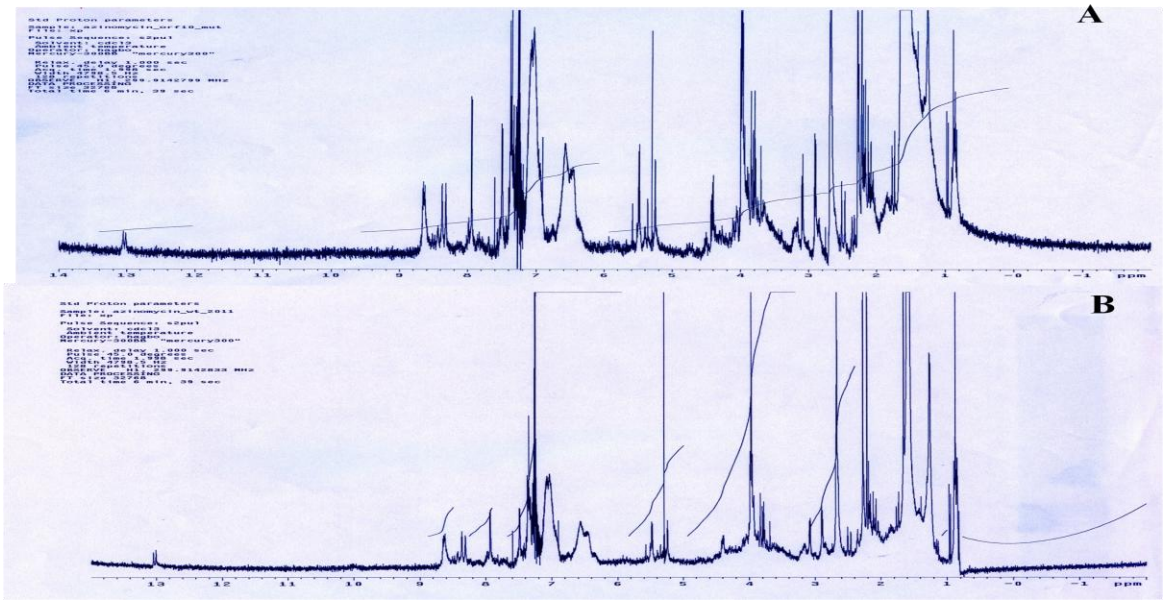

Figure 29.[1]H-NMR analysis of extracts from ORF10 disruptant (A) and wild-type (B) strains.

pathway intermediates is not rate-limiting in the biosynthesis of azinomycin. A minimal or no increase in azinomycin production would also be observed if even the incorporation of valine degradation products into the biosynthesis of azinomycin is rate-limiting but the intermediates (Figure 26) are being acted upon by other homologous enzymes of the valine degradation pathway. This finding also establishes the boundary of azinomycin biosynthetic gene cluster, which contains twelve open reading frames (orfs) at the end of the cluster. The promising results of work being done on putative azinomycin resistance genes by Felix Yu in our group, and this report demonstrates that Orf10 (with double strike) and the genes downstream, orf11 and orf12 (Figure 31) lie outside the gene cluster.

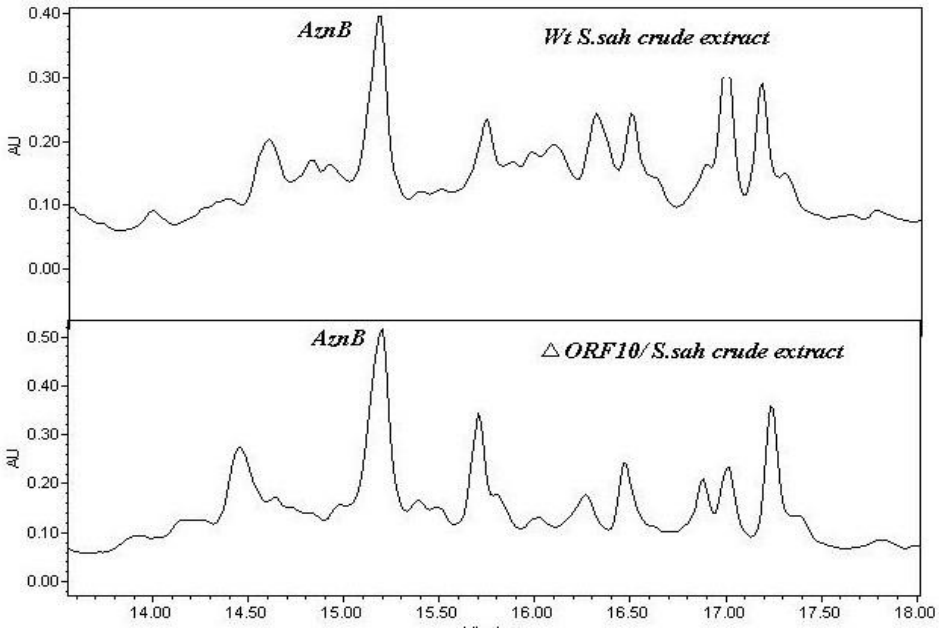

Figure 30.RP-HPLC analysis of *S.sahachiroi* wild-type and *ORF10* disruptant.

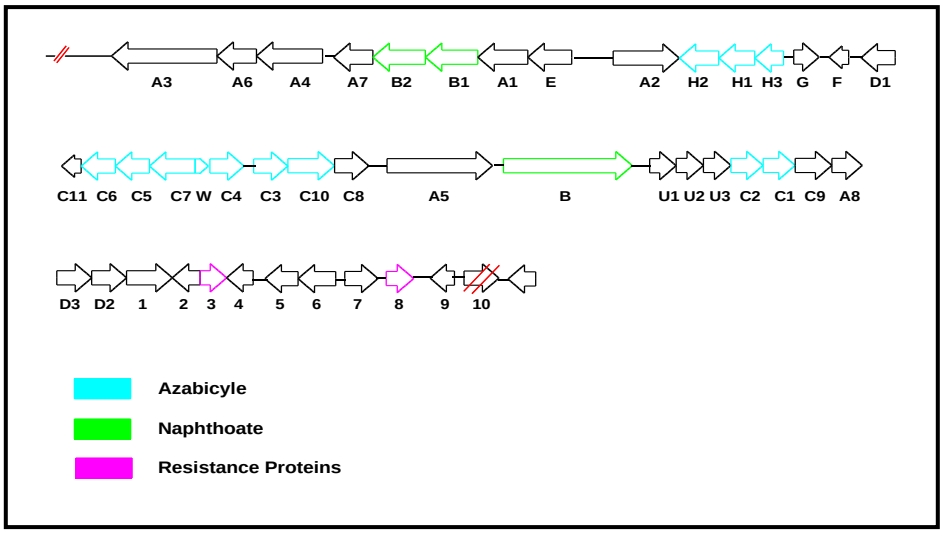

Figure 31.Revised azinomycin gene cluster showing boundary of the gene cluster.

CHAPTER III

PROBING THE ROLE OF *aziW*, A LYSINE BIOSYNTHETIC GENE (*lysW*) HOMOLOGUE IN AZINOMYCIN PRODUCTION

INTRODUCTION

The studies on azinomycin biosynthesis have continued to shed light on how nature stitched together this complex architectural structure. Feeding experiments with isotope-labeled precursors have shown that L-valine, L-threonine and L-glutamic acid are incorporated into azinomycin, whereas L-lysine is not.[123] L-valine is incorporated into the epoxide moiety and L-glutamic acid is incorporated into the azabicycle portion. L-threonine is found in the enol fragment of azinomycin B, which distinguishes azinomycin A from B (Figure 32). Based on the analysis of the draft genome sequence of *S. sahachiroi* by J. Foulke-Abel (Watanabe's group) and information gleaned from the azinomycin biosynthetic gene cluster,[29] a hypothetical path to the formation of the azibicyclic moiety using L-glutamic acid as a precursor was proposed (Figure 33). The enzymes involved in the proposed pathway have high sequence homology to those involved in bacterial lysine biosynthesis (Figure 34A) through the α-aminoadipic acid (AAA) pathway and arginine biosynthesis.[129] A putative open reading frame (ORF) that lies between *aziC7* and *aziC4* (Figure 34B) was discovered in the azinomycin gene cluster. This ORF had previously gone unnoticed in the azinomycin gene cluster. It encodes a protein of 59 amino acids that shows 46 % amino acid sequence identity to *lysW* from *T. thermophilus,* including four conserved cysteine residues and the C-

terminal EDWGE sequence.[130] The disruption of *lysW* in *T. thermophilus* resulted in lysine auxotrophy, and reconstitution of all the enzymes in Figure 32A except *lysW* was negative for lysine production.[130] This suggested that *lysW* is a critical enzyme in lysine biosynthesis in *T. thermophilus*.

Arginine biosynthesis in bacteria commonly starts with the protection of the α-amino group of glutamate by an acetyl group through a reaction catalyzed by N-acetylglutamate synthase, *argJ* (Figure 31).[131,132] This reaction produces N-acetylglutamate and avoids an undesirable cyclization to form Δ^1-pyroline-2-carboxylate (Figure 34).[130-132] *AziC2* is another gene in the azinomycin gene cluster; it is homologuous to *lysX* in *T. thermophilus*. *lysX* is involved in lysine biosynthesis in this organism. Recent experiments in our group showed that *aziC2* is capable of modifying both glutamate and α-amino adipic acid with an acetyl group (unpublished work by D. Simkhada, Watanabe's group). However, *lysX* encoded by *T. thermophilus* failed to catalyze the modification of α-amino adipic acid with an acetyl group.[128]

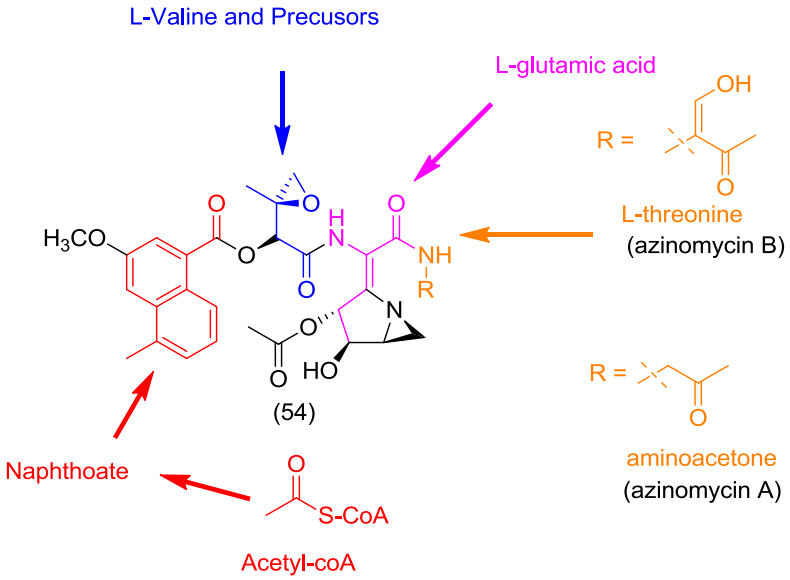

Figure 32. Some of the precursors that are incorporated into azinomycin.

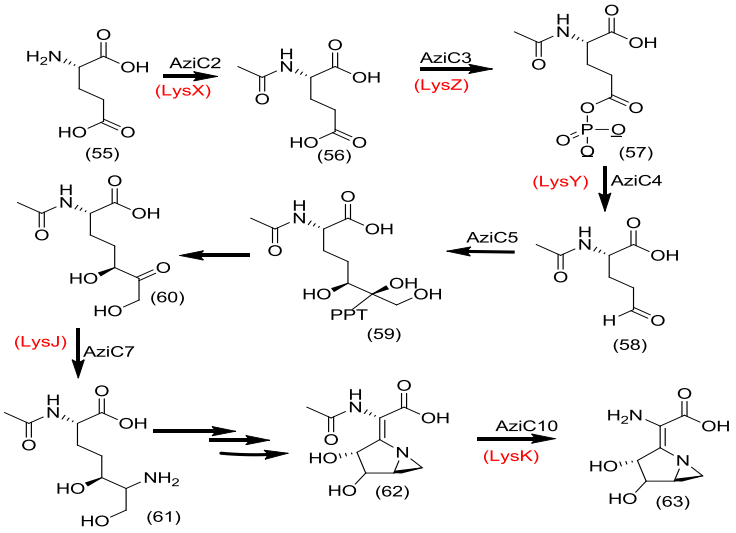

Figure 33.Proposed biosynthetic pathway of the azabicyclic ring.

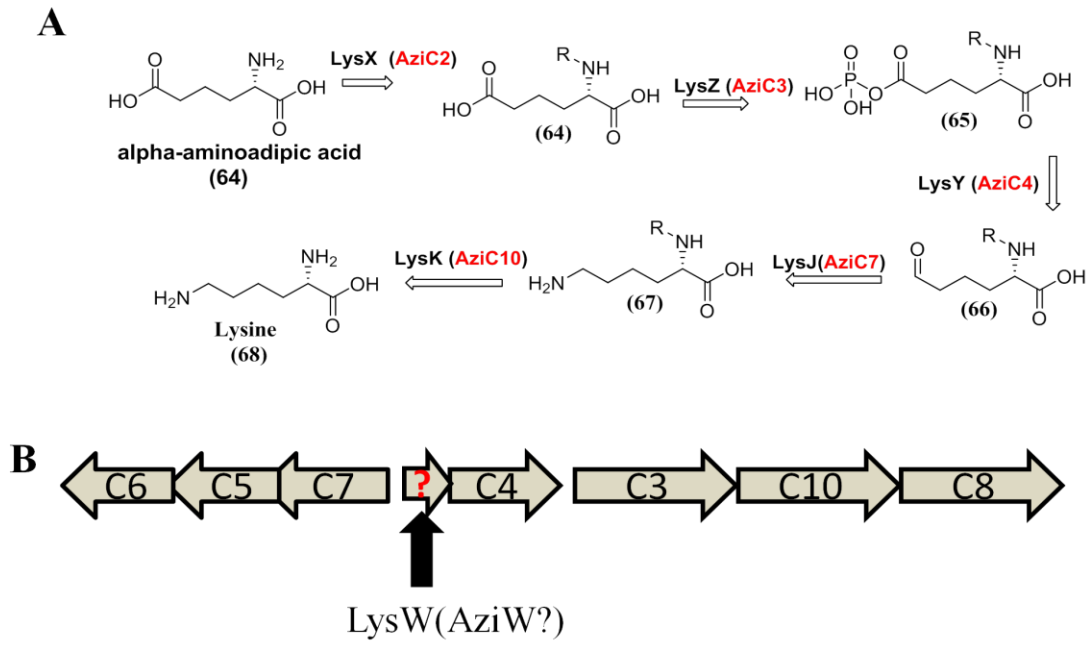

Figure 34. Lysine biosynthesis and location of *aziW* in azinomycin gene cluster. (A) Lysine biosynthesis in bacteria using alpha amino adipic acid (AAA). (B) Portion of aznomycinB gene cluster showing position of *aziW*.

It was discovered that *lysX* uses a C-terminal glutamate of *lysW* as the acceptor of α-amino adipic acid. It is suggested, based on experimental evidence, that *lysX* activates the carboxyl group of C-terminal glutamate of *lysW* through phosphorylation using ATP and ligates it to the amino group of α-amino adipic acid (Figure 35) thereby avoiding the formation of a cyclic compound, Δ^1-piperidine-2-carboxylate, Pip2C (Figure 35). Crystallization of *lysW* with a bound α-aminoadipic acid and co-crystallization of *lysW* with *lysZ* confirmed the role of *lysW* in *T.thermophilus* as a carrier of α-aminoadipic acid in lysine biosynthesis.[133] *lysW* in the lysine biosynthetic clusters of selected bacteria and archea (Figure 36) is located next to, and upstream of *lysX*. However, it is located upstream, but not next to *lysX* in the azinomycin gene cluster

(Figure 36). Lysine is the only known proteinogenic amino acid that has two distinct biosynthetic pathways: the diaminopimelate (DAP) pathway in plants, bacteria and lower fungi, and the α-aminoadipate pathway in higher fungi.[134]

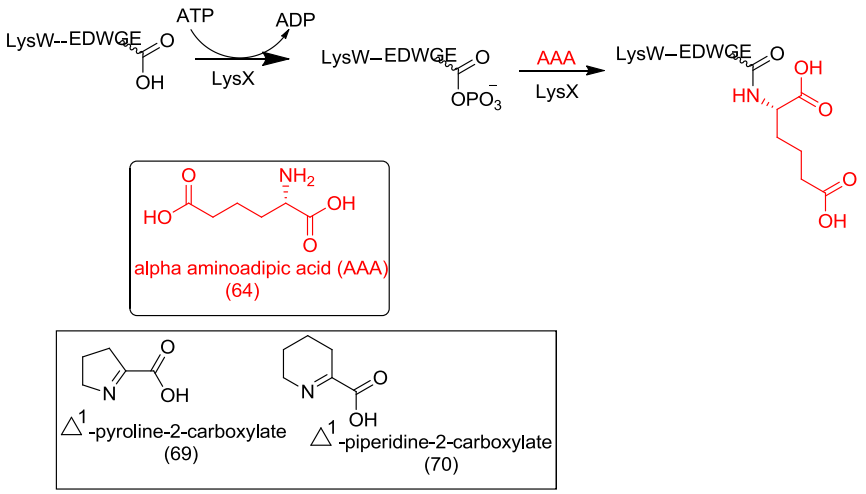

Figure 35.Enzymatic activities of lysW & lysX and structures of some truncation products of arginine and lysine biosyntheses. (Arginine (pyroline-2-carboxylate); lysine (piperidine-2-carboxylate).

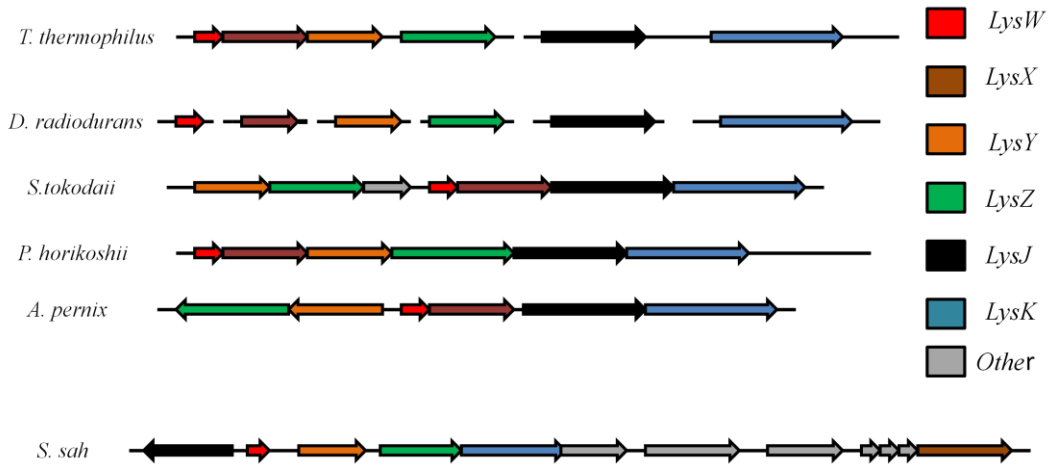

Figure 36.Comparison of gene orientation of lysine biosynthetic gene clusters. Homologues of *lysW*, *lysX*, *lysY*, *lysZ*, *lysJ* and *lysK* are color-coded as shown in the legend. Genomic sequence information used is for *S.sahachiroi*, *T.thermophilus*, *D. radiodurans*, *S. tokodaii*, *P. horikoshii* and *A. premix*.[130]

Lysine is not known to serve as a precursor of azinomycin biosynthesis. It is intriguing that *aziW*, a putative lysine biosynthetic enzyme, is clustered with other azinomycin biosynthetic enzymes. It is also known from the unpublished draft genome sequence of *S. sahachiroi* (Watanabe)[126] that this microorganism harbors a several genes involved in lysine biosynthesis through the diaminopimelate (DAP) pathway. The aim of this experiment is to probe the possible role of this largely forgotten gene, *aziW*, in azinomycin production.

MATERIALS AND METHODS

Unless otherwise specified, biochemical reagents were purchased from Sigma (ST Louis, MO). Oligonucleotide primers were ordered from Integrated DNA Technologies (Idtdna), USA while the PCR kit (Phusion DNA polymerase, buffer, dNTPs, DMSO), all enzymes and regular DNA ladders were obtained from NEB (Ipswich, MA). All PCR reactions were carried out with a PTC-200 Peltier Thermal cycler by MJ Research (Waltham, MA). All other media and reagents were purchased from VWR International (West Chester, PA). DNA miniprep (QIAprep) and Gel extraction (QIAquick) kits were purchased from Qiagen (Valencia, CA). The RNA extraction kit (RNeasy Mini Kit) was obtained from Qiagen (Valencia, CA) and the Northern hybridization kit (NorthernMax) was purchased from Ambion, a subsidiary of Life Technologies (Grand Island, NY). Oligonucleotide primers, plasmids and bacterial strains used in this study are summarized in Table 2**.** Reverse phase high performance

liquid chromatography (RP-HPLC) separations were conducted on a Waters 600 controller equipped with Waters 2487

Table 2 Bacterial strains, plasmids and primers used in *aziW* study

Strains, plasmids or primers	Relevant characteristics or primer sequence	Reference or source
Strains		
S. sahachiroi	Wild type azinomycin A and B-producing strain	ATCC
E.coli DH10B	General cloning host	Epicentre
E.coli S17-1	Conjugative donor	Rongfeng*
ΔLysW/*S.sah*	*S.sahachiroi* lacking LysW	This study
+LysW/*S.sah*	ΔLysW/*S.sah* + LysW	This study
Plasmids		
pKC1139	*Streptomyces-E.coli* shuttle vector	Rongfeng*
pSET-152	Streptomyces protein expression vector	Sohng*
pKC-LysW-KO	Gene disruption construct	This study
pSET-152-LysW	LysW Complementation construct	This study
Primers		
TSR –F	GCGTCTAGATGATCAAGGCGAATACTTCATATG	This study
TSR -R	CGCTCTAGAATCACTGACGAATCGAGGTCGAG	This study
LysW-UP-F	GTCAAGCTTCGGCGCGCAGGGCGCAGCGGTGCT	This study
LysW-UP-R	GCTTCTAGACCCTCCATGCTCGGAGAGTG	This study
LysW-DS-F	CTGTCTAGATCGTGAAGGTGAGCGTCGTCG	This study
LysW-DS-R	GACGAATTCCGGCGAGCGCCAGTTCGGCCA	This study
LysW-probe-1-F	CATCGTGGCGAAGGTGGCC	This study
LysW-probe-1-R	CAAGTTCGCGGCGTTCGCC	This study
LysW-F(probe-2)	ATAGGATCCAGGAGGCAACACATGACTACG	This study
LysW-R(probe-2)	TCTAGACTCGCCCCAGTCCTCTTCGACCTC	This study
LysW-probe-3-F	CCCGCAGCACCCGCGCCGTG	This study
LysW-probe-3-R	CCACAGCCGCTCTTGCTCG	This study
LysW -F	GCCATGCCCACCCCAAGCT	This study
LysW-R	CGGCGTTGTAGACCCGGAAG	This study
aziC3-F	GTGAACACGGCCCGTCCG	This study
aziC3-R	GTACGGTCCGGCCGTCCTG	This study
aziC10-F	CAGCGCACCGCCGACCGT	This study
aziC10-R	AGCCGATGCCGATACGTC	This study

*Prof. J.K.Sohng, Institute of Biolmolecular Reconstruction, Sunmoon University, South Korea
* Rongfeng- Johns Hopkins University.

dual λ absorbance detector (Milford, MA) by using a Phenomenex Prodigy 5µ C8 (250 x 4.6 mm) column (Torrance, CA). Radioactive labeled Adenosine Triphosphate (^{32}P ATP) was purchased from Perkin Elmer (Walthan, MA), while the 1 Kb Plus DNA ladder used in southern hybridization was obtained from Life Technologies (Carlsbad, CA).

Media Conditions

All components are per liter of deionized water and autoclaved before use.

R2YE (Required Growth Factor added/Yeast Extract): Yeast extracts, 4 g; Bacto-peptone, 4 g; Bacto-tryptone, 2 g; Glucose, 10 g; Sucrose, 103 g; K_2SO_4, 0.25 g; $MgCl_2.6H_2O$, 10.12 g; Casaminoacids, 1g; 10 mL KH_2PO_4 (0.5%); 80 mL $CaCl_2.2H_2O$ (3.68 %); 15 mL L-proline (20 %); 2 mL *Trace element solution; 5 mL NaOH (1N); 25 mL Tris-HCl (1M, pH 7.5); adjust to pH 6.8 with HCl or NaOH. *Trace element solution contained the following components per liter: $ZnCl_2$, 40 mg; $FeCl_3$ •$6H_2O$, 200 mg; $CuCl_2$ •$2H_2O$, 10 mg; $MnCl_2$•$4H_2O$, 10 mg; $Na_2B_4O_7$• $10H_2O$, 10 mg; $(NH_4)_6Mo_7O_2$ • $4H_2O$, 10 mg; and deionized water.MS (Manntol/Soy): Mannitol, 20 g; Soy Flour, 20 g PS5 (Pharmamedia/Starch): Pharmamedia (yellow cotton seed flour), 5 g; Soluble Starch, 5 g, adjust pH to 7 prior to sterilization. LB (Luria-Bertani): Bacto-Peptone, 10 g; Yeast Extract, 5 g; Sodium Chloride, 5 g. MOPS, 15 g; Trace elements, 10 mL.Dissolve in 1-liter and autoclave. RNase free water was prepared by incubation of 2 liter solution containing 0.1 % diethyl pyrocarbonate, DEPC (Sigma-Aldrich) at 42 ^{o}C for 24 hr followed by autoclave.

Minimal Media: Prepare 5X M9 salt by mixing $Na_2HPO_4.12\ H_2O$ 85.7 g, KH_2PO_4 15.0 g, NaCl 2.5 g in 1000 ml of milli-Q and autoclave. Dissolve 5 g $(NH_4)_2SO4$ in 15 ml of H2O, sterile filter. Prepare trace elements solution by dissolving 1 g EDTA, 29 mg $ZnSO_4.7H2O$, 198 mg $MnCl_2.\ 4H_2O$, 254 mg $CoCl_2.\ 6H_2O$, 13.4 mg $CuCl_2$ and 147 mg $CaCl_2$ in 100 ml of milli-Q and autoclave. Prepare each of the following solutions in milliQ water separately and sterile filter: 20 % (w/v) glucose: 25 g in 100 ml, 0.1 M $CaCl_2.2H_2O$: 1.47g in 100 ml, 1M $MgSO_4.7H_2O$:24.65g in 100 ml, 10 mM $FeSO_4.7H_2O$: 140 mg in 50 ml (prepare fresh), 1 % thiamine: 500 mg in 10 ml (prepare fresh). For 1 liter M-9 media, mix 200 ml of M-9 salts, 3 ml of $(NH_4)_2SO_4$, 1 ml of $CaCl_2.2H_2O$, 1 ml trace elements, 20 ml glucose, 1 ml $MgSO_4.7H_2O$, 1 ml $FeSO_4.7H_2O$ and 2 ml thiamine.

Cloning of the *aziW* Disruption Construct

Genomic DNA was isolated from *Streptomyces sahachiroi* cultured on R2YE for 2-days at 30 ^oC and 250 rpm shaker using the salting out method. This DNA was used as template to amplify the 950 base pair regions flanking the target gene, LysW. Primer pair (LysW-UP-F which has a *Hind*III restriction site and LysW-UP-R containing an *Xba*I restriction site, Table 2) was used in the amplification of upstream region. LysW-DS-F which contained an XbaI restriction site and LysW-DS-R that contained an *Eco*RI restriction site was used in the amplification of the downstream region. The selective marker gene, thiostrepton (TSR) was amplified from a plasmid, pRF, a gift from Rongfeng (Table 2) using the TSR primer pair containing an XbaI restriction sites on both the forward and reverse direction. Amplification was achieved as follows: 98 ^oC for

30 s followed by 29 iterative steps of 98 ^{o}C for 10 s, 63 ^{o}C for 20 s, and 72 ^{o}C for 30 s and a final 72 ^{o}C for 10 min. The PCR reaction mixtures were separated on a 1% agarose gel and the desired bands extracted from the agarose using a QIAquick Gel Extraction Kit. Purified PCR products were restriction digested with appropriate enzymes and purified on a mini-column packed with Sephadex G50 (GE Healthcare, Uppsala, Sweden). An *E.coli – Streptomyces* shuttle vector, pKC1139, a gift from Rongfeng (Table 2) was digested with HindIII and XbaI, separated on a 1 % agarose gel and purified using the QIAqick Kit. Digested upstream and pKC1139 fragments were ligated to produce intermediate plasmid pKC-LysW-UP. This was digested with XbaI and EcoRI and the fragment ligated to the rear-arm digest to generate intermediate plasmid pKC-LysW1. Finally, pKC-LysW1was digested with XbaI and ligated to TSR fragment to generate pKC-LysW-KO. All the ligation steps above were followed by transformation in *E.coli* DH10B (Table 2) and transformants were spread on LB-agar plates containing 25 µg/mL apramycin and incubated at 37 ^{o}C for at least 13 hr to allow for selection of positive clones. Positive clones were identified by both restriction digestion and plasmid sequencing performed using ABI Big Dye Chemistry at the Gene Technology Laboratory, Texas A&M University.

E. coli-S. sahachiroi **Interspecies Conjugation**

S. sahachiroi was inoculated onto MS-agar plates (mannitol 2 %; soy flour 2 %; bacto-agar 1.5 % in distilled water) and incubated at 28 ^{o}C for 5-days. The spores were scraped off the plate with a sterile scraper and suspended in a 15 mL falcon tube

containing 2xYT medium (1.6 % tryptone and 1% yeast extract in distilled water) and sterile glass beads. The spores were vortexed for one minute and filtered through sterile cotton followed by heat shock at 50 ^{o}C for 10 min. Spores were pre-germinated by shaking at 37 ^{o}C for 3 hr and the tube subsequently centrifuged at 6000 rpm for 10 min to pellet the spores. The pellets were re-suspended in fresh 2xYT medium. The spores were again centrifuged and re-suspended in 4 mL of 2xYTmedium. The donor, *E. coli* S17-1 carrying the disruption construct (pKC-LysW-KO), was prepared according to standard *E. coli* competent cell preparation.[135] The *E.coli* S17-1 carrying the pKC-LysW-KO plasmid was grown overnight at 37 ^{o}C with shaking and used to subculture 5 mL LB medium in a 15 mL falcon tube until the optical density, OD_{600} = 0.4. The cells were centrifuged at 5000 rpm for 8 min, washed twice with 2xYT medium while maintaining the temperature at 4 ^{o}C. The cells were re-suspended in 2 mL of 2xYT medium and 1 mL of each of the donor and recipient cells were mixed and plated on ISP4-agar medium supplemented with 10 mg/ml sterile magnesium chloride solution. After 18 hr of incubation at 28 ^{o}C, the plates were overlaid with 1 mL water containing 0.5 mg nalidixic acid and 1 mg apramycin. The *S. sahachiroi* exconjugants resulting from single crossover of the plasmid into the chromosome were first isolated after 5-days. Thiostrepton-resistant but apramycin-sensitive colonies derived from a second crossover were selected for further confirmation after 5-rounds of selection on MS – agar plates containing 50 µg/mL thiostrepton.

Generation of ^{32}P-dATP Labeled Gene Probes and Southern Hybridization

^{32}P-labeling of 1 kb Plus DNA ladder was carried out according to Life Technologies protocol using T4 DNA polymerase. Two 500-bp (probes 1 & 3) fragments located up and downstream of *aziW* respectively and 180-bp (*lysW*) probes were generated by PCR.The PCR consisted of a 20 µl reaction mixture containing 1µL ^{32}P-dATP in addition to 0.4 mM of each primer (Table 2); 0.25 mM of each of the 4 dNTPs, 1 µl of plasmid harboring the corresponding template DNA, 1 U of high fidelity phusion polymerase (NEB) in its recommended reaction buffer, 10% DMSO and other PCR components as described previously. A control PCR was set up under similar conditions except with water in place of 1µL ^{32}P-dATP. PCR mixture from the control reaction was analyzed for purity on a 1 % agarose gel electrophoresis. Unincorporated nucleotides from the PCR containing 1 µL ^{32}P-dATP were removed by purification using a Sephadex G-50 spin column and radioactive activity checked with a Gieger counter. For Southern hybridization, 40 µg genomic DNA (wild type and LysW disrupted *S. sahachiroi)* were digested with *Bgl*II restriction enzyme at 37 ^{o}C for 3 hr in a 50 µL reaction volume. The digested DNA was concentrated by ethanol precipitation and separated on 1 % agarose gel at 80 V for 3 hr. DNA transfer to positive nylon membrane (Ambion) was performed by upward transfer method as contained in the Molecular Cloning, a Laboratory Handbook, Volume1.[128] DNA transfer to the membrane (via alkaline transfer) took approximately 6 hr, at which time the set-up was disassembled and the membrane agitated in neutralization buffer for 5 min. Pre-

hybridization and hybridization, washing and detection were performed according to the protocol in the Molecular Cloning, a Laboratory Handbook ,Volume 1.[128]

Construction of Recombinant Integrative Plasmid, pSET152-lysW

For functional overexpression of the *aziW* gene in Δ aziW *S. sahachiroi*, a 200-bp DNA fragment including the entire *aziW* gene and its upstream ribosome binding site (RBS) was amplified by PCR using the wild type *S. sahachiroi* genomic DNA as a template with the primer pair LysW-F and LysW-R (Table 2) containing the restriction sites BamHI on the forward and XbaI on the reverse primers. PCR mixture (final volume of 20 µl) contained 0.4 mM of each primer, 0.25 mM of each of the 4 dNTPs, 1 µl of extracted DNA, 1 U of high fidelity phusion polymerase (NEB) in its recommended reaction buffer, and 10 % DMSO. Amplification was performed in a Thermal Cycler (BioRad, USA) according to the following profile: 98 ^{o}C for 30 s followed by 29 iterative steps of 98 ^{o}C for 10 s, 63 ^{o}C for 20 s, 72 ^{o}C for 30 s and a final step of 72 ^{o}C for 10 min. 1 U Taq DNA polymerase (NEB) was added to the mixture and extension was carried out in the thermal cycler at 72 ^{o}C for additional 10 min. The PCR reaction mixtures were separated on a 2 % agarose gel, the desired bands excised from the agarose gel and the DNA extracted using a QIAquick gel extraction kit. Purified PCR product was ligated into a pGEM T-easy vector (Promega) according to manufacturer's protocol and transformed in *E. coli* DH10B. Positive clones were selected followed by complete nucleotide sequence confirmation by Genetech Lab, Texas A&M University. The PCR product was finally subcloned into the pSET152 integrative plasmid containing

a strong constitutive promoter, ermE* and the resulting plasmid was designated pSET152-aziW. The sequence of this plasmid was verified and the plasmid was transformed in *E.coli* donor strain, S17-1 followed by selection on apramycin plates.

E. coli-S. sahachiroi **Interspecies Conjugation**

Conjugation with the streptomyces system was performed as described previously except that *S. sahachiroi ΔaziW* strain was used in place of wild type. Since the *ΔlysW* strain is already resistant to thiostrepton, the conjugation plates were overlaid with 1 mL water containing 0.5 mg nalidixic acid, 1 mg apramycin and 1 mg thiostrepton. *Streptomyces* spores that were resistant to both thiostrepton and apramycin were selected through one more cycle of incubation on MS-agar plate containing 25 μg/mL apramycin and 50 μg/mL of thiostrepton. Positive clones were used for fermentation.

Fermentation and Isolation of Metabolites

The spores of mutant, wild type and complement strains were spread separately on MS agar plates and incubated at 28 ^{o}C until brownish spores developed (usually 5 -7 days). Fermentation of the first and second stage starter cultures were performed as previously described,[125] except the volume of the second stage culture was 100 mL instead of 2x600 mL. The third stage culture was carried out under nutrient starved conditions fermentation was in 2x 2000 mL flask containing 1 L of medium at 28 ^{o}C and 225 rpm for 84 hr. Fermentation broths were extracted with dichloromethane and

concentrated *in vacuo* to recover amorphous yellowish extracts. The crude extracts were analyzed by HPLC. Each extract was dissolved in 50 % acetonitrile to a concentration of 1 mg/mL and passed through a 0.2 µm syringe filter. To each filtered solution, 10 µL was withdrawn and diluted 10 times; 20 µL was finally drawn from each sample for RP-HPLC analysis. A linear gradient of acetonitrile and water (solvent A = acetonitrile; solvent B = water; 0-1 min 10 % A; 1-14 min 10 % A to 95 % A; 14-15 min 95 % A; 15-20 min 95 % A to 10 % A; 20-25 min 10 % A) was used to separate metabolites with a Phenomenex Prodigy 5µ C8 (250 x 4.6 mm) column and a detector set at 254 nm and 320 nm. Mass spectral analyses of unique RP-HPLC peaks (Appendix) were performed at the mass spectrometer facility in chemistry department, Texas A&M University, using both APCI and ESI ionization mode.

RNA Isolation and Northern Hybridization

RNA isolation was carried out according to the manufacturer's protocol using the RNeasy mini kit (Qiagen). Briefly, glycerol stocks of both the *S.sahachiroi* wild type and the aziW deletion mutant were used to inoculate 5 mL of R2YE medium and cultured at 28 ^{o}C at 250 rpm for 2-days. The starter culture (100 µL) was used to inoculate 50 mL of APM medium (dextrose, 60 g; yeast extract, 8 g; malt extract, 20 g; sodium chloride, 2 g; MOPS, 15 g; trace elements, 10 mL). The culture flasks were agitated at 250 rpm and 28 ^{o}C for 24 hr. The bacterial cells were harvested by transferring 3x2 mL culture broth of each construct to 15 mL falcon tubes followed by centrifugation at 5000 x g for 5 min at 4 ^{o}C. The supernatant was decanted and the tubes

allowed to warm to room temperature. Bacterial cells were re-suspended in 100 µL of TE buffer containing 3 mg/mL lysozyme. The suspension was then transferred to 1.5 mL centrifuge tubes and incubated at room temperature for 10 min. Following incubation, 350 µL of buffer RLT containing 1% beta mercaptoethanol (β-ME) was added and the suspension mixed thoroughly by vortexing vigorously. The tubes and its contents were spun down at 14,000 rpm for 2 min. The supernatant was transferred to RNase–free centrifuges tube and 250 µL of ethanol (95 %) was added. The mixture was applied to RNeasy mini spin columns and centrifuged at 14,000 rpm for 2 min. The mini spin column was washed sequentially with RW1 and RPE buffers (Qiagen, RNeasy mini Handbook). RNA was eluted with 30 µL Rnase-free water. DNase treatment was carried out with a TURBO DNA-free kit (Ambion) to remove the contaminating DNA. Northern hybridization was performed according to NorthernMax® protocols (Ambion). Briefly, 10 µg of total RNA per sample was loaded on a 1% agarose-formaldehyde denaturing gel in 1× MOPS buffer (Ambion). The separated RNAs were transferred to the BrightStar-Plus membrane (Ambion), UV cross-linked and hybridized with ^{32}P-labeled DNA probe specific for AziC4 coding sequence (42 °C overnight in ULTRAhyb buffer, Ambion). The hybridized membrane was washed twice with high-stringency wash solution for 5 min and 15 min. The hybridization signals were detected between washes using a Gieger Counter and membrane exposed to an autoradiography plate for 12 hr. The autoradiographic image was visualized with a Fuji Phosphoimager (Texas A&M University, Biology Department).

Reverse Transcription (RT)-PCR Analysis of Genes Downstream of *aziW*

RNA isolation and purification was carried out as described previously. RT-PCR was performed according to C.M. Watanabe [136] to check the mRNA expression profile of the downstream genes following disruption of *aziW*. Specifically, the expression profile of aziC4, aziC3 and aziC10 were monitored. Following RNA extraction, total RNA (5µg) was transcribed to single-stranded cDNA by using SuperScript First-Strand (Invitrogen). PCR reactions with the cDNA aliquots were conducted with N-acetytransfrase (aziC2) as an amplification standard. The PCR primers used (Table 2) are lysW-probe-1 for aziC4, aziC3, aziC10 and aziC2. Each amplification cycle was conducted as described previously (cloning of *lysW* disruption construct).

Testing of Lysine Auxotrophy of *aziW* Mutant

The growth of the *S. sahachiroi,* lysW disruptant and wild type strains were monitored on both solid and liquid media. Minimal medium agar plates consisted of 0.5 g L-asparagine, 0.5 g potassium phosphate dibasic, 0.2 g magnesium sulfate, 10 g mannitol, 0.01 g iron sulfate and 10 g bacto agar and 1 L of distilled water. Wild type and mutant *S. sahachiroi* were grown on minimal agar plates supplemented with or without 0.1 mM sterile filtered lysine at 28 ^{o}C for 3-4 days. For examination of lysine auxotrophy in liquid culture, the first stage culture was carried out in R2YE as previously described. After 2-days, 50 µl of first stage culture was used to inoculate 50 mL of minimal medium supplemented with or without 0.1 mM lysine at 28 ^{o}C and 250 rpm for 2-3days. Liquid minimal media was prepared by mixing 200 mL of M9 salts

(autoclaved solution of 64 g/L sodium phosphate dibasic, 15 g/L potassium phosphate monobasic, 2.5 g/L sodium chloride and 5 g/L ammonium chloride.), 2 mL of 1 M magnesium sulfate, 20 mL of 20 % glucose, 100 µL of 1 M calcium chloride in 1 L of distilled water.

RESULTS AND DISCUSSION

Generation of *aziW* Disruptant

The thiostrepton antibiotic resistance marker (TSR) was introduced in place of *aziW*, a protein homologous to *lysW* of *T. thermophilus* in which it has been shown to be involved in lysine biosynthesis. The TSR gene was inserted by ligation between the genes flanking *aziW* within the azinomycin gene cluster and the cassette was ligated into the *E.coli-streptomyces* shuttle vector pKC1139. The resulting plasmid, pKC-LysW-KO (Figure 37A), contained sequences homologous to those flanking the *aziW* gene in addition to the selection marker gene, TSR. Sequence analysis of pKC-LysW-KO plasmid revealed that the TSR gene was placed in an orientation opposite to that of *aziW* and other downstream genes (Figure 34B). PKC-LysW-KO was first transformed into an *E. coli* donor strain, S17-1, and then introduced into wild-type *S. sahachiroi* by conjugation. Several rounds of selection for the antibiotic TSR resistance resulted in isolation of clones that had lost the shuttle vector, pKC1139 (Figure 37C). Figure 35 shows the strategy used to achieve *aziW* gene disruption by homologous recombination as well as the positive colonies that were generated on MS agar plates. Integration of the TSR gene into the *S. sahachiroi* genome was verified by PCR that targeted the TSR gene

(Table 3). Only mutant strains produced the expected TSR product from PCR performed with aziW mutant genomic DNA (Figure 38) as template. Site-specific integration of the TSR gene between the flanking regions of aziW was verified by Southern hybridization. Three different probes were used, each targeting different regions of the mutant azinomycin gene cluster. Probe-1, 500 bp long, targeted the upstream region of *aziW*, whereas probe-2 and probe-3 are 180 bp and 500 bp long respectively and targeted the *aziW* gene itself and the gene downstream of *aziW*. The strategy and results of Southern hybridization experiments are shown in Figure 36. Probe-1 produced two bands at ~ 8.4 kb and ~9.3 kb (Figure 38D) for the wild type and *aziW* mutant respectively. Probe-2, however, produced two bands in the wild type and one band in the mutant (Figure 38B). One of the two bands in the wild type corresponds to the ~8.4 kb fragment, whereas the second band is a low molecular weight DNA that also appeared in the *aziW* mutant and corresponds to the size of *aziW*. A close observation of band intensities also showed that low molecular weight DNA band in the mutant strain is more intense than the corresponding band in the wild type. Probe-3 (Figure 38C) produced bands which were consistent with those seen with probe-1. Taken together, these results confirm the site specific replacement of *aziW* by TSR selection marker. However, the appearance of an intense *aziW* band in the mutant is suggestive of the presence of another copy of *aziW* in the *S. sahachiroi* genome. This is strongly supported by the presence of a similar band in the wild-type strain as well as the band that represents our target, *aziW*.

Recombinant Integrative Plasmid, pSET152-lysW

The *aziW* sequence containing the native ribosome binding site (RBS) was cloned into the multiple cloning site of a recombinant integrative plasmid, pSET152, under the control of the erythromycin (ermE*) promoter (Figure 39). It was intorduced into *E.coli* DH10B strain, and the plasmid sequence verified. This plasmid was later intoduced into the *E.coli* donor strain, S17-1 and transferred into the *aziW* mutant strain by conjugation as described previously. Positive clones were selected on apramycin plates.

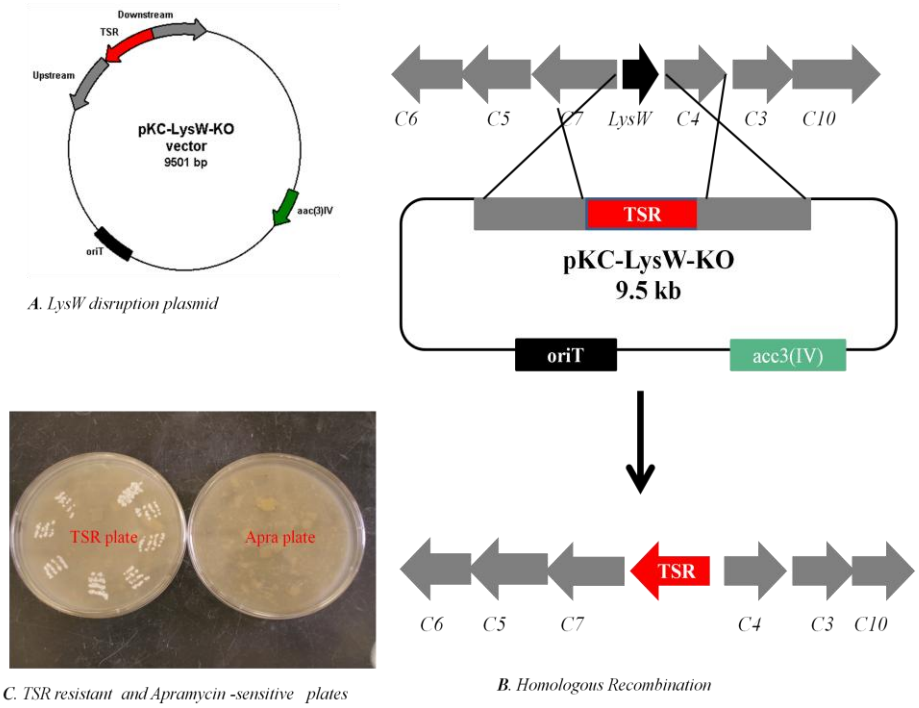

Figure 37.*aziW* disruption strategy. (A) *aziW* mutant plasmid. (B) Homologous recombination strategy. (C) *aziW* mutant strain on both apramycin and thiostrepton selective plates.

Fermentation and Characterization of Metabolites

The spores of mutant and wild-type strains were spread on MS agar plates and incubated at 28 ^{o}C until brownish spores developed (usually 5 -7 days). Fermentation of the first and second stage starter cultures were carried as described previously.[124] However, third stage fermentation was carried out in shake flask under nutrient-starved conditions.[124] Fermentation in the shake-flask system ensures that conditions were the same and creates a good platform for comparison of wild-type and mutant strains. This is in contrast to the standard third stage fermentation, in which only a 10-liter fermentation could be carried out.

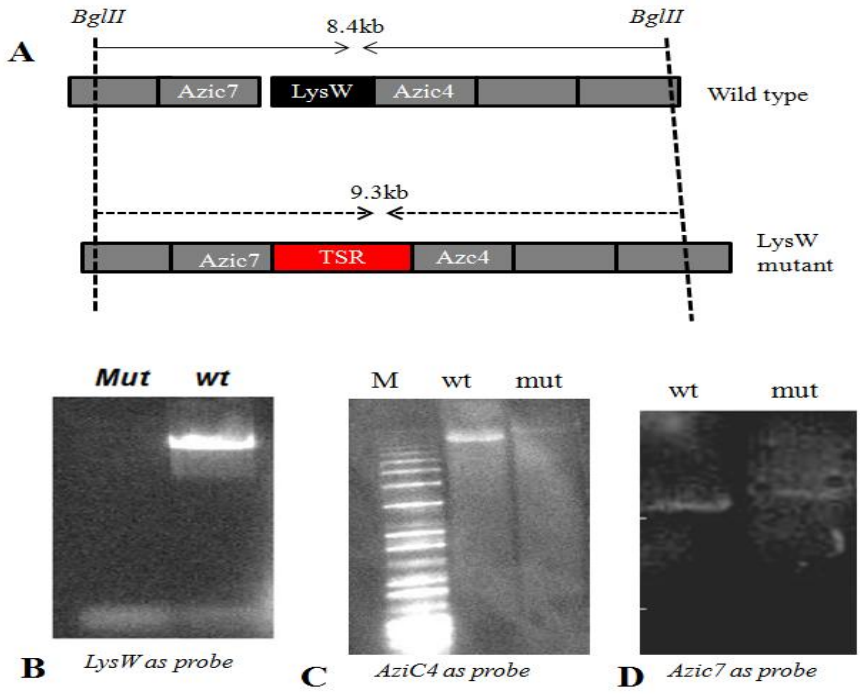

Figure 38.Confirmation of aziW disruption. (A) Enzyme digestion strategy. Southern hybridization with (B) *lysW* gene as probe;(C) aziC4 as probe and, (D) aziC7 as probe.

The third stage fermentation in all cases was extended by 24 hr and the fermentation broth extracted with dichloromethane separated *in vacuo,* and a crude sample was used for RP-HPLC analysis. RP-HPLC conditions are detailed in the materials and methods section.

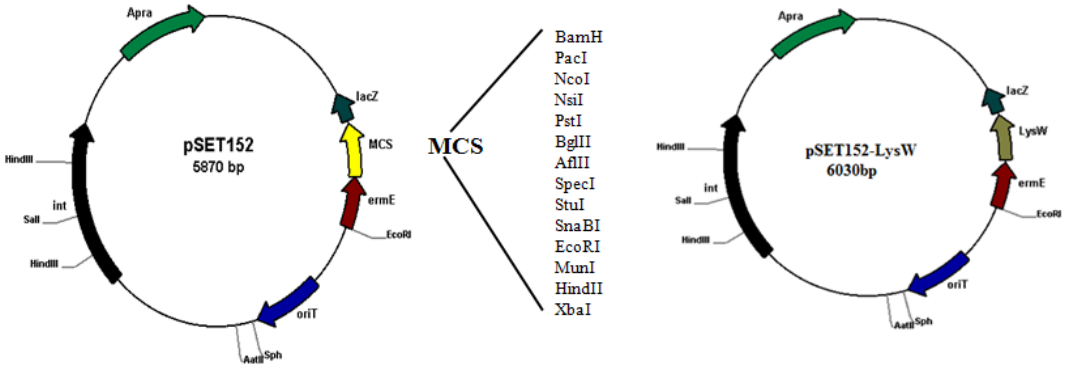

Figure 39.Vector diagram of pSET152 and complementation plasmid.

Genetic disruption of *aziW* completely abolished the production of azinomycin **(**Figure 40), suggesting that *aziW* might be a critical element in the biosynthesis. Individual peaks from the wild-type were analyzed and their identity confirmed by mass spectrometry (Appendix). Complementation of the disrupted gene by integration into the genome has been successfully used to restore the production of natural products.[134,137,138] However, complementation in our case failed to restore the production of azinomycin (Figure 41) to a detectable level. However, this might be due to the protein not being overexpressed. Alternatively, failure of restoration of azinomycin production in the *aziW* knockout by complementation with *aziW* might suggest existence of polar effects caused by the disruption.

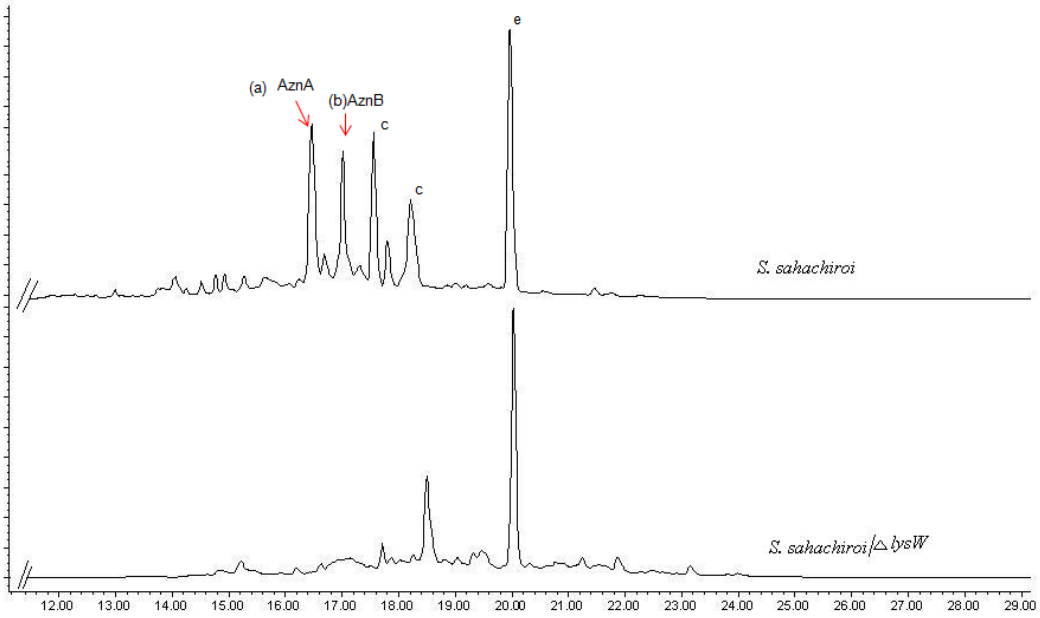

Figure 40.RP-HPLC analysis of metabolites from *S. sahachiroi* wild-type (top) and *aziW* deletion mutant (bottom).

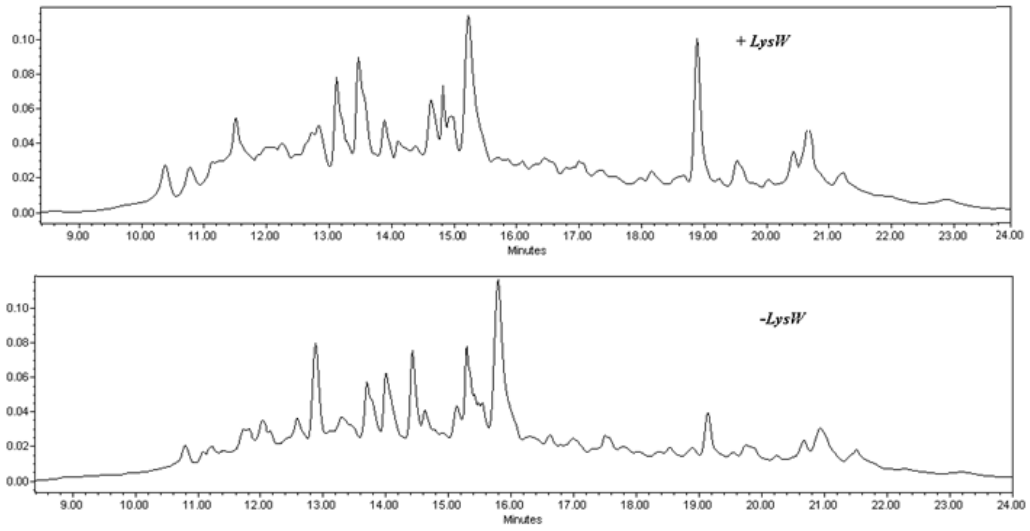

Figure 41.RP-HPLC analysis of *S. sahchiroi aziW* complement (top) and *aziW* deletion mutant (bottom).

Organization of lysW Operon and Northern Blot Analysis

A potential promoter was identified 49 bp upstream of the *lysW* translation start site, ATG, using the bacteria promoter identification software, BPROM (http://linuxl.softberry.com/berry.phtml) (Figure 42A). Northern blotting with a ^{32}P-dATP-labeled probe specific for the aziC4 sequence was conducted, and consistent with the speculation of a co-transcription of aziW with another downstream gene, one transcript of above 4 kb was observed (Figure 42B).

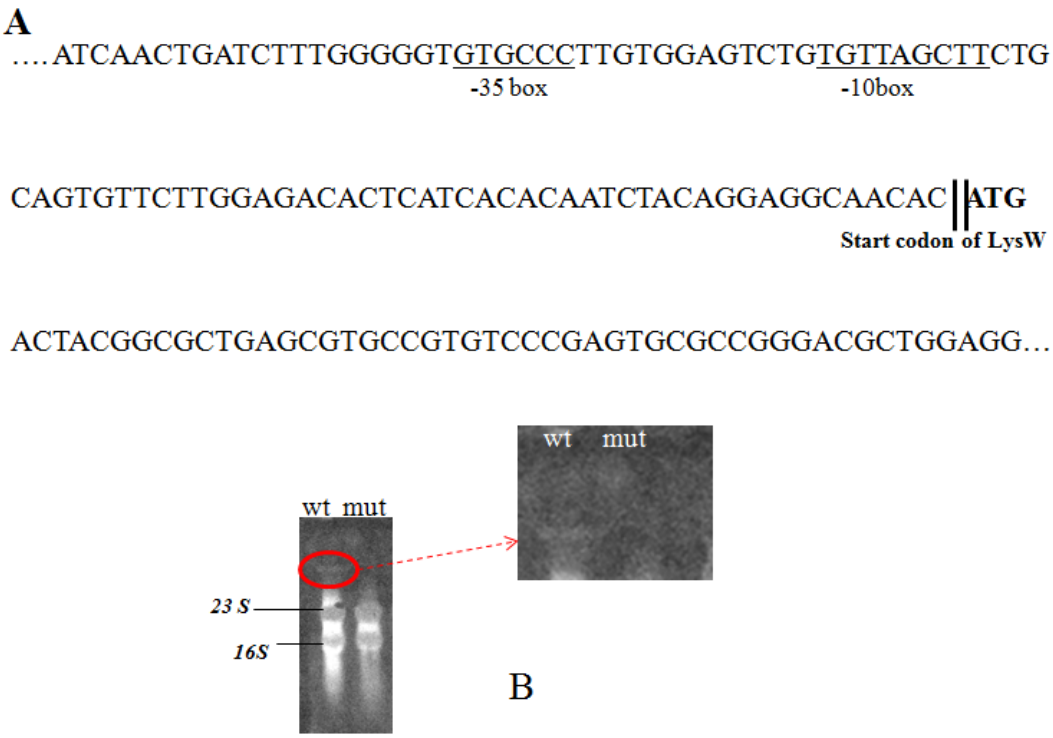

Figure 42.Promoter analysis of *aziW* sequence and Northern hybridization. (A) Promoter predicted by BPROM to drive the transcription of *LysW* operon. Underlined letters indicate -35 and -10 regions for the putative promoter. Bold letters indicated the predicted start codon (ATG). (B) Northern blot analysis (and zoom in) with ^{32}P-labeled probe specific to *azic4* sequence.

Sequence analysis of the pKC-LysW-KO plasmid showed that the TSR gene was integrated in the orientation opposite the *lysW* operon (Figure 34B). The implication of this is that the *aziW* operon cannot count on the native TSR promoter to efficiently drive the transcription of the operon. The promoter and transcription start site of the *lysW* operon were not affected by the gene disruption of *aziW*. This might imply that transcription in the presence of intervening TSR gene sequence would result in at least some amount of downstream gene transcripts. However, the preceding outcome is only possible if there is no activation of latent *rho*-dependent terminators in the TSR complement sequence.[139-141] Most *rho*-dependent termination message involved termination at the end of the bacterial operons;[142] however, *in vitro* transcription studies have revealed existence of *rho*-dependent termination sites within genes.[143] A search of TSR gene (1056 bp) using free online transcription termination predictor, ARNold: finding terminators, did not predict the presence of any terminator in either direction. Only one terminator site was predicted for the 63-kb sequence of azinomycin gene cluster in both directions.

The mRNA Expression Profile of Genes Downstream of *aziW*

Following the disruption of lysW and the inability of *lysW* complementation to restore azinomycin production to a detectable level, the mRNA expression level of the downstream genes were profiled. Single-stranded cDNA was generated by the use the SuperScript First-Strand and the PCR conditions normalized with *aziC2* as an endogenous amplification standard. a*ziC2* was selected as a standard because it is

located 17.8 kb downstream of *aziW* and may not under the control of the same promoter as *aziW*. The PCR of *aziC4*, *aziC3* and *aziC10* were performed under the standardized condition and equal amounts of PCR mixtures were analyzed on a 1 % agarose gel electrophoresis. Of the three genes whose mRNA exression levels were investigated, only *aziC4* showed similar expression levels in both wild-type and mutant. The expression of *aziC3* is lower in the *aziW* deletion mutant compared to the wild-type, whereas the expression of aziC10 is not detectable in the mutant. These results are shown in Figure 43. What these results suggest is that the replacement of *aziW* with TSR resulted in the transcriptional attenuation of the downstream genes. The impact is much stronger the further away the gene is from the transcription start site, which is located, upstream of *aziW*. It follows from this argument that the transcription of other genes *(aziC8, aziA5*, Figure 31) thought to be under the control of the same promoter as *aziW* (Figure 42) might be down-regulated or truncated. This, and a possible low expression level of aziW from the complementation plasmid might explain the inability of the *aziW* complementation to restore azinomycin production.

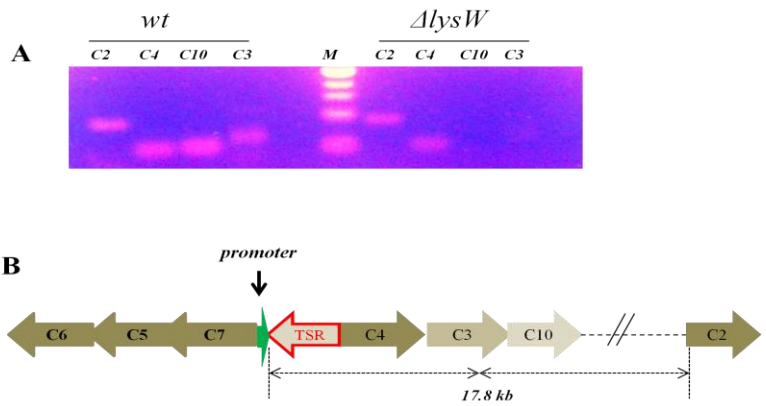

Figure 43.The mRNA expression profile of *aziW* downstream genes. (A) mRNA expression profile of downstream genes; C4, C3, C10. (B) Portion of the gene cluster in *aziW* disruptant showing the endogenous amplification standard, C2 located 17.8 kb downstream of aziW.

Lysine Auxotrophy in *aziW* Deletion Mutant

In order to probe the role of the *aziW* gene in lysine biosynthesis, a lysine auxotrophy experiment was carried out. First stage culture was carried in R2YE medium at 28 ^{o}C in a shaker. After 24 hr of incubation, 10 µl of each cultured sample was used to inoculate 5mL minimal medium, and incubation was continued for additional 24 hr. There was no difference in the phenotype of the wild-type or *aziW*-deleted *S. sahachiroi* with or without lysine after 24 hr. The growth of the cells in liquid media did not reflect the lack of a critical element in lysine biosynthesis as previously reported.[132] This observation supports the earlier indication of an additional copy of *aziW* by Southern hybridization (Figure 38B). It also lends credence to initial findings by isotope-labeled precursor feeding experiment, which strongly showed that lysine is not incorporated in azinomycin biosynthesis.[125] The *aziW*-deleted strain certainly grows on minimal media agar plates; however, growth is stunted and sporulation is very weak (Figure 44). This

might suggest that *aziW* and other lysine biosynthetic homologues are involved in the sporulation process.

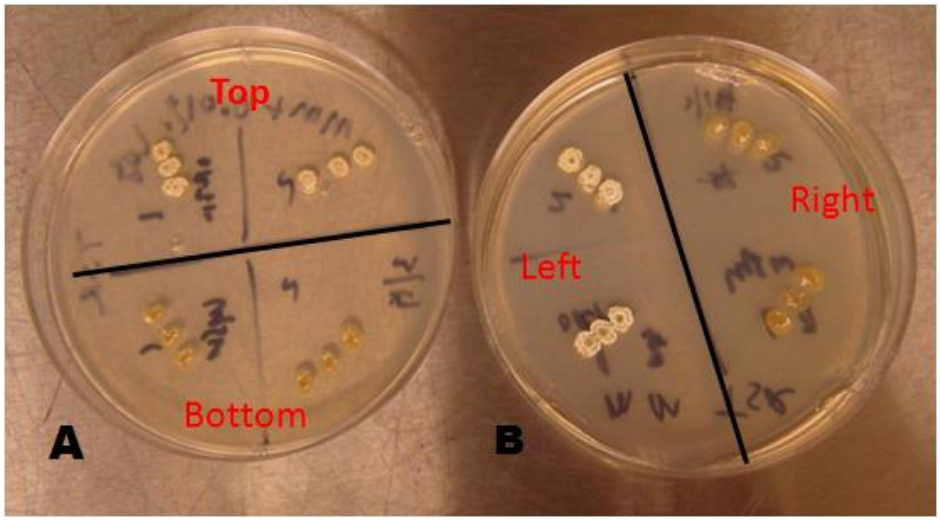

Figure 44.Lysine auxotrophy experiment on minimal media agar plates. (A) supplemented with 0.1mM lysine, top – wild type strain; bottom – LysW deletion strain. (B) without supplement, left – wild type strain; right – lysW deletion strain.

Perhaps, *aziW* deletion has blocked production of some intermediate compounds required for sporulation as regulators or maybe components of the spore cell wall.

CHAPTER IV

BIOCHEMICAL EVALUATION OF THE ROLE OF CYTOCHROME P450 (*aziC9*) IN AZINOMYCIN BIOSYNTHESIS

INTRODUCTION

Cytochrome P450 was first discovered over five decades ago when it was reported that an enzyme complex located in the liver was able to oxidatively metabolize certain xenobiotic compounds.[144,145] Shortly after the discovery of P450, a carbon monoxide (CO) binding pigment that gave an absorption maximum (λ_{max}) at 450nm was detected in liver microsomes.[146,147] This pigment was later identified as a hemoprotein of the b-type cytochrome, hence the name cytochrome P450.[148-150] Cytochrome P450 enzymes are found in all five biological kingdoms.[151] In the mammalian system, P450s are found in most tissues; however, a greater proportion is located in the hepatocyte cells of the liver.[152] Cytochrome P450 enzymes constitute a large family of oxidative heme-containing proteins that catalyze a wide range of nature's oxidative transformations. The generic type of reaction catalyzed by P450s is hydroxylation. The reaction requires two

$$R\text{-}H + O_2 + 2H^+ + 2e^- \longrightarrow R\text{-}OH + H_2O$$

electrons (supplied b redox partners), molecular oxygen and two protons. All P450 enzymes display close structural similarity despite their low sequence identity. In prokaryotes, there exists a P450 heme signature motif: F G x G x H/R x C L /A (where x is any amino acid residue F is phenyalanine, G is glycine, H is histidine, R is arginine, C is cysteine, L is leucine and A is alanine).[153] The heme group consists of the

protoporphyrin IX and a central iron (III) atom. The protoporphyrin IX consists of a core tetrapyrrole ring formed from four pyrrole rings linked by methylene bridges. Each ring contains a methyl group side chain and two consecutive rings contain either a propionate or vinyl side chain (Figure 45). Several distinct types of enzymes and redox proteins have historically been termed cytochromes based on the presence of a heme group in the enzymes; however, their primary, secondary and tertiary structures vary markedly.[154]

The use of the term "cytochrome," as applied to P450s (EC1.14.14.1) is a misnomer since these proteins are now regarded as heme-thiolate proteins or enzymes. The distinction is that whereas other cytochromes tend to possess at least one histidine residue that ligates the heme iron, the P450s ligate iron with cysteine.[154] The peroxidases that break down hydrogen perioxide to water contain the heme-moiety, but the ligand is usually histidine (except in chloroperoxidase which contains cysteine heme and displays spectral characters common to P450s).[155,156] One distinguishing feature of peroxidases is that they possess active sites that have just enough space to bind a single molecule of hydrogen peroxide, whereas P450s have larger active sites due to varying size of substrates. P450s are grouped into ten different classes based on the type of redox partner used by the enzyme (Table 3).[157]

Typical reactions in which P450 enzymes are involved include metabolism of foreign compounds, such as drugs, carcinogens and plant products.[158] They generally promote the conversion of hydrophobic compounds to hydrophilic derivatives to enhance their excretion from the body. In secondary metabolic pathways in *Streptomyces*, P450s are typically located within the biosynthetic gene cluster, where

they have been shown to increase the structural complexities and bioactivities of natural products through the regio- and stereospecific oxidation of precursors.[159-162] However, the NADPH-dependent redox partners (NADPH-cytochrome P450 reductase and ferredoxin) are not usually clustered with the genes encoding the P450 enzymes. Recent advances in genome sequencing and other biological tools have revealed a large number of genes encoding the P450 enzymes in *Streptomyces*.[163,164]

Cytochrome P450 enzymes usually function as monooxygenases that insert one atom of oxygen from molecular oxygen into a substrate while reducing the second oxygen atom to water. This is usually mediated by two-electron transfer from NAD(P)H via a flavoprotein or ferredoxin. The activation of molecular oxygen is common to all P450s, and this reaction takes place at the heme center. The proposed catalytic cycle of P450s is depicted in Figure 46. [165]

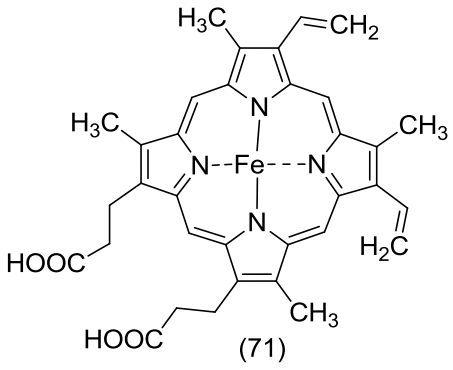

(71)

Figure 45.Protoporphyrin IX with a bound iron.

Table 3. Classes of P450 systems classified based on components involved in the electron transfer to the P450 enzyme		
Class/source	**Electron transport chain**	**Localization/ remarks**
Class I		
Bacterial	NAD(P)H ▸ [FdR] ▸ [Fdx] *▸ [P450]	Cytosolic, soluble
Mitochondrial	NADPH ▸ [FdR] ▸ [Fdx] ▸ [P450]	P450: inner mitochondrial membrane, FdR: membrane associated, Fdx: mitochondrial matrix, soluble
Class II		
Bacterial	NADH ▸ [CPR] ▸ [P450]	Cytosolic, soluble; *Streptomyces carbophilus*
Microsomal A	NADPH ▸ [CPR] ▸ [P450]	Membrane anchored, ER
Microsomal B	NADPH ▸ [CPR] ▸ [cytb5] ▸ [P450]	Membrane anchored, ER
Microsomal C	NADH ▸ [cytb5Red] ▸ [cytb5] ▸ [P450]	Membrane anchored, ER
Class III		
Bacterial	NAD(P)H ▸ [FdR] ▸ [Fldx] ▸ [P450]	Cytosolic, soluble, *Citrobacter braakii*
Class IV		
Bacterial	Pyruvat, CoA ▸ [OFOR] ▸ [Fdx] ▸ [P450]	Cytosolic, soluble, *Sulfolobus tokadaii*
Class V		
Bacterial	NADH ▸ [FdR] ▸ [Fdx–P450]	Cytosolic, soluble, *Methylococcus capsulatus*
Class VI		
Bacterial	NAD(P)H ▸ [FdR] ▸ [Fldx–P450]	Cytosolic, soluble, *Rhodococcus* strain *11Y*
Class VII		
Bacterial	NADH ▸ [PFOR–P450]	Cytosolic, soluble, *Rhodococcus* sp strain NCIMB 9784, Burkholderia sp., *Ralstonia metallidurans*
Class VIII		
Bacteria, fungi	NADPH ▸ [CPR–P450]	Cytosolic, soluble, *Bacillus megaterium*, *Fusarium oxysporum*
Class IX		
Only NADH dependent, fungi	NADH ▸ [P450]	Cytosolic, soluble, *Fusarium oxysporum*
Class X		
Independent in plants/mammals	[P450]	Membrane bound, ER

Redox center key: Fdx- iron-sulfur cluster; FdR- Ferredoxin reductase(FAD); CPR – cytochrome P450 reductase (FAD, FMN); Fldx – Flavodoxin (FMN); OFOR – 2-oxoacid:ferredoxin oxidoreductase (TPP, [4Fe-4S] cluster); PFOR – phthalate-family oxygenase reductase (FMN, [2Fe-2S] cluster); *Fdx – iron-sulfur cluster of type: [2Fe-2S], [4Fe-4S],[3Fe-4S], [3Fe-4S]/[4Fe-4S].[157]

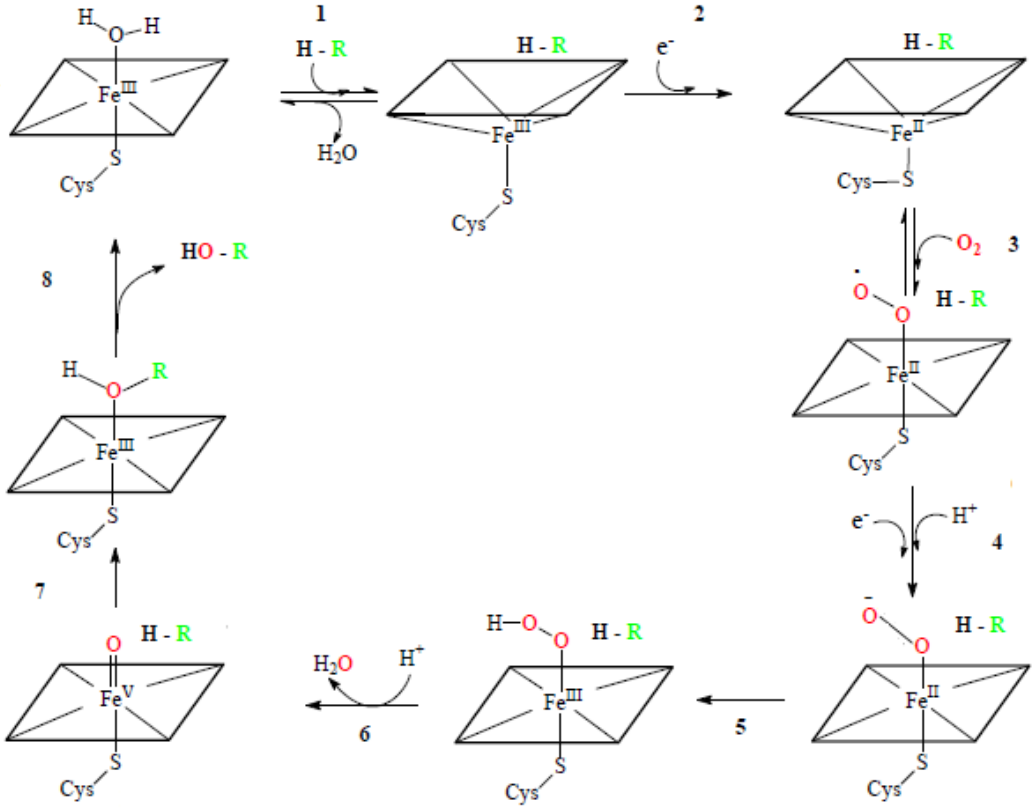

Figure 46.Proposed catalytic cycle of cytochrome P450.

Applications of Cytochrome P450

P450s play indispensible roles in both primary and secondary metabolic pathways. Drug metabolism and excretion would almost impossible without the intervention of P450s. Industrial biotransformations are carried out by P450; well-established commercial applications of P450 monooxygenase are in the biotransformation of steroids. Examples include the Reichstein S to hydrocortisone conversion through 11β-hydroxylation mediated by P450 in *Curvularia* sp, transformation of progesterone to cortisone by *Rhizopus* sp and the oxidation of

campactin to pravastatin (blood cholesterol lowering agent) by *Streptomyces* sp strain Y-110.[166-168] Other areas that have seen increased application of P450s are the environmental biodegradation of harmful compounds like pesticides, insecticides and other agro chemicals. CYP101 (P450cam) from *Pseudomonas putida* has been successfully used for the environmentally friendly biodegradation of pentachlorobenzene in the absence of either surfactant or organic co-solvents.[169] Bioremediation of highly toxic polychlorinated dibenzo-p-dioxins by hydroxylation was achieved by the use of mammalian P450,[170] and that of another toxic compound, 2,3,7-trichlorodibenzo-p-dioxin was effected with a triple mutant CYP102A1 from *Bacillus megaterium.*[171]

Cytochrome P450s have great potential in biotechnological and other industrial applications and giant strides have already been made; however, the co-factor requirement in P450 catalysis is a major setback. An enzyme-coupled system for the regeneration of NADPH/NADH is therefore necessary for successful application of P450 at the industrial level. Success in the industrial application of P450s also depends on an in-depth understanding of the redox partner requirement for each P450. Some of these limitations are being addressed by efforts in the recycling of NADH through an enzyme-coupled system for the CYP105D1 from *Streptomyces griseus* using formate dehydrogenase.[172]

Cytochrome P450 as Epoxidases

Cytochrome P450 catalyzes many reactions one of which is the epoxidation of olefins across the double bond by insertion of an oxygen atom. In some cases, epoxidation result in new compounds of physiological importance being made from naturally occurring substrate such as arachidonic acid.[173] Some foreign compounds have also been known to exert their mutagenic and carcinogenic effects after undergoing cytochrome P450-mediated epoxidation.[174] However, epoxidation by cytochrome P450 in natural product biosyntheses have produced compounds with remarkably increased potency. Cryptophycins are potent anticancer agents with about 25-analogues; and they have isolated from *Nostoc* sp. ATCC 53789. Studies have shown that *CrpE* (cyctochrome P450) - mediated epoxidation at the C2' and C3' of de-epoxycryptophycin-1 produces cryptophycin-1 (Figure 47), which exhibits >100 times more potency than its precursor.[175] Genetic disruption of *pimD* (cytochrome P450) in *Streptomyces natalensis* produced a novel polyene macrolide with decreased antifungal activity.[176,177] The cytochrome P450 epoxidase, *pimD* was discovered to convert the intermediate, 4, 5-de-epoxypiramicin to piramicin, a 26-member polyene macrolide antifungal antibiotic (Figure 47).

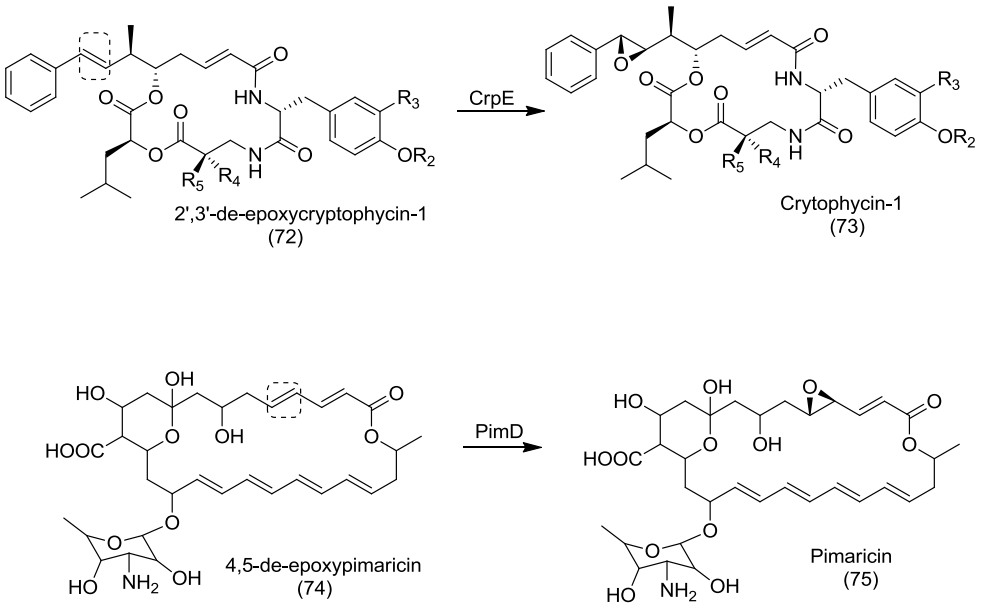

Figure 47.Cytochrome P450 catalyzed epoxidation reactions.

aziC9, a Cytochrome P450 in the Azinomycin Gene Cluster

The azinomycin gene cluster contains two cytochrome P450 hydroxylase genes, *aziB1* and *aziC9* (Figure 48). The role of *aziB1* has been established as being responsible for the catalysis of the regiospecific hydroxylation of free 5-methyl-naphthoic acid to produce 3-hydroxy-5-methyl-naphthoic acid. The hydroxyl group is later O-methylated by *az1B2*, a SAM-dependent O-methyltransferase to produce the methoxy functionality (Figure 49).[178] *aziC9,* on the other hand, has not been characterized and there are three oxidation events in the azinomycin B structure (Figure 50) for which no functional assignment of enzymes have been carried out. One of these oxidation steps is the formation of the epoxide moiety, which is known to strongly contribute to the DNA alkylation effect of azinomycin B.[117]

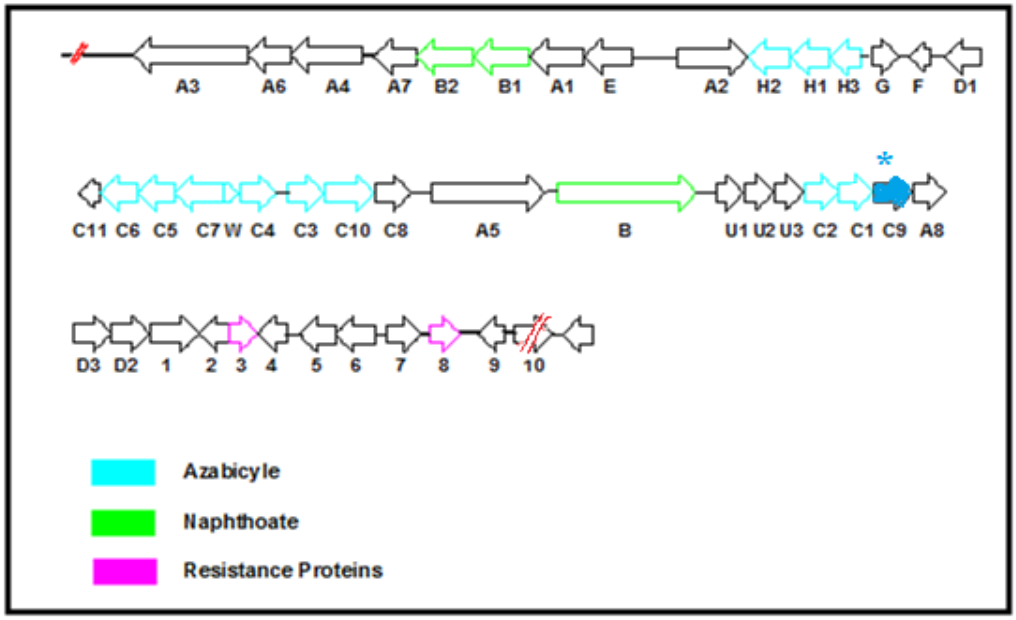

Figure 48.Azinomycin gene cluster showing cytochrome P450 in blue color.

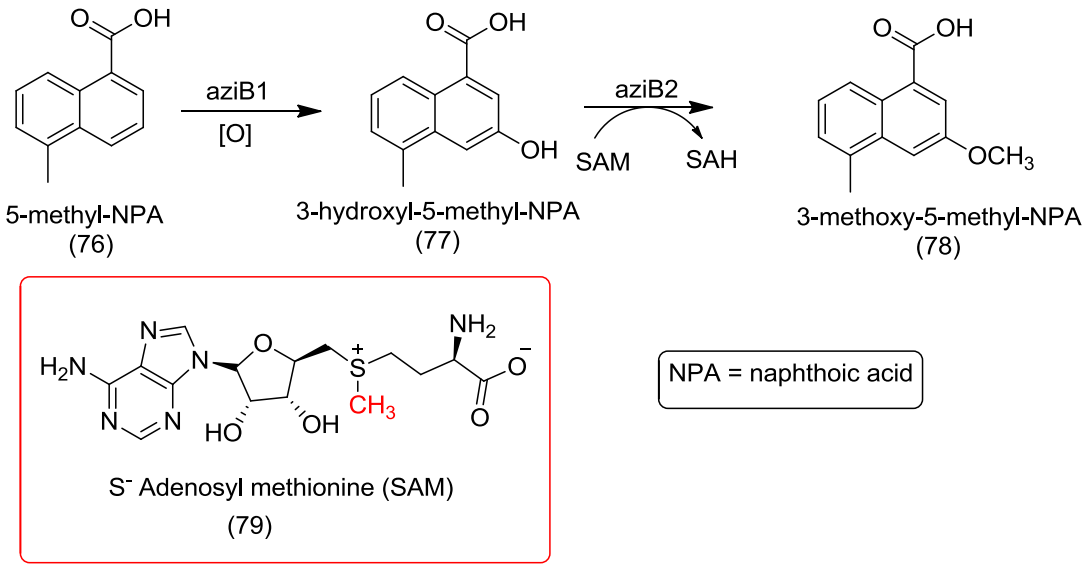

Figure 49.*aziB1*, cytochrome P450 catalyzed hydroxylation of 5-methyl-NPA.

Here, we aim to biochemically evaluate the role of the *aziC9*, cytochrome P450 in azinomycin B biosynthesis.

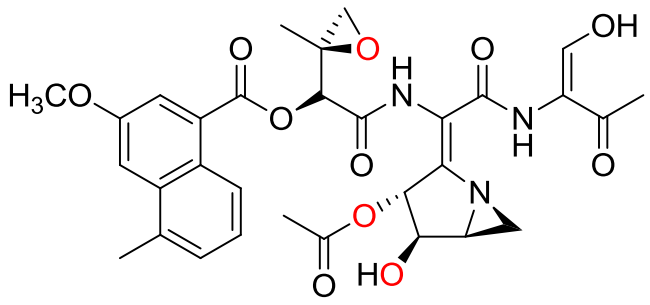

(37)

Figure 50.Oxidation steps in azinomycin shown in red color.

MATERIALS AND METHODS

Cloning, Overexpression and Purification of *aziC9*

All chemicals were bought from either Sigma or VWR. aziC9 gene was amplified by PCR using the wild type *S. sahachiroi* genomic DNA as a template with the primer pair AziC9-F and AziC9-R (Table 4) containing the restriction sites NdeI on the forward and XhoI on the reverse primers. PCR was performed in a final volume of 20 µl containing 0.4mM of each primer, 0.25 mM of each of the 4 dNTPs, 1 µl of extracted genomic DNA, 1 U of high fidelity phusion polymerase (NEB) in its recommended reaction buffer, and 10 % DMSO. Amplification was performed in a Thermal Cycler (BioRad, USA) according to the following profile: 98^{o}C for 30 s followed by 29 iterative steps of 98 ^{o}C for 10 s, 63 ^{o}C for 20 s, 72 ^{o}C for 30 s and a final 72 ^{o}C for 10 min. 1 U Taq DNA polymerase (NEB) was added to the mixture and

Table 4 Bacterial strains, plasmids and primers used in *aziC9* study

Strains, plasmids or primers	Relevant characteristics or primer sequence	Reference or source
Strains		
S. sahachiroi	Wild type azinomycin A and B-producing strain	ATCC
E.coli DH10B	General cloning host	Epicentre
E.coli BL21 (DE3)	Expression host	Invitrogen
Plasmids		
pGEM T-Easy	Cloning vector	Promega
pET24b	*E.coli* protein expression vector	Invitrogen
pET24b-AziC9	Protein expression plasmid	This study
Primers		
aziC9 -F	GCCATATGATTATTTCCAAGCCCCCGTTC	This study
aziC9 -R	GACTCGAGCCGTACGTGTGCCTCACGAGGA	This study

extension carried in the thermal cycler at 72 ^{o}C for 10 min. The PCR reaction mixtures were separated on a 1% agarose gel, the desired bands were excised from the agarose gel and the DNA extracted using a QIAquick gel extraction kit. Purified PCR product was ligated into a pGEM T-easy vector (Promega) according to the manufacturer's protocol and transformed in *E.coli* DH10B. Positive clones were selected followed by complete nucleotide sequence confirmation by Genetech Lab, Texas A&M University. The PCR product was finally subcloned into the pET24b (Invitrogen) and the resulting plasmid was designated pET24b-AziC9. This plasmid was transformed in *E.coli* BL21 (DE3) (Strategene) cells for inducible expression under a T7 promoter. A 5 mL overnight culture in LB Miller media and 50 μg/mL kanamycin was used to inoculate 1 L media and grown to 0.7 OD_{600}. The culture was induced with 1 mM IPTG (Sigma) and 0.5 mM aminolevulenic acid (Sigma); culture flask was transferred to 16 °C for 24 hr to achieve

optimal soluble expression. All remaining steps were performed on ice. Cells were collected by centrifugation, resuspended in 30 mL column binding buffer (50 mM Tris-HCl pH 7.5, 500 mM NaCl, 5 mM imidazole, 5% glycerol, 1 mM β-mercapoethnol (BME)) containing 1 mM phenylmethylsulfonyl fluoride, and lysed by sonication with a Branson Sonifier 450 (Branson Ultrasonics, Danbury, CT) fitted with a 5 mm microtip, output setting 6, duty cycle 50 %, for 8 cycles of 30 sec each. Cellular debris was pelleted by centrifugation, and the supernatant filtered with a 0.2 μm filter before applying to a pre-equilibrated HisTrap FF 5 mL column (GE Healthcare Life Sciences, Piscataway, NJ) at 1.5 mL/min. The column was washed with 300 mL column buffer containing 20 mM imidazole, and AziC9 was eluted with 30 mL column buffer containing 250 mM imidazole. The eluate was dialyzed by centrifugal ultrafiltration (Amicon Ultra-15 Centrifugal Filter Unit, Millipore, Billerica, MA) to a final concentration of 1 mg/mL in 50 mM NaH_2PO_4 pH 7.5, 5 % glycerol. To determine the purity of the protein, 10 μL of purified protein was mixed with 10 μl of 2x protein loading dye under denaturing condition (125 mM Tris-HCl pH 6.8, 4 % SDS, 20 % glycerol, 10 % BME, 0.004 % bromophenol blue). The mixture was boiled for 10 min at 100 ^{o}C, loaded on a 12 % SDS PAGE and separated by electrophoresis at 200 V for 30 min. The SDS PAGE was stained in Coomasie blue dye by boiling for 45 s and destained after 5 min.

Carbon Monoxide (CO) Binding Assay

The absorbance spectra of P420 and P450 were recorded in 50 mM phosphate buffer, pH 7.5, using a Genesys 2 spectrophometer (Thermo Spectronic, USA) at 25 ^{o}C with a 1-cm light path cuvette. P420 was reduced by the addition of 1 mg of pure sodium dithionite; CO gas was bubbled into the sample for about 20 s and the tube capped to saturate the sample with CO. The absorbance of unreduced P420 was measured versus the reduced sample.

***aziC9*, Cytochrome P450 Assay**

The activity of *aziC9* was tested by reaction with the substrate, 3-methyl-2-oxobut-3-enoate according to the protocol below. 1 µM *aziC9*, 2 mM substrate, 5 µM ferredoxin, and 0.1 U spinach ferredoxin reductase were mixed and reaction volume brought up to 200 µL with 50 mM phosphate buffer. The mixture was incubated at 37 ^{o}C for 3 min followed by the addition of 0.5 mM NADPH and the incubation continued for 60 min. Reaction mixture was extracted with ethyl acetate and the sample analyzed by mass spectrometry under electron spray ionization mode (ESI).

RESULTS AND DISCUSSION

Expression and Purification of *aziC9*

To evaluate the function of AziC9, the gene was cloned into pET24b (Figure 51A) and overexpressed in *E.coli* Bl21 (DE3) (Table 4) under the control of the T7 promoter. Protein purification was performed by the affinity method using a HisTap FF

column (see methods). A brownish-yellow protein (Figure 51B) was recovered after elution with 250 mM imidazole. SDS PAGE analysis showed an approximately 98 % pure protein migrating at about 51 kDa (Figure 51C), a mass which corresponds to the calculated molecular weight of AziC9 plus the His_6-tag (M_r = 51351). The protein buffer was changed to 50 mM phosphate buffer, pH 7.5 and the concentration measured by UV absorbance at 280 nm and extinction coefficient of 4630 M^{-1} cm^{-1}. 1 mL of 2 µM was recovered.

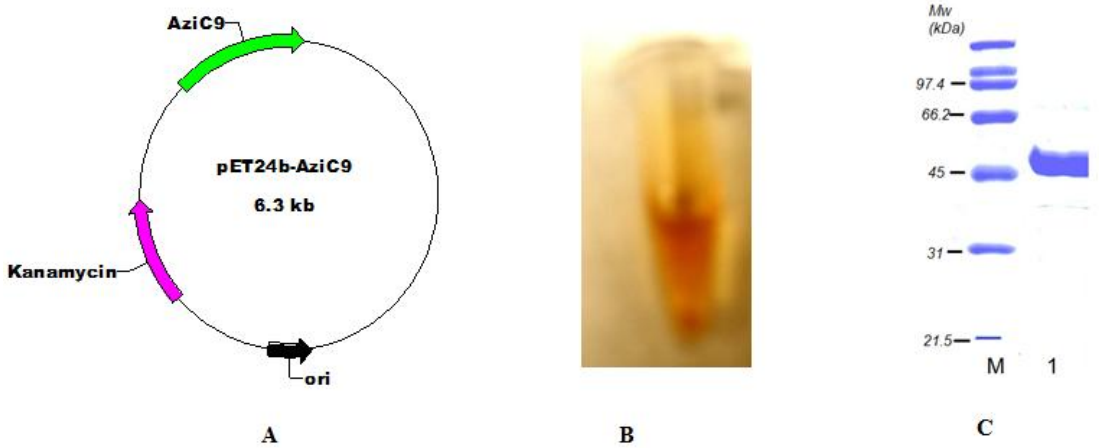

Figure 51. pET24b-aziC9 plasmid and SDS PAGE analysis of *aziC9*.(A) Expression plasmid, pET24b-AziC9. (B) Brownish yellow pure *aziC9*. (C) SDS PAGE analysis of *aziC9*, M is protein marker while lane 1 is purified AziC9.

Spectral Properties of *aziC9*

Purified *aziC9* has a P420 absorbance but it displays a small shift in absorbance corresponding to P450 upon reduction with sodium dithionite and carbon monoxide (Figure 52). However, the difference absorbance spectra (reduced P420 as control and reduced P420 + CO for 20 s as sample) that showed absorbance at above 420 nm cannot

be said to have peaked at 450 nm (Figure 52). Overall these results are suggestive of the identity of *aziC9* as a cytochrome P450. The reduction of P420 under atmospheric conditions instead of anaerobic conditions might be responsible for the less-than-expected CO binding result in *aziC9*.

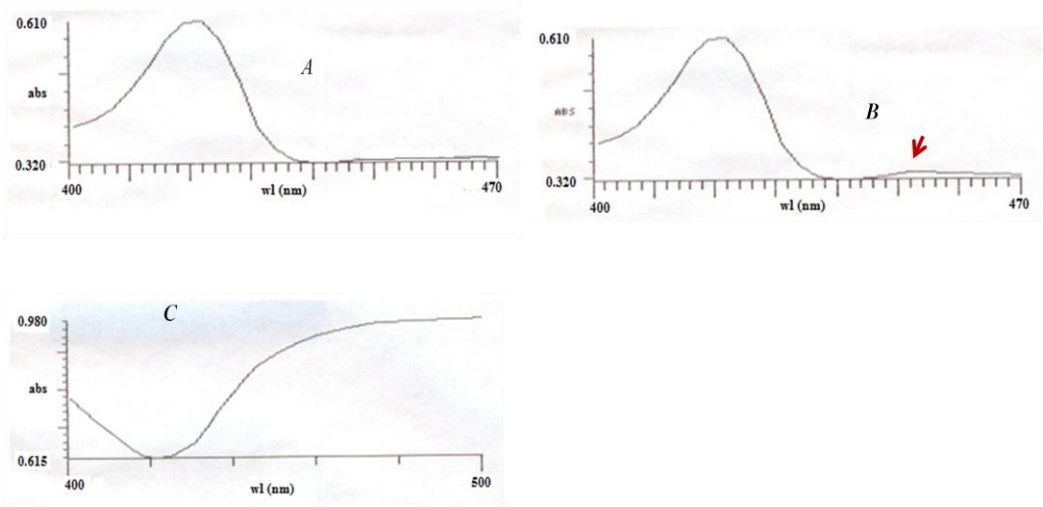

Figure 52.Carbon Monoxide (CO) binding study of a*ziC9*. (A) Oxidized P420; (B) Reduced P450 + CO and P420; (C) difference spectra of reduced P420 and B above.

Sequence Alignment of *aziC9*

To further confirm that *aziC9* is an authentic cytochrome P450, the translated amino acid sequence was searched against other bacterial genome sequences using the NCBI BLAST tool and some homologous sequence aligned and analyzed by Gene doc free software. As expected, *aziC9* harbors the signature heme-binding motif containing the unique cysteine residue which co-ordinates the heme center (Figure 53).

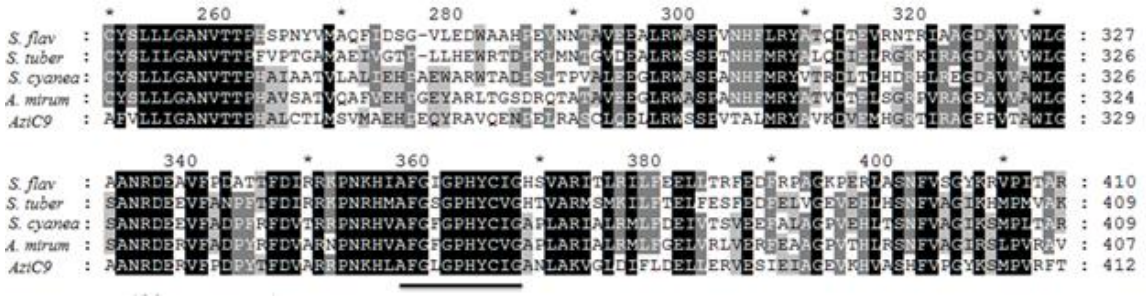

Figure 53.Multiple sequence alignment of *aziC9* with its homologues. (S. flav*: Streptomyces flavogriseus*, 41% identity; S. tuber: *Streptomyces tubercidius*, 39% identity; S. cyanea: *Saccharomonospora cyanea* NA-134, 43% identity; A. mirum: *Actinosynnema mirum* DSM 43827, 45% identity. Heme binding motif (AFGXGXHXCXG) is underlined.

Protein sequence alignment of *aziC9* and other well characterized epoxidases (*pimD*, *OleP*, *CrpE*) showed marked reduction in sequence identity (Figure 54). However, the unique heme binding motif is conserved is all sequences. This apparent reduction in sequence identity may be attributed to differences in substrate requirements for individual enzymes. This further identifies *aziC9* as a cytochrome P450; maybe more specifically, an epoxidase.

Figure 54.Multiple sequence alignment of *aziC9* with other P450 epoxidases. PimD from *Streptomyces natalensis*; Olep from *Streptomyces antibioticus* and CrpE from *Nostoc* sp. ATCC 53789. Underlined is the heme binding motif (See Figure 45).

Conversion of 3-methyl-2-oxobut-3-enoate to the Epoxide

The enzymatic activity of *aziC9* was measured by testing its ability to convert 3-methyl-2-oxobut-3-enoate to the epoxy-3-methyl-2-oxobutanoate. Purified *aziC9* was incubated with 3-methyl-2-oxobut-3-enoate; the redox partners and NADPH for 60 min at 37 ^{o}C (see methods) (Figure 55). The ethyl acetate extract of the reaction mixture was concentrated *in vacuo* and subjected to mass analysis. The result is promising but not definite owing to the low concentration of enzyme and substrate available at the time. The reaction is being optimized and will be repeated to confirm the product of this reaction. However, it is not clear at what stage the oxidation takes place in the biosynthesis of azinomycin. A preponderance of data support post PKS/NRPS tailoring of intermediates by cytochrome P450s. If this is this case here, it is then expected that reaction with 3-methyl-2-oxobut-3-enoate, a non-natural substrate of *aziC9*, might not result in any substantial amount of the corresponding epoxide. Gene disruption of AziC9 still remains one of the most viable routes to the full characterization of this enzyme. Disruption would most likely result in the accumulation of an intermediate which could be isolated and used as a natural substrate for *aziC9*.

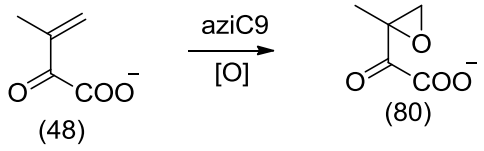

Figure 55.*aziC9* reaction with 3-methyl-2-oxobut-3-enoate.

CHAPTER V

CONCLUSION

The importance of natural products to the survival of humans and other living organisms cannot be over-emphasized. It is still being used extensively in folk medicine especially in developing countries. Understanding how microorganisms and plants make these complex medicinal compounds is a crucial step in taking advantage of nature's gift to humanity. This era has certainly witnessed an upsurge in evolutionary diseases and emergence of superbugs.

The advancement in science and technology, and the existing downward trend in the cost of sequencing of bacterial genomes marked a shift towards genetic and biomolecular approaches toward understanding these biochemical transformations in microbes. These efforts are already paying off in terms of successful natural products approved as drugs by the FDA and more detailed understanding of many complex product pathways.

Azinomycin B has continued to attract the interest of researchers since its initial discovery due to its biological activity and unique structural features. The identification of the biosynthetic gene cluster has inched us closer to the biosynthetic rationalization of this complex architectural anticancer/antitumor compound. Until the enzymatic transformations leading to the aziridine and epoxyvaline moieties and the entire structure are fully understood, the prospect of engineering a more stable and target-specific azinomycin B will remain elusive. Our research group's effort at developing an *in situ*

drug delivery system via a plasmid bearing cancer cell inducible promoter will receive a boost when a more complete understanding of azinomycin biosynthesis is brought to bear.

Gene disruption of ORF10, a putative dehydrogenase and the analysis of the metabolite revealed no apparent change in the production of azinomycin B. The native substrate of this enzyme was not biochemically established and this substrate could as well be the product of some other enzymatic reactions. The involvement of ORF10 in a shunt pathway to azinomycin could not be categorically determined based on the foregoing. However, it did firmly confirm that ORF10 is not part of the azinomycin B gene cluster.

AziC9 was evaluated and shown to be an authentic cyctochrome P450. This family of enzymes catalyzes oxidative reactions which increase both the complexity and bioactivities of natural product. Full characterization of *aziC9* will rely on gene disruption and gene complementation followed by the analysis of the metabolites in each case.

The azinomycin gene cluster contains genes whose products have not been characterized. For example, *aziW* had not been previously annotated and the disruption of which abolished the production of azinomycin. Sequence analysis suggests that this gene is transcribed as polycistronic RNA with the downstream genes. The mRNA expression profile showed a polar effect on downstream genes following disruption of *aziW*. Further studies will be needed to evaluate the role of *aziW* in azinomycin biosynthesis.

Three experiments were discussed here and they open up platforms for the further study of azinomycin biosynthesis. These studies established the boundary of the azinomycin gene cluster and identified *aziC9* as a true cytochrome P450. The identification of specific roles of these genes will be invaluable to combinatorial and protein engineering groups who are interested in biosynthetic solutions to bioactive compounds.

REFERENCES

1. Butler, M. S. (2004). The role of natural product chemistry in drug discovery. *J Nat Prod. 67*, 2141- 2153.

2. Newman, D.J., and Cragg, G.M. (2012). Natural products as sources of new drugs over the 30 years from 1981 to 2010. *J Nat Prod.75*, 311 - 355.

3. Ueda, H., Nakajima, H., Hori, Y., Fujita, T., Nishimura, M., Goto, T., and Okuhara, M. (1994) FR901228, a novel antitumor bicyclic depsipeptide produced by *Chromobacterium violaceum* No. 968. I. Taxonomy, fermentation, isolation, physico-chemical and biological properties, and antitumor activity. *J. Antibiot. 47*, 301-310.

4. Ueda, H., Nakajima, H., Hori, Y., Goto, T., and Okuhara, M. (1994) Action of FR901228, a novel antitumor bicyclic depsipeptide produced by *Chromobacterium violaceum* no. 968, on Ha-ras transformed NIH3T3 cells. *Biosci. Biotechnol. Biochem*. *58*, 1579-1583.

5. Wang, H. C.R. (1999) Antineoplastic antibiotic. *Drugs Future 24*, 1184-1188.

6. VanderMolen, K. M., McCulloch, W., Pearce, C. J., and Oberlies, N. H. (2011) Romidepsin (Istodax, NSC 630176, FR901228, FK228, depsipeptide): a natural product recently approved for cutaneous T-cell lymphoma. *J. Antibiot. 64,* 525-531.

7. Li, K.W., Wu, J., Xing, W., and Simon, J.A. (1996) Total synthesis of the antitumor desipeptide FR-901,228. *J. Am.Chem. Soc. 118*, 7237-7238.

8. Wani, M.C., Taylor, H.L., Wall, M.E., Coggon, P., and McPhail, A.T. (1971) Plant antitumor agents. VI. Isolation and structure of taxol, a novel antileukemic and antitumor agent from *Taxus brevifolia*. *J. Am.Chem. Soc. 93*, 2325-2327.

9. Fuchs, D.A., and Johnson, R.K. (1978) Cytologic evidence that taxol, an antineoplastic agent from *Taxus brevifolia*, acts as a mitotic spindle poison. *Cancer Treatment Reports 62*, 1219-1222.

10. Stephenson, F. (2002) A tale of taxol. Available: rnr.fsu/2002/taxol.html.

11. Goodman, J., and Walsh, V. (2001) *The story of taxol: nature and politics in the pursuit of an anti-cancer drug*. Cambridge University Press, New York. p17.

12. Kingston, D.G.I. (2001) Taxol, a molecule for all seasons. *Chemical Communications*, 867-880.

13. Levine, Donald P. (2006) Vancomycin: a history. *Clinical Infectious Diseases 42*, S5-S12.

14. Collie, J. N. (1907) Derivatives of the multiple keten group. *J. Chem. Soc*. 1806-1813.

15. Georgievski Z,, Koklanis K., and Leone J. (2008) Fixation behavior in the treatment of amblyopia using atropine. *Clinical and Experimental Ophthalmology 36* (Suppl 2), A764–A765.

16. *Robinson,* R. (1917) The structural relations of natural products. *J. Chem. Soc.* (London) *111*, 762-776.

17. Birch, A. J., Massy-Westropp, R. A., and Moye, C. J. (1955) The biosynthesis of 6-hydroxy-2-methylbenzoic acid. *Chem. and Ind*. 683-688

18. Shoolingin-Jordan, P. M., and Campuzano, I. D. G. (1999) Polyketides and other secondary metabolites including faty acids and their derivatives. *Comprehensive natural products chemistry*. Edited by Sankawa, U., Elsevier, Oxford. pp. 345-365.

19 Alberts, A.W., Strauss, A.W., Hennessy S., and Vagelos, P.R. (1975). Regulation of synthesis of hepatic fatty acid synthetase: binding of fatty acid synthetase antibodies to polysomes. *Proc.Natl. Acad. Sci. U.S.A. 72*, 3956-3960.

20. Stoops, J. K., Arslanian, M. J., Oh, Y. H., Aune, K.C., Vanaman, T.C., and Wakil, S. J. (1975) Presence of two polypeptide chains comprising fatty acid synthetase. *Proc.Natl. Acad. Sci. U.S.A. 72*, 1940-1944.

21. Smith, S., Agradi, E., Libertini, L., and Dileepan, K.N. (1976) Specific release of the thioesterase component of the fatty acid synthetase multienzyme complex by limited trypsinization. *Proc.Natl. Acad. Sci. U.S.A. 73*, 1184-1188.

22. Fischbach, M. A., and Walsh, C. T. (2006) Assembly-line enzymology for polyketide and nonribosomal peptide antibiotics: logic, machinery, and mechanisms. *Chem. Rev. 106*, 3468-3496.

23. Cortes, J., Haydock, S.F., Roberts, G.A., Bevitt, D.J., and Leadlay, P.F. (1990) An unusually large multifunctional polypeptide in the erythromycin-producing polyketide synthase of *Saccharopolyspora erythraea*. *Nature 348*, 176-178.

24. Bevitt, D.J., Cortes, J., Haydock, S.F., and Leadlay, P.F. (1992) 6-deoxyerythronolide-B synthase 2 from *Saccharopolyspora erythraea*: cloning of the structural gene, sequence analysis and inferred domain structure of the multifunctional enzyme. *Eur J Biochem. 204*, 39.

25. Staunton, J., and Weissman, K.J. (2001) Polyketide biosynthesis: a millennium review. *Nat. Prod. Rep. 18*, 380-416.

26. Otsuka,M., Ichinose, K., Fujii, I., and Ebizuka, Y. (2004) Cloning sequencing, and functional analysis of an iterative type I polyketide synthase gene cluster for biosynthesis of the antitumor chlorinated polyenone neocarzilin in *Streptomyces carzinostaticus*. *Antimicrobial Agents and Chemotherapy 48*, 3468- 3476.

27. Shao, L., Qu, X. D., Jia, X.Y., Zhao, Q. F., Tian, Z. H., Wang, M., Tang, G. L., and Liu, W. (2006) Cloning and characterization of a bacterial iterative type I polyketide synthase gene encoding the 6-methylsalicyclic acid synthase. *Biochemical and Biophysical Research Communications 345*, 133-139.

28. Liu, W., Nonaka, K., Nie, L., Zhang, J., Christenson, S.D., Bae, J., Van Lanen, S. G., Zazopoulos, E., Farnet, C. M., Yang, C. F., and Shen, B (2005) The neocarzinostatin biosynthetic gene cluster from *Streptomyces carzinostaticus* ATCC 15944 involving two iterative type I polyketide synthases. *Chemistry & Biology 12*, 293-302.

29. Zhao, Q., He, Q., Ding, W., Tang, M., Kang, Q., Yu, Y., Deng, W., Zhang, Q., Fang, J., Tang, G., and Liu, W. (2008) Characterization of the azinomycin B biosynthetic gene cluster revealing a different iterative type I polyketide synthase for naphthoate biosynthesis. *Chemistry & Biology 15*, 693-705.

30. Moriguchi, T., Kezuka, Y., Nonaka, T., Ebizuka, Y., and Fujii, I. (2010) Hidden function of catalytic domain in 6-methylsalicylic acid synthase for product release. *J. Biol. Chem. 285*, 15637-15643.

31. Staunton, J., and Weissman, K. J. (2001) Polyketide biosynthesis: a millennium review. *Nat. Prod. Rep. 18*, 380-416.

32. Jez, J. M., Austin, M. B., Ferrer, J.L., Bowman, M. E., Schroder, J., and Noel, J. P. (2000) Structural control of polyketide formation in plant-specific polyketide synthases. *Chem. Biol. 7*, 919-930.

33. Jez, J. M., Bowman, M. E., and Noel, J. P. (2001) Structure-guided programming of polyketide chain-length determination in chalcone synthase . *Biochemistry 49*, 14829-14838.

34. Jez, J. M., Bowman, M. E., and Noel, J. P. (2002) Expanding the biosynthetic repertoire of plant type III polyketide synthases by altering starter molecule specificity. *Proc. Natl. Acad. Sci. U.S.A. 99*, 5319 -5324.

35. Ducki, S., Forrest, R., Hadfield, J.A., Kendall, A., Lawrence, N.J., McGown, A.T., and Rennison, D. (1998) Potent antimitotic and cell growth inhibitory properties of substituted chalcones. *Bioorganic and Medicinal Chemistry Letters 8*, 1051-1056.

36. Yarishkin, O. V., Ryu, H. W., Park, J. Y., Yang, M. S., Hong, S. G., and Park, K. H. (2008) Sulfonate chalcone as new class voltage-dependent K+ channel blocker. *Bioorganic & Medicinal Chemistry Letters 18*, 137-140.

37. Belmont, P., Bosson, J., Godet, T., and Tiano, M. (2007) Acridine and acridone derivatives, anticancer properties and synthetic methods: where are we now? *Anticancer Agents Med Chem 2*, 139-169.

38. Kelly, J.X., Smilkstein, M.J., Brun, R., Wittlin, S., Cooper, R. A., Lane, K.D., Janowsky, A., Johnson, R.A., Dodean, R.A., Winter, R., Hinrichs, D.J., and Riscoe, M. K. (2009) Discovery of dual function acridones as a new antimalarial chemotype. *Nature 459*, 270-273.

39. Ferrer, J. L. Jez, J. M., Bowman, M. E., Dixon, R. A., and Noel, J. P. (1999) Structure of chalcone synthase and the molecular basis of plant polyketide biosynthesis. *Nat. Struct. Biol. 6*, 775-784.

40. Widdick, D. A., Dodd, H. M., Barraille, P., White, J., Stein, T. H., Chater, K.F., Gasson, M.J., and Bibb, M. J. (2003) Cloning and engineering of the cinnamycin biosynthetic gene cluster from *Streptomyces cinnamoneus* DSM 40005. *Proc.Natl. Acad. Sci. U.S.A. 100*, 4316-4321.

41. Wilkinson, B., and Micklefield, J. (2007) Mining and engineering natural-product biosynthetic pathways. *Nat. Chem. Biol. 3*, 379-386.

42. McIntosh, J. A., Donia, M. S., and Schmidt, E. W. (2009) Ribosomal peptide natural products: bridging the ribosomal and nonribosomal worlds. *Nat. Prod. Rep. 26*, 537-559.

43. van Kraaij, C., de Vos, W. M., Siezen, R. J., and Kuipers, O. P. (1999) Lantibiotics: biosynthesis, mode of action and applications. *Nat. Prod. Rep. 5*, 575-585.

44. Chatterjee, C., Paul, M., Xie, L., and van der Donk, W.A. (2005) Biosynthesis and mode of action of lantibiotics. *Chem. Rev. 105*, 633- 684.

45. Morris, S. L., Walsh, R. C., and Hansen, J. N. (1984) Identification and characterization of some bacterial membrane sulfhydryl groups which are targets of bacteriostatic and antibiotic action. *J. Biol. Chem. 259*, 13590-13594.

46. Hancock, J.F., Paterson, H., and Marshall, C.J. (1990) A polybasic domain or palmitoylation is required in addition to the CAAX motif to localize p21ras to the plasma membrane. *Cell 63*, 133-139.

47. Bulaj, G. (2005) Formation of disulfide bonds in proteins and peptides. *Biotechnol Adv. 23*, 87- 92.

48. Eijsink, V.G, Skeie, M., Middelhoven, P. H., Brurberg, M. B., and Nes, I. F. (1998) Comparative studies of class IIa bacteriocins of lactic acid bacteria. *Appl Environ Microbiol*. *64*, 3275-3281.

49. Schmidt, E.W., Nelson, J.T., Rasko, D.A., Sudek, S., Eisen, J.A., Haygood, M.G., and Ravel, J. (2005) Patellamide A and C biosynthesis by a microcin-like pathway in Prochloron didemni, the cyanobacterial symbiont of *Lissoclinum patella*. *Proc. Natl. Acad. Sci. U.S.A.* 102, 7315-7320.

50. Metlitskaya, A., Kazakov, T, Kommer, A., Pavlova, O., Praetorius-Ibba, M., Ibba, M., Krasheninnikov, I., Kolb, V., Khmel, I., and Severinov, K. (2006) Aspartyl-tRNA synthetase is the target of peptide nucleotide antibiotic, Microcin C. *J. Biol. Chem. 281*, 18033-18042.

51. van der Meer, J.R., Rollema, H.S., Siezen, R.J., Beerthuyzen, M.M., Kuipers, O.P., and De Vos, W.M. (1994) Influence of amino acid substitution in the nisin leader peptide on biosynthesis and secretion of nisin by *Lactococcus lactis*. *J. Biol.Chem 269*, 3555-3562.

52. van der Meer J.R., Polman, J., Beerthuyzen, M.M., Siezen, R.J., Kuipers, O.P., and De Vos, W.M. (1993) Characterization of the *Lactococcus lactis* nisin A operon genes, *nisP*, encoding a subtilisin-like serine protease involved in the precursor processing, and *nisR*, encoding a regulatory protein involved in nisin biosynthesis. *J. Bacteriol 175*, 2578-2588.

53. Furgerson Ihnken, L.A., Chatterjee, C., and van der Donk, W.A. (2008) In vitro reconstitution and substrate specificity of a lantibiotic protease. *Biochemistry 47*, 7352-7363.

54. Chen, P., Qi, F.X., Novak, J., Krull, R.E., and Caufield, P.W. (2001) Effect of amino acid substitutions in conserved residues in the leader peptide on biosynthesis of the lantibiotic mutacin II. *FEMS Microbiol. Lett. 195*, 139-144.

55. Allali, N., Afif, H., Couturier, M., and Van Melderen, L. (2002) The highly conserved TldD and *TldE* proteins of *Escherichia coli* are involved in microcin B17 processing and in CcdA degradation. *J. Bacteriol. 184*, 3224-3231.

56. Wirawan, R. E., Swanson, K. M., Kleffmann, T., Jack, R.W., and Tagg, J. R. (2007) Uberolysin: a novel cyclic bacteriocin produced by *Streptococcus uberis. Microbiology 153*, 1619-1630.

57. Fujita, K., Ichimasa, S., Zendo, T., Koga, S., Yoneyama F., Nakayama, J., and Sonomoto, K. (2007) Structural analysis and characterization of lacticin Q, a novel bacteriocin belonging to a new family of unmodified bacterocins of gram-positive bacteria. *Appl. Environ. Microbiol. 73*, 2871-2877.

58. Qiu, R., Pei, W., Zhang, L., Lin, J., and Ji, G. (2005) Identification of the putative staphylococcal *AgrB* catalytic residues involving the proteolytic cleavage of *AgrD* to generate autoinducing peptide. *J. Biol. Chem. 280*, 16695-16704.

59. Guijarro J, I., Gonzalez-Pastor, J. E., Baleux, F., San Millan, J.L., Castilla, M. A., Rico, M., Moreno, F., and Delepierre, M. (1995) Structure and organization of plasmid genes required to produce the translation inhibitor microcin C7. *J. Biol. Chem. 270*, 23520-23532.

60. Thomas, X., Destoumieux-Garzon, D., Peduzzi, J., Afonso, C., Blond, A., Birlirakis, N., Goulard, C., Dubost, L., Thai, R., Tabet, J.C., and Rebuffat, S. (2004) Siderophore peptide, a new type of posttranslationally modified antibacterial peptide with potent activity. *J. Biol. Chem. 279*, 28233-28242.

61. Caboche, S., Pupin, M., Leclere, V., Fontaine, A., Jacques, P., and Kucherov, G. (2008) NORINE: a database of nonribosomal peptides. *Nucleic Acids Research 36*, D326-331.

62. Byford, M.F., Baldwin, J.E., Shiau, C.Y, Schofield, C.J. (1997) The mechanism of ACV synthetase. *Chem. Rev. 97*, 2631-2650.

63. Hori, K., Yamamoto, Y., Minetoki, T., Kurotsu, T., Kanda, M., Miura, S., Okamura, K., Furuyama, J., and Saito, Y. (1989) Molecular cloning and nucleotide sequence of the gramicidin S synthetase 1 gene. *J Biochem. 106*, 639-645.

64. Fischbach, M. A., and Walsh, C. T. (2006) Assembly-line enzymology for polyketide and nonribosomal Peptide antibiotics: logic, machinery, and mechanisms. *Chemical Reviews 106*, 3468-3496.

65. Marahiel, M.A. (1997) Protein templates for the biosynthesis of peptide antibiotics. *Chem. Biol. 4*, 561-567.

66. Eriani, G., Delarue, M., Poch, O., Gangloff, J., and Moras, D. (1990) Partition of tRNA synthetases into two classes based on mutually exclusive sets of sequence motifs. *Nature 347*, 203-206.

67. Ehmann, D.E., Shaw-Reid, C. A., Losey, H. C., and Walsh, C. T. (2000) The *EntF* and *EntE* adenylation domains of *Escherichia coli* enterobactin synthetase: sequestration and selectivity in acyl-AMP transfers to thiolation domain cosubstrates. *Proc. Natl. Acad. Sci. U.S.A. 97*, 2509-2514.

68. Stachelhaus, T., Mootz, H.D., Bergendahl, V., and Marahiel, M.A. (1998) Peptide bond formation in nonribosomal peptide biosynthesis.Catalytic role of the condensation domain. *J. Biol. Chem. 273*, 22773-22781.

69. Weber, G., Schorgendorfer, K., Schneider-Scherzer, E., and Leitner, E. (1994) The peptide synthetase catalyzing cyclosporine production in *Tolypocladium niveum* is encoded by a giant 45.8-kilobase open reading frame. *Curr. Genet. 26*,120-125.

70. Guenzi, E., Galli, G., Grgurina, I., Gross, D. C., and Grandi, G. (1998) Characterization of the syringomycin synthetase gene cluster. A link between prokaryotic and eukaryotic peptide synthetases. *J. Biol. Chem. 273*, 32857-32863.

71. Marahiel, M. A., Stachelhaus, T., and Mootz, H. D. (1997) Modular peptide synthetases involved in nonribosomal peptide synthesis. *Chem. Rev. 97*, 2651-2674.

72. Guenzi, E., Galli, G., Grgurina, I., Pace, E., Ferranti, P., and Grandi, G. (1998) Coordinate transcription and physical linkage of domains in surfactin synthetase are not essential for proper assembly and activity of the multienzyme complex. *J. Biol. Chem. 273*, 14403-14410.

73. Mootz, H.D., Schwarzer, D., and Marahiel, M. A. (2002) Ways of assembling complex natural products on modular nonribosomal peptide synthetases. *ChemBioChem. 3*, 490-504.

74. Peypoux, F., Bonmatin, J. M., and Wallach, J. (1999) Recent trends in the biochemistry of surfactin. *Appl. Microbiol. Biotechnol. 51*, 553-563.

75. Kratzschmar, J., Krause, M., and Marahiel, M.A. (1989) Gramicidin S biosynthesis operon containing the structural genes *grsA* and *grsB* has an open reading frame encoding a protein homologous to fatty acid thioesterases. *J. Bacteriol. 171*, 5422-5429.

76. Turgay, K., Krause, M., and Marahiel, M. A. (1992) Four homologous domains in the primary structure of *GrsB* are related to domains in a superfamily of adenylate-forming enzymes. *Mol. Microbiol. 6*, 529-546.

77. Du, L., Chen, M., Zhang, Y., and Shen, B. (2003) *BlmIII* and *BlmIV* nonribosomal peptide synthetase-catalyzed biosynthesis of the bleomycin bithiazole moiety involving both in *cis* and in *trans* aminoacylation. *Biochemistry 42*, 9731-9749.

78. Marshall, C. G., Hillson, N. J., and Walsh, C. T. (2002) Catalytic mapping of the vibriobactin biosynthetic enzyme VibF. *Biochemistry 41*, 244-250.

79. Eberhard, B. (2006) *Terpenes: flavors, fragrances, pharmaca, pheromones*. Wiley, New York.

80. Davis, E. M., and Croteau, R. (2000) Cyclization enzymes in the biosynthesis of monoterpenes, sesquiterpenes, and diterpenes, *Biosynthesis: aromatic polyketides, isoprenoids, alkaloids 209*, 53-95.

81. Dewick, P.M. (2009) *Medicinal natural products: a biosynthetic approach*, 3rd ed. Wiley, New York.

82. Eisenreich, W., Schwarz, M., Cartayrade, A., Arigoni, D., Zenk, M. H., and Bacher, A. (1998) The deoxyxylulose phosphate pathway of terpenoid biosynthesis in plants and microorganisms. *Chem. Biol. 5*, R221-R233.

83. Dogbo, O., Laferriere, A., D' Harlingue, A., and Camara, B. (1988) Isolation and characterization of a bifunctional enzyme catalyzing the synthesis of phytoene. *Proc. Natl. Acad. Sci. U.S. A. 85*, 7054-7058.

84. Krinsky, N. I. (1994) The biological properties of carotenoids. *Pure Appl. Chem. 66*, 1003-1010.

85. Di Mascio, P., Kaiser, S., and Sies, H. (1989) Lycopene as the most efficient biological carotenoid singlet oxygen quencher. *Arch. Biochem. Biophys 274*, 532-538.

86. Goodman, D. S., Huang, H. S. Kanai, M., and Shiratori, T. (1967) The enzymatic conversion of *all-trans* β-carotene into retinal. *J. Biol. Chem.*, *242*, 3543-3554.

87. Goodman, D. S., Huang, H. S., Kanai, M., and Shiratori, T. (1966) Mechanism of the biosynthesis of vitamin A from β-carotene. *J. Biol. Chem.* 241, 1929-1932.

88. Leuenberger, M. G., Engeloch-Jarret, C., and Woggon, W. D. (2001) The reaction mechanism of the enzyme-catalysed central cleavage of beta-carotene to retinal. *Angew. Chem. 40*, 2614-2616.

89. Wald, G. (1968) The molecular basis of visual excitation. *Nature 219*, 800-807.

90. Sparrow, J. R., and Boulton, M. (2005) RPE lipofuscin and its role in retinal pathobiology. *Exp. Eye Res. 80*, 595-606.

91. Newman, D. J. (2008) Natural products as leads to potential drugs: an old process or the new hope for drug discovery? *J. Med. Chem. 51*, 2589-2599.

92. Borman, S. (2002) Combinatorial chemistry: advances in synthesis, purification, and analysis further refine the combinatorial approach, now a mainstream tool in drug discovery, *C&EN Washington 45*, 43-57.

93. Shen, B. (2004) Accessing natural products by combnatorial biosynthesis. *Science: STKE,* pe14.

94. Strohl, W. R. (2001) Biochemical engineering of natural product biosynthesis pathways. *Metab. Engin. 3*, 4-14.

95. Cane, D.E., Walsh, C.T., and Khosla, C. (1998) Harnessing the biosynthetic code: combinations, permutations, and mutations. *Science 282*, 63-68.

96. Walsh, C. T. (2002) Combinatorial biosynthesis of antibiotics: challenges and opportunities. *ChemBioChem. 3*, 125-134.

97. Paradkar, A., Trefzer, A., Chakraburtty, R., and Stassi, A. (2003) *Streptomyces* genetics: a genomic perspective. *Crit. Rev. Biotechnol. 23*, 1-27.

98. August, P. R., Lang, L. T., Yoon, Y. J., Ning, S., Muller, R., Yu, T.W., Taylor, M., Hoffmann, D., Kim, C. G., Zhang, X., Hutchinson, C. R., and Floss, H.G (1998) Biosynthesis of the ansamycin antibiotic rifamycin: deductions from the molecular analysis of the rif biosynthetic gene cluster of *Amycolatopsis mediterranei* S699.*Chem Biol. 5*, 69-79.

99. Kakavas, S. J., Katz, L., and Stassi, D. (1997) Identification and characterization of the niddamycin plyketide synthase genes from *Streptomyces caelestis*. *J. Bacteriol. 179*, 7515-7522.

100. Denoya, C. D., Fedechko, R. W., Hafner, E. W., McArthur, H. A. I., Morgenstern, M. R., Skinner, D. D., Stutzman-Engwall, K., Wax, R. G., and Wernau, W. C. (1995) A second branched-chain alpha-keto acid dehydrogenase gene cluster (bkdFGH) from *Streptomyces avermitilis*: its relationship to avermectin biosynthesis and the construction of a bkdF mutant suitable for the production of novel antiparasitic avermectins. *J. Bacteriol. 177*, 3504-3511.

101. Cortes, J., Wiesmann, K. E. H., Roberts, G. A., Brown, M. J., Staunton, J., and

Leadley, P. F. (1995) Repositioning of a domain in a modular polyketide synthase to promote specific chain cleavage. *Science 268*, 1487-1489.

102. Kao, C. M., Luo, G., Katz, L., Cane, D. E., and Khosla, C. (1995) Manipulation of macrolide ring size b directedmutagenesis of a odular polyketide synthase. *J. Am. Chem. Soc. 117*, 9105-9106.

103. Oliynyk, M., Brown, M. J. B., Cortes, J., Staunton, J., and Leadley, P. F. (1996) A hybrid modular polyketide synthase obtained by domain swapping. *Chem. Biol. 3*, 833-839.

104. McDaniel, R., Kao, C. M., Fu, H., Hevezi, P., Gustafsson, C., Betlach, M., Ashley, G., Cane, D. E. and Khosla, C. (1997) Gain-of-function mutagenesis of a modular polyketide synthase. *J. Am. Chem. Soc. 119*, 4309-4310.

105. Ruan, X., Pereda, A., Stassi, D. L., Zeidner, D., Summers, R. G., Jackson, M., Shivakumar, A., Kakavas, S., Stavers, M. J., Donadio, S. and Katz, L. (1997) Acyltransferase domain substitutions in erythromycin polyketide synthase yield novel erythromycin derivatives *J. Bacteriol. 179*, 6416-6425.

106. Weissman, K. J., and Leadlay, P.F. (2005) Combinatorial biosynthesis of reduced polypeptides. *Nat. Rev Microbiol*, *105*, 543-936.

107. Weissman, K.J. (2006) The structural basis for docking in modular polyketide biosynthesis. *ChemBioChem*, *7*, 485-494.

108. Pfeifer, B.A., and Khosla, C. (2001) Biosynthesis of polyketides in heterologous hosts. *Microbiol. Mol. Biol. Rev*. *65*, 106-118.

109. Kao, C.M., Katz, L., and Khosla, C. (1994) Engineered biosynthesis of complete macrlactone in a heterologous host. *Science 265*, 509-512.

110. McDaniel, R., Thamchaipenet, A., Gustafsson, C., Fu, H., Betlach, M., and Ashley, G. (1999) Multiple genetic modifications of the erythromycin polyketide synthase to produce a library of novel "unnatural" natural products. *Proc. Natl. Acad. Sci. U.S.A. 96*, 1846-1851.

111. Keiser, T., Bibb, M. J., Chater, K.F., and Hopwood, D. A. (2000) *Practical Streptomyces Genetics*. The John Innes Fondation, Norwich, UK.

112. Menzella, H.G., Reid, R., Carney, J. R., Chandran, S. S., Reisinger, S.J., Patel, K.G., Hopwood, D. A., and Santi, D. V. (2005) Combinatorial polyketide bioosynhesis by de novo design and rearrangement of modular polyketide synthase genes. *Nat Biotechnol*. *23*, 1171-1176.

113. Hata, T., Koga, F., Sano, Y., Kanamori, K., Matsumae, A., Sugawara, R., Hoshi, T., Shimi, T., Ito, S., and Tomizawa, S. (1954) Carzinophilin, a new tumor inhibitory substance produced by streptomyces.I. *Journal of Antibiotics, Ser.* A 7, 107-112.

114. Nagaoka, K., Matsumoto, M., Oono, J., Yokoi, K., Ishizeki, S., and Nakashima, T. (1986) Azinomycins A and B, new antitumor antibiotics I. Producing organism, fermentation, isolation, and characterization. *J. Antibiot. 39*, 1527-1532.

115. Ishizeki, S., Ohtsuka, M., Kazuhiko, I., Kukita, K., Nagaoka, K., and Nakashima, T. (1987) Azinomycins A and B, new antitumor antibiotics III. Antitumor activity. *Journal of Antibiot. 40*, 60-65.

116. Hashimoto, M., Matsumoto, M., Yamada, K., and Terashima, S. (2003) Synthetic studies of carzinophilin. Part 4: chemical and biological properties of carzinophilin analogues. *Tetrahedron 59*, 3089-3097.

117. Coleman, R.S., Perez, R. J., Burk, C. H., and Navarro, A. (2002) Studies on the mechanism of action of azinomycin B: definition of regioselectivity and sequence selectivity of DNA cross-link formation and clarification of the role of the naphthoate. *J. Am. Chem. Soc*. *124*, 13008-13017.

118. Mao, Y., Varoglu, M., and Sherman, D.H. (1999) Molecular characterization and analysis of the biosynthetic gene cluster for the antitumor antibiotic mitomycin C from *Streptomyces lavendulae* NRRL 2564. *Chemistry & Biology 6*, 251-263.

119. Ogasawara, Y. and Liu, H.W. (2009) Biosynthetic studies of aziridine formation in azicemicins. *J. Am. Chem. Soc 131*, 18066-18068.

120. Van Lanen, S. G., Oh, T. J., Liu, W., Wendt-Pienkowski, E., and Shen, B. (2007) Characterization of maduropeptin biosynthetic gene cluster from *Actinomadura madurae* ATCC 39144 supporting a unifying paradigm for enediyne biosynthesis. *J. Am.Chem. Soc*. *129*, 13082-13094.

121. Sthapit, B., Oh, T., Lamichhane, R., Liou, K., Lee, H. C., Kim, C., and Sohng, J.K. (2004) Neocarzinostatin naphthoate synthase: an unique iterative type I PKS from neocarzinostatin producer *Streptomyces carzinostaticus*. *FEBS Letters 566*, 201-206.

122. Armstrong, R. W., Salvati, M. E., and Nguyen, M. (1992) Novel interstrand cross-links induced by the antitumor antibiotic carzinophilin/azinomycin B . *J. Am. Chem. Soc. 114*, 3144-3145.

123. Liu, C., Kelly, G. T., and Watanabe, C. M. H. (2006) In vitro biosynthesis of the antitumor agent azinomycin B. *Org. Lett*. *8*, 1065-1068.

124. Sharma, V., Kelly, G. T., and Watanabe, C. M. H. (2008) Exploration of the molecular origin of the azinomycin epoxide: timing of the biosynthesis revealed. *Org. Lett*. 4815-4818.

125. Kelly, G. T., Sharma, V., and Watanabe, C. M. H. (2008) An improved method for culturing *Streptomyces sahachiroi*: biosynthetic origin of the enol fragment of azinomycin B. *Bioorganic Chem*. *36*, 4-15.

126. Foulke-Abel, J., Agbo, H., Zhang, H., Mori, S., and Watanabe, C.M. (2011) Mode of action and biosynthesis of the azabicycle-containing natural products azinomycin and ficellomycin *Nat Prod Rep*. *28,* 693-704.

127. Sanchez, A.M., Bennett, G.N., and San, K.Y. (2005) Novel pathway engineering design of the anaerobic central metabolic pathway in *Escherichia coli* to increase succinate yield and productivity. *Metab. Eng*. *7*, 229-239.

128. Sambrook, J., and Russell, D. W. (2001) *Molecular cloning: a laboratory manual, Volume 1*. 3rd edition. Cold Spring Harbor Laboratory Press, Cold Spring Harbor, NY.

129. Kobashi, N., Nishiyama, M., and Tanokura, M. (1999) Aspartate kinase-independent lysine synthesis in an extremely thermophilic bacterium, *Thermus thermophilus*: lysine is synthesized via α-aminoadipic acid, not via diaminopimeric acid. *J. Bacteriol*. *181*, 1713-1718.

130. Horie, A., Tomita, T., Saiki, A., Kono, H., Taka, H., Mineki, R., Fujimura, T., Nishiyama, C., Kuzuyama, T., and Nishiyama, M. (2009) Discovery of proteinaceous N-modification in lysine biosynthesis of *Thermus thermophilus*. *Nature Chem. Biol. 9*, 673-679.

131. Leisinger, T., and Haas, D. (1975) N-Acetylglutamate synthase of *Escherichia coli* : regulation of synthesis and activity by arginine. *J. Biol. Chem*. *250*, 1690-1693.

132. Baetens, M., Legrain, C., Boyen, A., and Glansdorff, N. (1998) Genes and enzymes of the acetyl cycle of arginine biosynthesis in the extreme thermophilic bacterium *Thermus thermophilus* HB27. *Microbiology 144*, 479-492.

133. Yoshida, A., Tomita,T., Kuzuyama, T., and Nishiyama, M. (2010) The crystal structures of amino acid kinase *lysZ* and carrier protein *lysW* involved in lysine biosynthesis of *Thermus thermophilus*. *Riken Symposium,* 8/20/2010-8/22/2010.

134. Zabriskie, T. M., and Jackson, M. D. (2000) Lysine biosynthesis and metabolism in fungi. *Nat. Prod. Rep*. *17*, 85-97.

135. Ausubel, F.M., Brent, R., Kingston, R.E., Moore, D. D., Seidman, J.G., Smith, J. A. and Struhl, K. (2001) *Current protocols in molecular biology*. Wiley, New York.

136. Watanabe, C.M., Wolffram S., Ader, P., Rimbach, G., Packer, L., Maquire, J. J., Schultz, P. G., and Gohil, K. (2001) The *in vivo* neuromodulatory effect of herbal medicin *Ginkgo biloba*. *Proc. Natl. Acad. Sci. U. S.A. 98*, 6577- 6580.

137. Mi-Jin, L., Kyuboem, H., and Eung-Soo, K. (2011) Targeted gene disruption and functional complementation of cytochrome P450 hydroyxlase involved in cyclosporin A hydroxylation in *Sebekia benihana*. *J. Microbiol. Biotechnol. 21*,14-19.

138. Kim, J.N., Ahn, S., Seaton, K., Garrett, S., and Burne, R.A. (2012) Transcriptional organization and physiological contributions of the relQ operon of *Streptococcus mutans*. *J. Bacteriol. 194*, 1968-1978.

139. Morse, D., and Primakoff, P. (1970) Relief of polarity in *E. coli* by *suA*. *Nature 226*: 28.

140. Richardson, J. P., Grimley, C., and Lowery, C. (1975) Transcription termination factor *rho* activity is altered in *Escherichia coli* with *suA* gene mutations. *Proc. Natl. Acad. Sci. U.S.A. 72*, 1725.

141. Roberts, J. (1969) Termination factor for RNA synthesis. *Nature 224*, 1168.

142. Wu, A. M., Christie, G. E., and Platt, T. (1981) Tandem termination sites at the end of the tryptophan operon in *E. coli*. *Proc. Natl. Acad. Sci. U.S.A. 78*, 2913-2917.

143. Ciampi, M.S., and Roth, J.R. (1988) Polarity effects in the hisG gene of *Salmonella* require a site within the coding sequence. *Genetics 118*, 193-202.

144. Axelrod, J. (1955) The enzymatic demethylation of ephedrine. *J. Pharmacol. Exp. Ther. 114*, 430 - 438.

145. Brodie, B., Axelrod, J., Cooper, J.R., Gaudette, L., LaDu, B.N., Mitoma, C., and Udenfriend, S. (1955) Detoxication of drugs and other foreign compounds by liver microsomes. *Science 121*, 603-604.

146. Garfinkel, D. (1958) Studies on pig liver microsomes. I: Enzymic and pigment composition of different microsomal fractions. *Arch. Biochem. Biophys. 77*, 493-509.

147. Klingenberg, M. (1958) Pigments of rat liver microsomes. *Arch. Biochem. Biophys. 75*, 376-386.

148. Omura, T., Sato, R. (1962) A new cytochrome in liver microsomes. *J. Biol. Chem. 237,* 1375-1376.

149. Omura, T., and Sato, R. (1964a) The carbon monoxide-binding pigment of liver microsomes. I. Evidence for its hemoprotein nature. *J. Biol. Chem. 239*, 2370-2378.

150. Omura, T., and Sato, R. (1964b) The carbon monoxide-binding pigment of liver microsomes. II. Solubilization, purification and properties. *J. Biol. Chem. 239*, 2378-2385.

151. Nelson, D.R., Kamataki, T., Waxman, D.J., Guengcrich, F.P., Estabrook, R.W., Feyereisen, R., Gonzalez, F.J., Coon, M.J., Gunsalus, I.C., Gotoh, O., Okuda, K., and Nebert, D.W. (1993) The P450 superfamily: update on new sequences, gene mapping, accession numbers, early trivial names of enzymes, and nomenclature. *DNA Cell Biol. 12*, 1-51.

152. Janig, G.R., Makower, A., Rabe, H., Bernhardt, R., and Ruckpaul, K. (1984) Chemical modification of cytochrome *P*-450 LM2: characterization of tyrosine as axial heme iron ligand *trans* to thiolate. *Biochim. Biophs. Acta*. *787*, 8-18.

153. Nelson, D. R., Koymans, L., Kamataki, T., Stegeman, J. J., Feyereisen, R., Waxman, D. J., Waterman, M. R., Gotoh, O., Coon, M. J., Estabrook, R. W., Gunsalus, I. C., and Nebert, D. W. (1996) P450 superfamily: update on new sequences, gene mapping, accession numbers and nomenclature. *Pharmacogenetics 6,* 1- 42.

154. Lehninger, A.L., Nelson, D.L., and Cox, M.M. (1993) *Principles of biochemistry.* Worth, New York.

155. Li, H., and Poulos, T.L. (1994) Structural variation in heme enzymes: a comparative analysis of peroxidase and P450 crystal structures. *Structure 2*, *461*- 464.

156. Marnett, L. J., and Kennedy, T. A. (1995) Comparison of the peroxidase activity of hemoproteins and cytochrome P450, in: *Cytochrome P450* (P.R.Ortiz de Montellano, ed.) Plenum, New York, 49 - 80.

157. Hannemann, F., Bichet, A., Ewen, K. M., and Bernhardt, R. (2007) Cytochrome P450 systems-biological variations of electron transport chains. *Biochim. Biophys. Acta, 1770*, 330-344.

158. Guengerich, F. P. (1999) Cytochrome P-450 3A4: regulation and role in drug metabolism. *Annu. Rev. Pharmacol. Toxicol*. *39*, 1-17.

159. Lamb, D.C., Ikeda, H., Nelson, D.R., Ishikawa, J., Skaug, T., Jackson, C., Ōmura, S., Waterman, M. R., and Kelly, S. L. (2003) Cytochrome P450 complement (CYPome) of the avermectin-producer *Streptomyces avermitilis* and comparison to that of *Streptomyces coelicolor A3(2)*. *Biochem. Biophys. Res. Commun*. *307*, 610-619.

160. Rix, U., Fischer, C., Remsing, L.L., and Rohr, J. (2002) Modification of post-PKS tailoring steps through combinatorial biosynthesis. *Nat. Prod. Rep*. *19*, 542-580.

161. Bentley, S.D., Chater, K.F., Cerdeño-Tárraga, A.M., *et.al*.(2002) Complete genome sequence of the model actinomycete *Streptomyces coelicolor* A3(2). *Nature 417*, 141-147.

162. Carlson, C., Li, S., Gunatilleke, S.S., Anzai, Y., Burr, D. A., Podust, L.M., and Sherman, D.H. (2011) Tirandamycin biosynthesis is mediated by co-dependent oxidative enzymes. *Nat Chem*. *3*, 628- 633.

163. Parajuli, N, Basnet, D.B., Chan, L. H., Sohng, J.K., and Liou, K. (2004) Genome analyses of *Streptomyces peucetius* ATCC 27952 for the identification and comparison of cytochrome P450 complement with other *Streptomyces*. *Arch Biochem Biophys. 425*, 233-241.

164. Ikeda, H., Ishikawa, J., Hanamoto, A., Shinose, M., Kikuchi, H., Shiba T., Sakaki, Y., Hattori, M., and Omura, S. (2003) Complete genome sequence and comparative analysis of the industrial microorganism *Streptomyces avermitilis Nat. Biotechnology 21*, 526 – 531.

165. Wong, L. L. (1998) Cytochrome P450 monooxygenases. *Curr. Opin. Chem. Biol. 2*, 263-268.

166. Petzoldt, K. Schering Aktiengesellschaft : Process for the preparation of 11-beta-hydroxy steroids . (Berlin, Germany*). Patent 4353985.*

167. Peterson, D.H. (1952) Microbial transformation of steroids. Introduction of oxygen at carbon-11 of progesterone. J. *Am. Chem. Soc. 74*, 5933-5936.

168. Park, J.W. (2003) Bioconversion of compactin into pravastatin by *Streptomyces* sp. *Biotechnol. Lett. 25*, 1827-1831.

169. Jones, J.P. (2001) Oxidation of polychlorinated benzenes by genetically engineered CYP101 (cytochrome P450cam). *Eur. J. Biochem. 268*, 1460-1467.

170. Sakaki, T. (2002) Biodegradation of polychlorinated dibenzo-pdioxins by recombinant yeast expressing rat CYP1A subfamily. *Arch. Biochem. Biophys*. *401*, 91-98.

171. Sulistyaningdyah, W.T. (2004) Metabolism of polychlorinated dibenzo-p-dioxins by cytochrome P450 BM-3 and its mutant. *Biotechnol. Lett. 26*, 1857-1860.

172. Taylor, M., Lamb, D. C., Cannell, R. J., Dawson, M. J., and Kelly, S. L. (2000) Cofactor recycling with immobilized heterologous cytochrome P450 105D1 (CYP105D1). *Biochem. Biophys. Res. Commun. 279*, 708-711.

173. Capdevila, J.H., Falck, J.R., and Estabrook, R.W. (1992) Cytochrome P450 and the arachidonate cascade. *FASEB J. 6*,731-736.

174. Oesch, F., Doehmer, J., Friedberg, T., Glatt, H.R., Oesch-Barthlomowicz, B., Platt, K.L., Steinberg, P., Utesch, D., and Thomas, H. (1990) Toxicological implications of enzymatic control of reactive metabolites. *Hum Exp Toxicol. 9*, 171-177.

175. Ding, Y., Seufert, W.H., Beck, Z.Q., and Sherman, D.H. (2008) Analysis of the cryptophycin P450 epoxidase reveals substrate tolerance and cooperativity. *J. Am. Chem. Soc. 130*, 5492 -5498.

176. Mendes, M.V., Recio, E., Fouces, R., Luiten, R., Martin, J.F., and Aparicio, J.F. (2001) Engineered biosynthesis of novel polyenes: a pimaricin derivative produced by targeted gene disruption in *Streptomyces natalensis*. *Chem Biol. 8*, 635-644.

177. Mendes, M.V., Anton, N., Martin, J.F., and Aparicio, J.F. (2005) Characterization of the polyene macrolide P450 epoxidase from *Streptomyces natalensis* that converts de-epoxypimaricin into pimaricin. *Biochem J. 386*, 57- 62.

178. Ding, W., Deng, W., Tang, M., Zhang, Q., Tang, G., Bi, Y., and Liu, W. (2010) Biosynthesis of 3-methoxy-5-methyl naphthoic acid and its incorporation into the antitumor antibiotic azinomycin B. *Mol BioSyst. 6*, 1071-1081.

APPENDIX

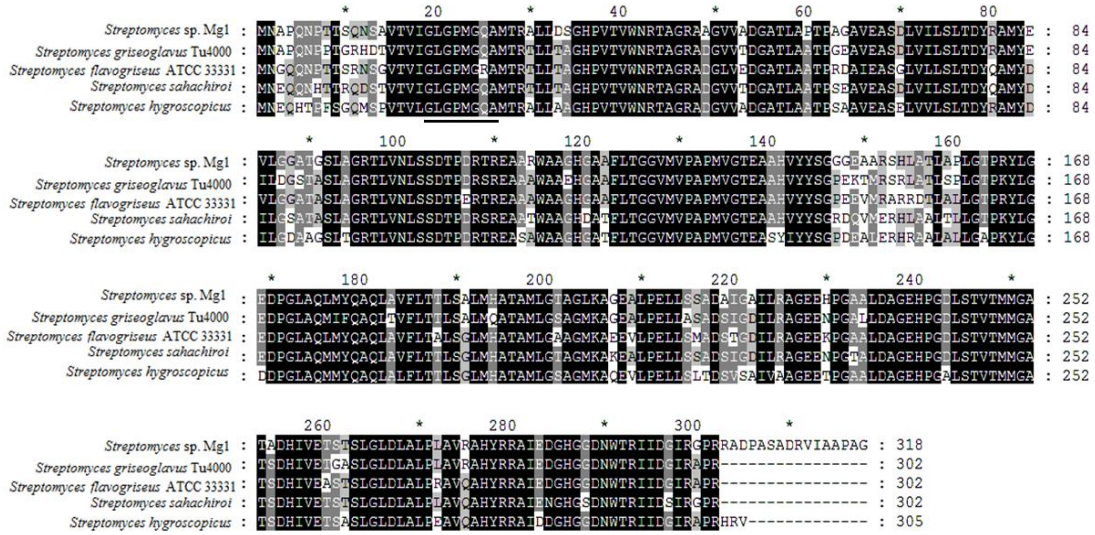

Figure 56. Multiple sequence alignment of *ORF10* with its homologues. (*S.* sp. Mg1; 84% identity, *S. griseoflavus* Tu4000; 85% identity, *S. flavogriseus* ; 84% identity and *S. hygroscopicus* ; 81% identity). Co-factor NAD+/NADP+ bindings motif is underlined.

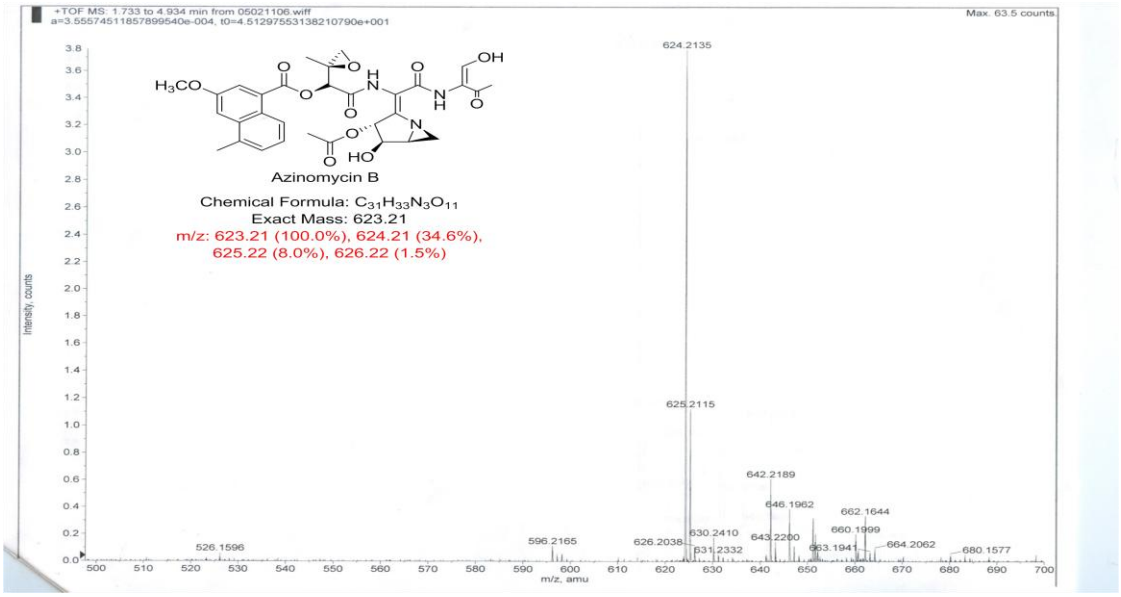

Figure 57.Mass spectrum of azinomycin B (peak B) collected from RP-HPLC.

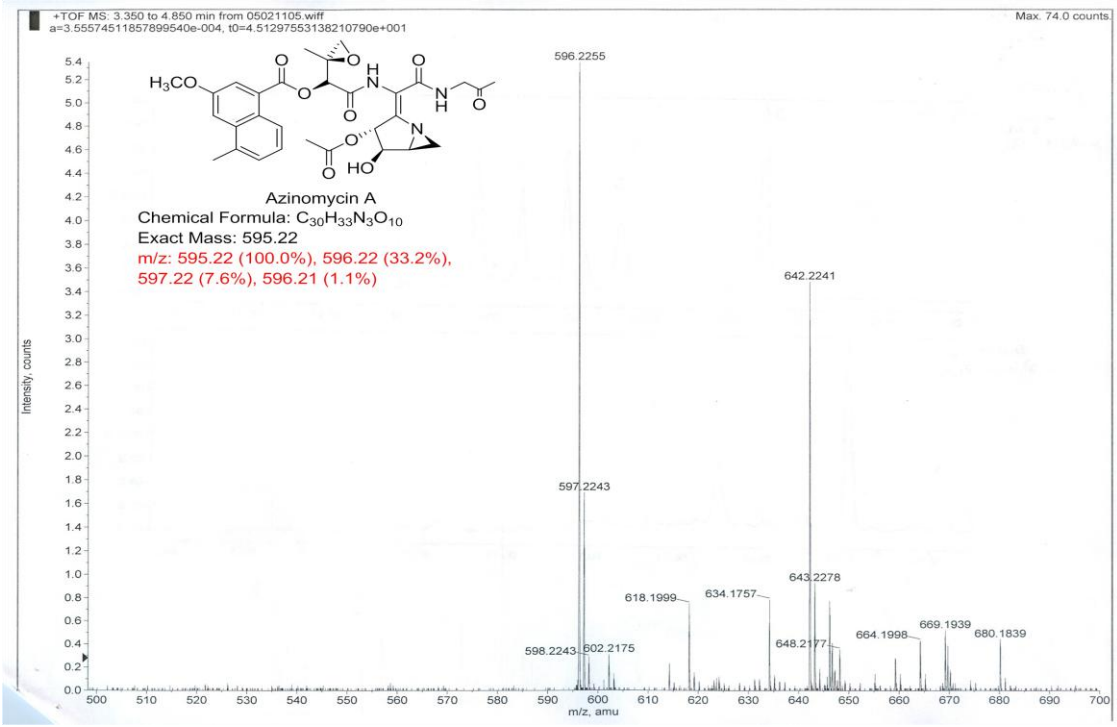

Figure 58.Mass spectrum of azinomycin A (peak A) collected from RP-HPLC.